The Role of Natural Organic Matter and Phosphorus in a Changing Environment

Dissertation for the degree of *Philosophiae Doctor*

by

Christian Wilhelm Mohr

Department of Chemistry
Faculty of Mathematics and Natural Sciences
University of Oslo
2017

Contents

Abstract

Eutrophication is globally a growing concern, as freshwater bodies are becoming more and more exposed to nutrient pollution. Excessive P loading is often the main cause of eutrophication, as P is often the limiting nutrient to phytoplankton growth. P pollution to lakes and reservoirs generally comes both from non-point sources, such as runoff from agricultural areas, and point sources, such as sewage from wastewater outlets. Abatement actions regulating the application of fertilisers and ploughing regimes for agricultural areas, and re-routing of sewage outlets, greatly lowers the P loading to the waterbodies. As such, eutrophication problems can generally be easily solved given the right incentives.

Lake Vansjø, located in an agricultural district in south eastern Norway, has experienced a continues worsening in water quality over the last 30 to 40 years, as a of result eutrophication. However, in the case of Lake Vansjø, over 500 million of Norwegian kroner has been spent on sewage infrastructure upgrade and abatement actions over the years, without achieving the expected improvements. In 2009 the EUTROPIA project was funded, partly with the aim to improve our understanding of the catchment as a whole and better understand why the abatement actions have not had the desired affects. It is this part of the project which is the focus of this study.

The study found that the decline in acid rain over the last 30 to 40 years is one of the main explanations for why the abatement actions have not had the desired affects. The decline in acid rain, has resulted in a 3 times reduction in the concentration of labile Al. The study predicts that the orthophosphate/phosphate concentration in the lake, in the 1980's, would have been $\approx \frac{1}{5}$ of the concentration of what is today, due to Al co-precipitation with phosphate.

Additionally, over the same period there has been a doubling in the concentration of Dissolved Organic Matter (DOM), partly explained by climate change and partly by the decline in acid rain. DOM photo- and biodegradation studies were conducted to better assess what impact an increase in DOM may have on the lake water quality. The study found that photodegradation greatly enhances the biodegradability of the DOM: Photodegradation alone after 20 hours exposure contributed to 26% mineralisation of the original Dissolved Organic Carbon (DOC). Of the remaining DOC, 3 to 39% was mineralised by micro-organism, for 0 to 20 hours exposure, respectively. The study suggests that humic substances become more biodegradable after irradiation, particularly humic acids (HA). Fulvic acids (FA) seem to be a product of HA degradation, in addition to bioavailable DOM fragments. It is postulated that the increase in the DOM concentration may have a significant impact on the microbial biodiversity in shollow lake basins, such as *Vanemfjorden*, Lake Vansjø's western basin. The reduction in light attenuation, and the higher degree of low-molecular-weight bioavailable DOM, suggests migration of bacteria and phytoplankton to the surface in search for energy. However, the production of rad-

icals from DOM photodegradation most likely will also result in a deathly environment for micro-organisms. The DGT study in the lake seems to confirms these findings, since more bioavailable P was found near the surface of the lake than any other depths.

The Diffusive Gradients in Thin films (DGT) were found be useful as passive sampler for two bioavailable P fractions; Dissolved Reactive Phosphorus (DRP; approx. orthophosphate) and Low-Molecular-Weight Organic Phosphorus (LMWOP). The concentration of LMWOP is approx. equal or larger than orthophosphate in forested steams. If the concentration of LMWOP, along with the rest of the DOM, has doubled over the last 30 to 40 years; and considering that 85% of the catchment is forested area, and the largest contributor of DOM to the lake; then it is highly likely that climate change and acid rain decline have had an impact on eutrophication.

Acknowledgement

I would like to thank my supervisor and mentor throughout this work, Rolf D. Vogt. It has been a great pleasure working with you all these year. Your support, guidance, and trust in my abilities is truly appreciated. I have enjoyed our intellectual discussions in your office, our trips to China, and our field trips collecting water and soil while fighting off mosquitoes. I have learned so much from you over the years we have worked together. And for that I am truly grateful. I hope we will have the opportunity to work together again in the future.

To my co-supervisor Tom Andersen thank you for all your help and support. Still after all theses years I am baffled with the extent of your knowledge. I have enjoyed our discussion, and hope to have more in the future.

I would like to thank my co-supervisor Grethe Wibetoe for your guidance.

I would like to give a special thanks to Claus Jørgen Nielsen for all the advice and help. Thank you for taking the time to help me better understand physical chemistry and spectroscopy.

To my fellow student, colleague and dear friend Catherine, who I have got to know over so many years. I have enjoyed our time together discussing, arguing :) and lots and lots of laughing! Thanks for all the good times!

To my Chinese brother Bin, who is no longer in Norway, thanks for your friendship, kindness and hospitality. I hope to see you again soon and my Chinese parents!

And to Goran, Kristine, Asfaw, Kaja, Xie, Alexander E., Koji, Su Ming, Yemane, Dejene, Neha, Ykalo, Sahle, Pauline, Alexis, Liang, Lü, Yang, Frøydis, Ellen, Andreas S., Erlend, Wycliffe, Lena, Wen, Tomas, Alexander H., Elena, Gao, Emilie, Nina, Andreas L., Raoul, and so many others that I have come to know over the 8 years that I have been at UiO. Thanks for the talks, laughs, outings, and friendship.

Finally I would like to thank my family. I could never imagine getting through this Ph.D. without all of your support. You are all forever in my debt!

List of Papers

1. C. W. Mohr, R. D. Vogt, O. Røyset, T. Andersen, and N. A. Parekh. An in-depth assessment into simultaneous monitoring of dissolved reactive phosphorus (DRP) and low-molecular-weight organic phosphorus (LMWOP) in aquatic environments using diffusive gradients in thin films (DGT). *Environ. Sci.: Processes Impacts*, 17(4):711-727, 2015. ISSN 2050-7887. doi:10.1039/C4EM00688G.

2. C. W. Mohr, A. J. Baxter, C. B. Gundersen, T. Andersen, and R. D. Vogt. Spectroscopic and Chemical Analyses of Short-term Photo- and Biodegradation of Freshwater Dissolved Natural Organic Matter. *Environ. Sci.: Processes Impacts*. pages 1-14, 2017 [Submitted].

3. C. W. Mohr, Y. Kidanu, A. Løken, and R. D. Vogt. Solution to acid rain pollution and the onset of eutrophication: A biogeochemical perspective., pages 1-16, 2017 [manuscript].

Other papers

1. C. W. Mohr and R. D. Vogt. Sorption of Nitramines to Soil. Final report of a preliminary assessment study. Technical report, University of Oslo, Oslo, 2012.

2. R. D. Vogt, A. Engebretsen, and C. W. Mohr. The Effect of Increased Dissolved Natural Organic Matter on Eutrophication. In J. Xu, J. Wu, and Y. He, editors, *Functions of Natural Organic Matter in Changing Environment*, chapter Part VII, pages 895-899. Springer Netherlands, Dordrecht, 2013. ISBN 9787308102711.

3. B. Zhou, R. D. Vogt, X. Lu, X. Yang, C. Lü, C. W. Mohr, and L. Zhu. Land use as an explanatory factor for potential phosphorus loss risk, assessed by P indices and their governing parameters. *Environ. Sci.: Processes Impacts*, 17(8):1443-1454, aug 2015. ISSN 2050-7887. doi: 10.1039/C5EM00244C.

4. C. Lü, J. He, L. Zuo, R. D. Vogt, L. Zhu, B. Zhou, C. W. Mohr, R. Guan, W. Wang, and D. Yan. Processes and their explanatory factors governing distribution of organic phosphorous pools in lake sediments. *Chemosphere*, 145:125-134, feb 2016. ISSN 00456535. doi: 10.1016/j.chemosphere.2015.11.038.

Abbreviations

Al_i	Labile Al
APA	Agarose Polyacrylamide
BCE	Before Current Era
CA	Cellulose Acetate
DGT	Diffusive Gradients in Thin films
DPSIR	Driving forces Pressures States Impacts Responses
DOC	Dissolved Organic Carbon
DOM/DNOM	Dissolved Organic Matter/Dissolved Natural Organic Matter
EDX	Energy-Dispersive X-ray Spectroscopy
EEA	European Economic Area
EEM	Fluorescence Excitation-Emission Matrix Spectroscopy
EU	European Union
EUTROPIA	Watershed EUTROphication management through system oriented process modelling of Pressures, Impacts and Abatement actions
FA	Fulvic Acid
FTIR	Fourier Transform Infrared Spectroscopy
HA	Humic Acid
HCPC	Hierarchical Clustering on Principal Components
HMW	High-Molecular-Weight
HMWOP	High-Molecular-Weight Organic Phosphorus
HS	Humic Substances
LMW	Low-Molecular-Weight
LMWOP	Low-Molecular-Weight Organic Phosphorus
LMWOM	Low-Molecular-Weight Organic Matter
LOD	Limit of Detection
LOQ	Limit of Quantification
Mw	Molecular Weight

NIBR	Norwegian Institute for Urban and Regional Research
NINA	Norwegian Institute for Nature Research
NIVA	Norwegian Institute for Water Research
NMBU	Norwegian University of Life Sciences
NPOC	Non-Purgeable Organic Carbon
NMR	Nuclear Magnetic Resonance Spectroscopy
PCA	Principal Component Analysis
PM	Particulate Matter
RCN	Research Council of Norway
SEM	Scanning Electron Microscopy
TWA	Time-Weighted Average
WFD	The EU Water Framework Directive
UiO	University of Oslo
UNECE	The United Nations Economic Commission for Europe
UV-Vis	UV-Visible Absorption Spectroscopy
WP	Work Packages

1 Introduction

1.1 EUTROPIA

There has been an increasing demand from citizens and environmental organisations in the European Union (EU) to improve the quality of their water resources. An opinion poll cast in 25 EU countries, prior to 2000, showed that out of the five main environmental issues, 47% of Europeans were most concerned with water pollution. As such, the EU set in motion a thorough reconstruction of the European Water Policy, and in 2000 the Water Framework Directive (WFD) was established. WFD is a framework that was set in place for the protection of inland surface waters, transitional waters, coastal waters and groundwater. It encompasses defining these different resources, classification of "good water quality", and policies with milestones enforcing; the identification of river basin districts and authorities; characterisation of river basins: pressures, impacts and economic analysis; establishment of monitoring programs; river basin management plan; establishing pricing policies; and meeting future environmental objectives [European Commission, 2010].

As part of the European Economic Area (EEA) agreements, Norway implemented WFD policies into their framework *Den norske vannforskriften*. In the wake of stricter polices and deadlines, there was an increasing amount of pressure placed on improving the quality of freshwater systems in Norway. An assessment of the quality of freshwater in Norway from 1980-2008, found that many lakes, especially in Østfold county (SE Norway), were suffering from eutrophication, with little sign of improvement [Solheim and Moe, 2008]. Lake Vansjø, the largest lake located in Morsa Catchment, Østfold, Norway, had especially poor water quality, due largely to the close proximity to agricultural land. However, despite over 500 million kroner spent in sewage infrastructural upgrades and a large number of abatement actions, including reduction in P runoff from agricultural land into the waterbodies draining into Lake Vansjø, little improvement was found [Solheim, 2001, Blankenberg et al., 2008].

In 2009, the Research Council of Norway (RCN) funded a four year interdisciplinary project titled "Watershed EUTROphication management through system oriented process modelling of Pressures, Impacts and Abatement actions", known informally as EUTROPIA. The aim of the project was to help meet future demands of WFD for Lake Vansjø, which requires among other things an integrated approach to managing water resources. As such, the EUTROPIA project adapted the DPSIR model (Driving forces Pressures States Impacts Responses) approach to better understand what mechanisms are driving the eutrophication in Lake Vansjø and what cost-benefit social responses are required to resolve the problem.

The project, lead by Prof. Rolf David Vogt (Department of Chemistry, University of Oslo (UiO)) was an interdisciplinary collaboration between the Department of Chemistry, UiO; Department of Biosciences, UiO; Department of Geosciences, UiO; Norwegian Institute for Water Research (NIVA); Norwegian Institute for Nature Research (NINA); Norwegian Institute for Urban and Regional Research (NIBR); Norwegian University of Life Sciences (NMBU); and Bio-Forsk.

The research strategy undertaken was an integrated approach, where tasks were assigned to work packages (WP), 1-5, encompassing different fields of science (Fig. 1). Description of WP are as follows: "WP1: Develop sampling and analytical methods for P fractionation in water; WP2: Describe catchment processes governing mobilization, transport and nutrient flux; WP3: Integrate the developed system and process understanding of the terrestrial and aquatic environments in the models; WP4: Use Bayesian network to integrate the simulation models with probability of stakeholder response and develop a better measure of uncertainty in prediction power for future changed pressures; and WP5: Develop systematic societal response analysis based on identified nutrient sources with focus on behavioural modelling the likelihood of implementation of different abatement strategies" [Vogt et al., 2008].

The studies in this thesis were partly funded by the EUTROPIA project and fall under the tasks of WP1 and WP2.
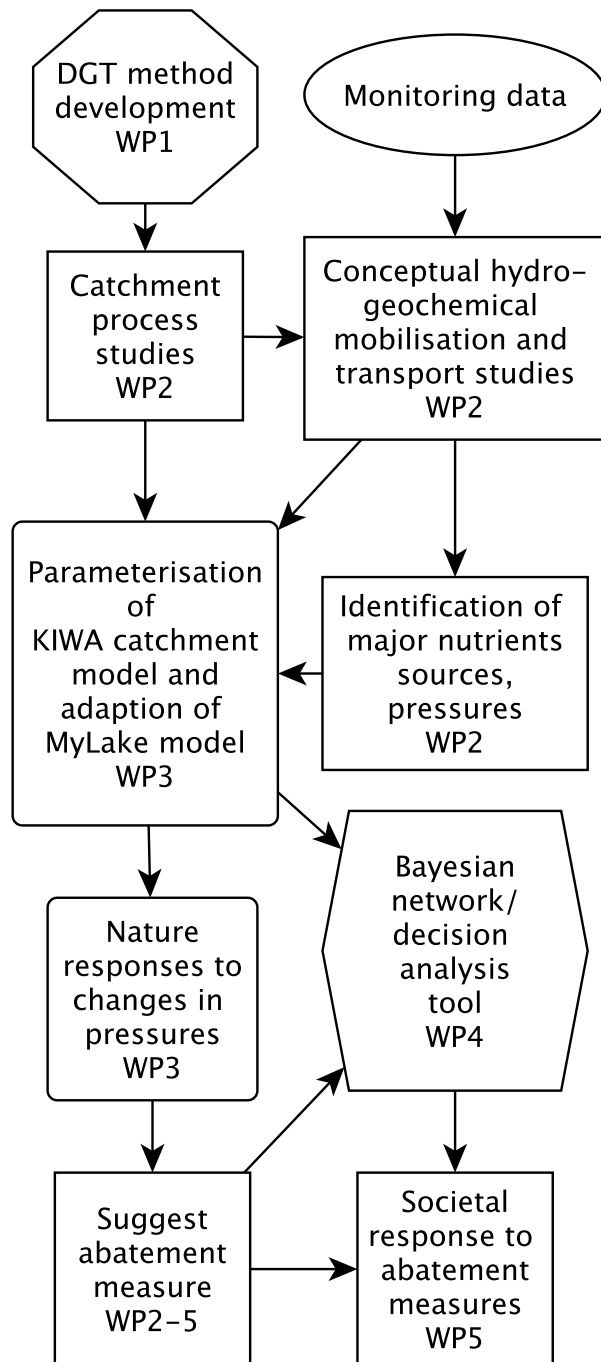

Figure 1: Work package research strategy for EUTROPIA project. Source: Adapted from Vogt et al. [2008].

1.2 A Historical Overview

To get a better understanding of possibly why abatement actions on reducing nutrient loading to Lake Vansjø have not had the expected improvements on the water quality, we need to understand the environmental changes that the Østfold region has undergone over time.

1.2.1 The End of an Ice Age

Around 23,000 and 19,000 BCE the last ice age was at a point at which the ice sheets were at their greatest coverage, referred to as the *Last Glacial Maximum*. Vast parts of North America, Eurasia, all of Greenland and Antarctica were covered under ice sheets as thick as 3 - 4 km (Fig. 2), placing enormous weight on the tectonic plates [Bowen, 2007].
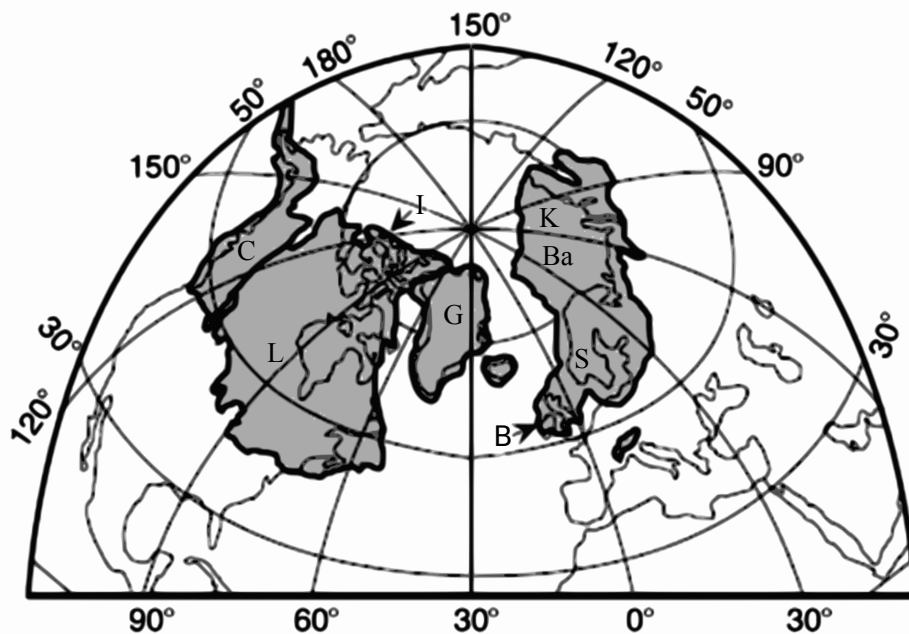
Figure 2: Illustration of the maximum estimated ice sheet coverage in the northern hemisphere. L: Laurentide Ice Sheet; C: Cordilleran Ice Sheet; I: Innuitian Ice Sheet; G: Greenland Ice Sheet; B: Great Britain and Ireland Ice Sheet; S: Scandinavian (Fenno-Scandian) Ice Sheet; Ba: Barents Sea Ice Sheet; K: Kara Sea Ice Sheet. Source: Adapted from Bowen [2007].

Since that time, the ice sheets have slowly retreated. This has resulted in what is known as post-glacial rebound, a process in which the land mass rises as the weight of the ice on top declines with the ice retreat (Fig. 3). Collectively these up and down elevation shifts in the crustal surface with change in glacial mass is known as glacial isostasy [Lambeck, 2007].

In the southern part of Norway, land rose up by as much as 200 m. Most of Østfold is below 200 m.a.s.l. (referred as the marine limit), and was therefore once bellow the ocean surface. For this reason most of Østfold has soil with marine sediment deposits
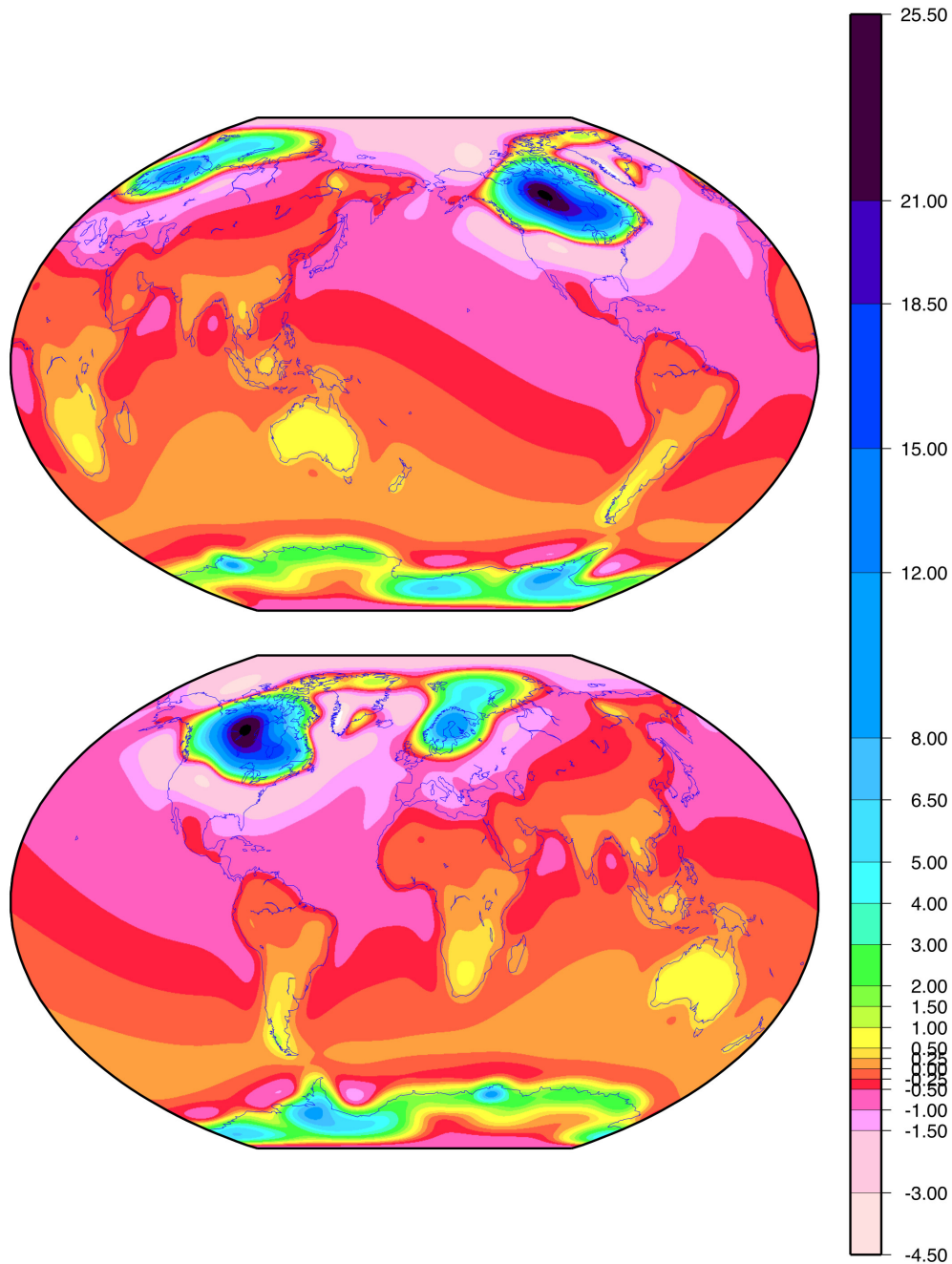
Figure 3: Modelled global crustal uplift in mm/year [Ivins et al., 1993]: Southern and Northern Hemisphere loading/unloading described by Ivins and James [2004, 2005], Peltier [2004]. Source: With permission from Erik Ivins.

[Klemsdal, 2002]. The soil is therefore rich in calcite and phosphate minerals, making it a naturally fertile land, suited for agriculture. It is also an area in which nutrients from land and lake sediments naturally provide a rich and diverse lake ecosystem [Spikkeland, 2003]. That being the case, there is very little additional nutrient input to the aquatic system that is required to tip the scale in the direction of eutrophication.

1.2.2 Climate Change and Acid Rain

Along with the great advances to civilization, contributed by the industrial revolution, came also new environmental challenges. One of which was the pollution brought on from the burning of fossil fuels. As the population and energy consumption grew rapidly over 20th Century, so did the emissions of CO_2, SO_2 and NO_x from burning fossil fuels. The increasing atmospheric concentration of CO_2, a greenhouse gas, has contributed to a rise in the global mean temperature, resulting in climate change [Collins et al., 2007]. Significantly warmer temperatures (Fig. 4) and increased rainfall (Fig. 5) have been observed in Norway. There are also far more frequent short period (∼1 hour) heavy rainfall episodes in the entire southern coastal region [Hanssen-Bauer et al., 2015]. The impact of this type of harsh frequent rainfall is increased erosion in areas with loose soil matter and a lack of vegetation, such as agricultural land after harvest and ploughing. Furthermore, due to warmer winters, there are more frequent freezing and thawing episodes which may be enhancing the erodability of the soil [Kværnø and Øygarden, 2006]. This in turn is resulting in increased runoff of particulate bound P from agricultural sites in Morsa Catchment [Skarbøvik et al., 2016], potentially providing more bioavailable P to the phytoplankton in the lake. Furthermore, the increase in lake temperatures due to warmer summers provides generally better conditions for phytoplankton growth, especially cyanobacteria [Kosten et al., 2012].
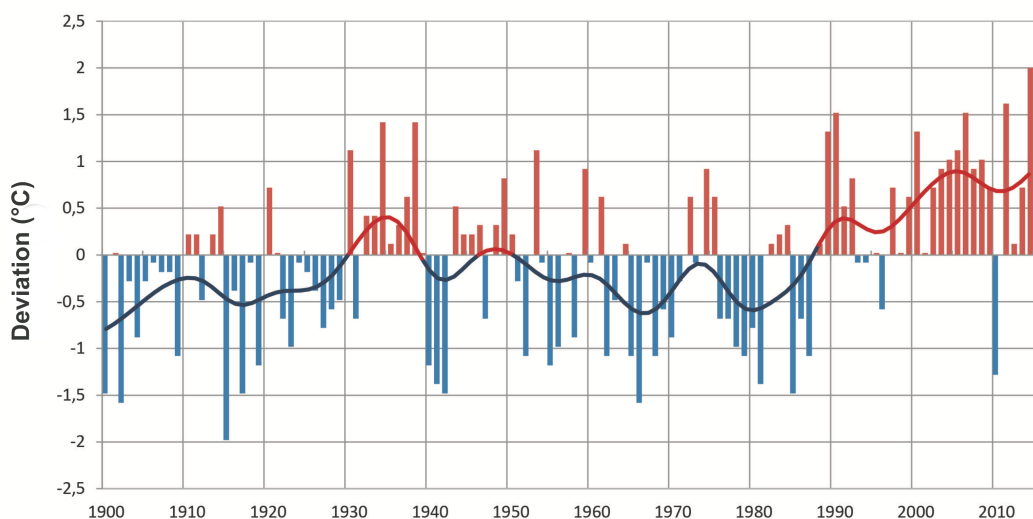
Figure 4: Trend in yearly mean temperature for mainland Norway 1900-2014. Change is presented as deviation (°C) from the mean temperature of the reference period 1971-2000. Source: Adapted from Hanssen-Bauer et al. [2015].

While combating CO_2 emissions is still a major global challenge, far more progress has been made on reducing anthropogenic SO_2 and NO_x emissions. Anthropogenic SO_2 emissions come mainly from coal power plants. As SO_2 reacts with the H_2O in the atmosphere,
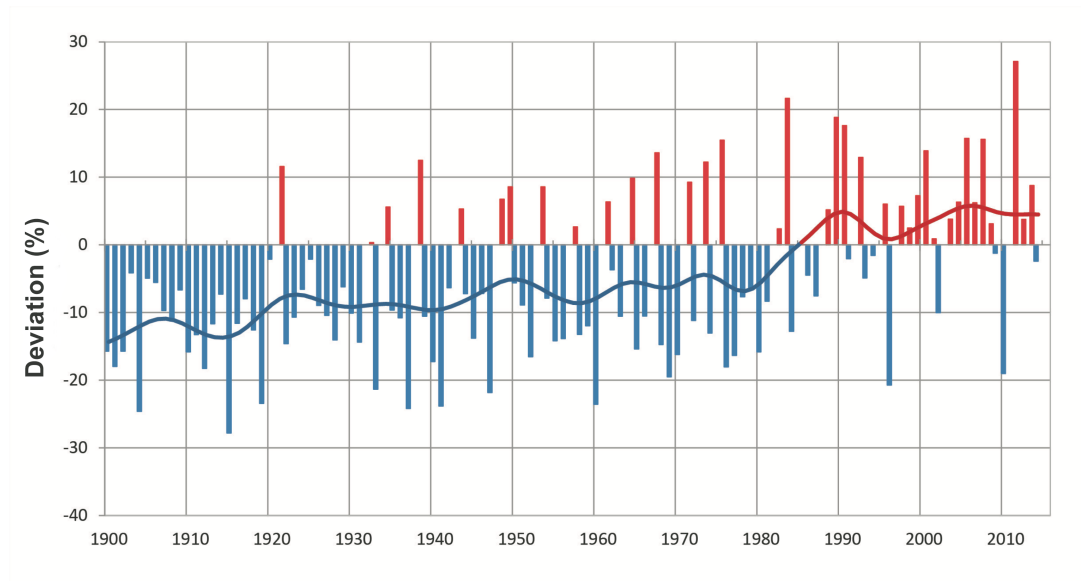
Figure 5: Trend in yearly rainfall for mainland Norway 1900-2014. Change is presented as percent deviation from the mean yearly rainfall for reference period from 1971-2000. Source: Adapted from Hanssen-Bauer et al. [2015].

it produces H_2SO_4, eventually returning back to land as either dry or wet deposition, the latter known commonly as acid rain. Anthropogenic NO_x emissions come primarily from internal combustion engines. In a similar manner, anthropogenic NO_x emissions react with H_2O producing HNO_3, which eventually deposits back to land. Acid rain was a major environmental problem in Europe and North America. Even Scandinavia, which did not have particularly high emissions of SO_2 and NO_x, received acid deposition via long range transport from industries in Great Britain and Germany [Skjelkvåle et al., 2001b, Odén, 1976, Brown and Sadler, 1981]. This resulted in increased leaching of Al from acid forested soil, resulting in fish deaths from toxic concentrations of labile Al (Al_i) in the aquatic environment [Gensemer and Playle, 1999, Rosseland et al., 2001]. In 1979, the United Nations Economic Commission for Europe (UNECE) agreed to enforce regulations to reduce the SO_2 emissions in European countries [UNECE, 1979]. Today, this collaborative agreement among European nations stands testament to one of the most successful interventions to combating a near environmental disaster. Acid deposition has dropped dramatically since the 1980's (Fig. 6).

In southern Norway there has been as much as ∼80% reduction in anthropogenic $SO_4{}^{2-}$ deposition from 1986 - 2013. As a result, over the same period there has been a ∼3 times reduction in Al_i concentrations in lakes in southern Norway. There has also been a doubling in the concentration of Dissolved Organic Carbon (DOC) [Garmo et al., 2014], which is a proxy for Dissolved Organic Matter (DOM), also referred to as Dissolved Natural Organic Matter (DNOM). The DOC trend has been linked to both the decline in acid rain and climate change [Weyhenmeyer et al., 2014, Köhler et al., 2013, Arvola et al., 2010, Haaland et al., 2010, Jennings et al., 2010, Monteith et al., 2007, Roulet and
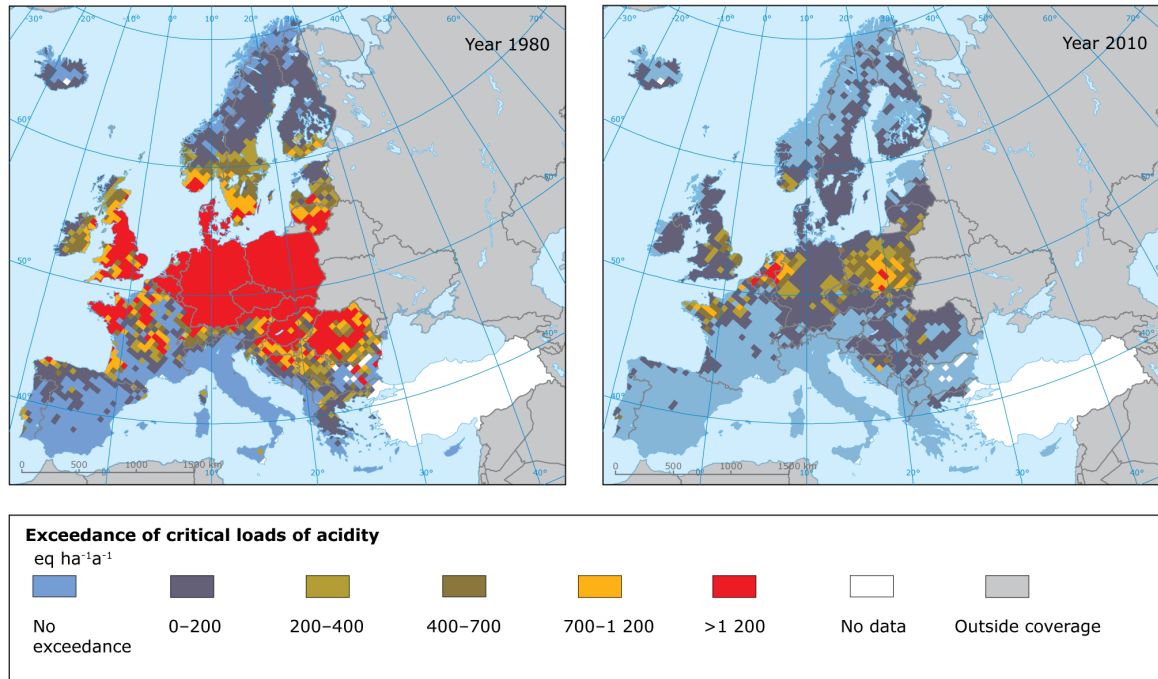
Figure 6: Maps showing the extent of change in European ecosystems which are exposed to acid deposition. The maps presents the exceedance of critical load limits for acidic cation. Source: Jones [2010] with permission.

Moore, 2006, Hongve et al., 2004, Vogt, 2003, Skjelkvåle et al., 2001a,b].

So what does this mean for P bioavailability? Al_i is a precipitating agent for phosphate in wastewater treatment plants and acts as an acute remedy for eutrophic lakes [Hsu, 1968, Auvray et al., 2006]. It is therefore possible that the decline in Al has resulted in more bioavailable P, thereby masking the effect of any abatement actions to reduce P loading to the lake. With regards to DOM, the impact is more complex and therefore more uncertain. The increase in DOM is potentially followed naturally with an increase in organic bound P. As mentioned in Sec. 1.2.1, the soil in Østfold is rich in phosphorus. With increased plant growth, due to warmer summers [Hanssen-Bauer et al., 2015], and increased DOM leaching from soil, it is highly possible that there is more organic P in the stream waters. Some of the organic P will be Low-Molecular-Weight (LMW; <1000 Da) molecules that are bioavailable to phytoplankton [Turner et al., 2002]. Furthermore, High-Molecular-Weight (HMW; >1000 Da), such as humic substances (HS), have P, which may become bioavailable in the lake through degradation processes of DOM, such as photodegradation. Furthermore, photodegradation of DOM may also render recalcitrant DOM more biodegradable, particularly important for heterotrophs. On the other hand, Al and Fe complexed with HS may become labile with HS photodegradation, and precipitate with bioavailable P. As such, the role of DOM remains far more unclear.

2   Scope of Study

The aim of this research is to get a better understanding of what role the changes in the environment over the last 30-40 years have had on the water quality of Lake Vansjø. Particular focus is directed towards the water draining from forested catchments. This is an area that is generally overlooked in regards to eutrophication, as the main source of nutrient pollution generally derives from anthropogenic activities, such as agriculture, sewage, etc. However, given that approx. 85% of the catchment draining into the lake is from forested areas, it cannot be overlooked how changes in these environments may have influenced the lake water chemistry. Furthermore, a large number of infrastructural changes and abatement actions have been taken to reduce nutrient loading from sewage and agricultural practices. Yet, little or less than expected improvements in lake water quality had been observed, which was incentive enough to explore elsewhere and thereby get a more complete understanding of the catchment as a whole.

The synopsis of the research presented in this thesis takes a biogeochemical perspective of the problem, looking particularly into the role of DOM and P fractions in the aquatic environment. The papers explore chemical processes utilising a variety of scientific techniques:

Paper I assesses the use of Diffusive Gradients in Thin films (DGT) as passive samplers for dissolved P fractions. The paper explores different models to estimate diffusion coefficients of organic P molecules, in order to determine the time-weighted average (TWA) concentration of the low-molecular-weight organic P fraction (LMWOP < 1000 Da). Furthermore it assess the molecular weight range of the organic P molecules sampled.

Paper II explores how photodegradation of DOM influences the biodegradation of DOM and the transformation of humic substances (HS). The idea is to simulate the processes that are occurring in Lake Vansjø, and thereby assess the impact the rise in DOM concentration may have. The study utilises a variety spectroscopic techniques, multivariate statistics, and speciation modelling, in order to assess physicochemical changes to DOM.

Paper III assesses how the mixing of forest and agricultural water, currently (technically 2015) and back in the 1980's, affected the bioavailability of P. The study looks into how mixing at different ratios affect the chemical speciation. The mixing is conducted both theoretically and experimentally and utilises a variety of physicochemical analysis methods.

3 Materials and Methods

3.1 Sampling Sites

The Morsa or Vansjø-Hobøl Catchment and Lake Vansjø, located in SE Norway (59.4°N 10.8°E), are the study areas which are the focus of the EUTROPIA project. The catchment and the lake are approx. 690 km² and 36 km², respectively. Predominantly 85% and 15% of the land-use, which is draining into the lake, are forest (including bog) and agriculture (Fig. 7). Approx. 90% of the catchment is below the marine limit [Skarbøvik et al., 2011]. This study mainly focuses on the stream water from two subcatchments within the Morsa Catchment, *Dalen* and *Støa*, located at close proximity to the lake. *Dalen* (area = 0.88 km²) and *Støa* (area = 0.16 km²) are pure forest and agriculture subcatchments, respectively. They are chosen specifically, because they are not mixed and thereby can represent the 85% and 15% land-use water draining into the lake.
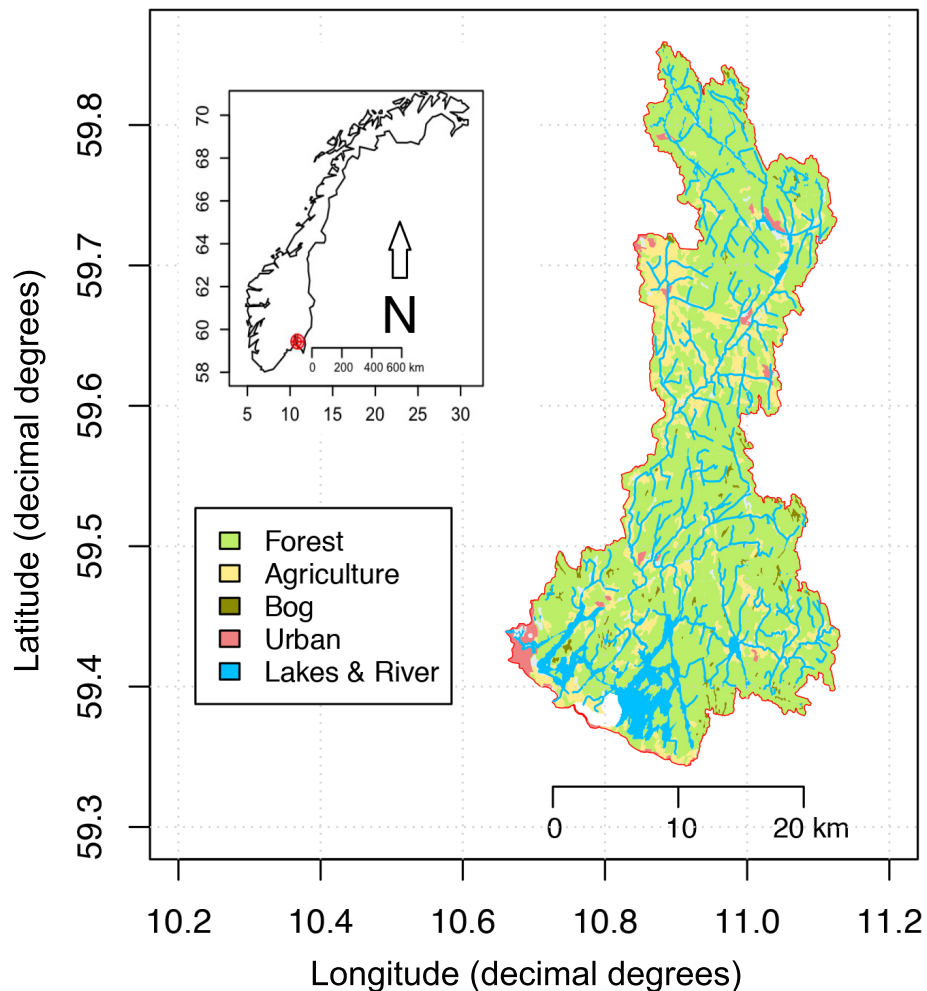
Figure 7: Land-use map of Morsa Catchment. Lake Vansjø is located in the southern part of the catchment. Source: Data from Norges vassdrags- og energidirektorats (NVE) [2016] and Kartverket [2016].

Paper I also studies the stream water from one mixed subcatchment, *Huggenes* (approx. 32% forest, 59% agriculture and 9% other land-use), and lake water from *Grepperødfjorden*, a small sub-basin part of Lake Vansjø (Fig. 8). **Paper II**, only studies the water from *Dalen*, since the focus is on DOM from forested areas, which predominantly is where the DOM in the lake originates from.

Table 1: Morphometrics of Lake Vansjø's two major basins [Bjørndalen et al., 2007].

	Storefjorden	Vanemfjorden
Surface area (km^2)	23.8	12
Average depth (m)	9.2	3.7
Greatest depth (m)	41	17
Theoretical Water Residence Time (years)	0.85	0.21
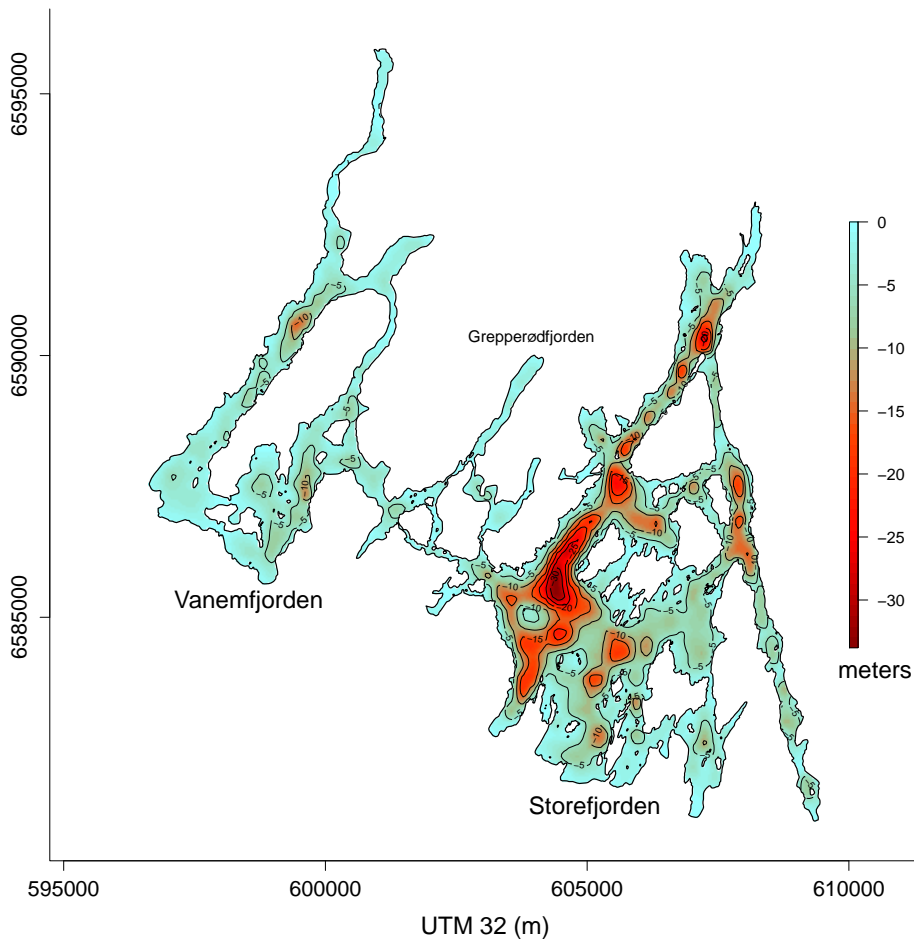
Figure 8: Lake Vansjø Morphology: The lake consist of many basins divided by narrow passages. It is however usually divided into two main basins, *Vanemfjorden* the shallow western basin and *Storefjorden* the larger and deeper eastern basin [Bjørndalen et al., 2007]. Source: Data courtesy of Tuomo M. Saloranta, Tom Andersen and Norges vassdrags- og energidirektorats (NVE) [2016].

3.2   Passive Sampling of P fractions with Diffusive Gradients in Thin films (Paper I)

Paper I, deals with the development of using Diffusive Gradients in Thin films for simultaneous determination of two P fractions in the aquatic environment: Orthophosphate (sum of H_3PO_4, $H_2PO_4^-$, HPO_4^{2-} and PO_4^{3-}) and Low-Molecular-Weight Organic Phosphorus (LMWOP). The three main advantage of using DGTs over conventional grab sample techniques is; A) you get a TWA concentration for a given period; B) because the DGTs accumulate the species over time you can measure below the limit of detection (LOD) of conventional methods; C) you separate species from the solution matrix, thereby reducing interference during chemical analysis (see more on this topic in Sec. 3.5)

Utilising DGTs, for determining the concentration of a specie in the aquatic environment, requires the diffusion coefficient (D) of that specie. The approach is therefore to first determine D for orthophosphate and for LMWOP molecules under laboratory conditions. Orthophosphate D was previously determined by Zhang et al. [1998]. For the LMWOP fraction, two common LMWOP molecules, adenosine monophosphate (AMP) and inositol hexaphosphate (IP6) were chosen and had their D determined. DGT application relies on the principles of Fick's first law for steady-state diffusion in dilute solutions [Cussler, 2009]. For DGTs the diffusive flux (J) of the species into the DGT can be calculated by Eq. 1,

$$J = \frac{m}{t} = AD\frac{c}{x} \tag{1}$$

where m is total mass of the specie collected on the adsorbent, t is the time accumulating the specie, A is the area of the DGT "window" exposed to the solution, D is the diffusion coefficient, c is the concentration of the specie in the solution, and x is the thickness of the membrane (Δg) and the diffusive boundary layer (DBL, δ) combined (Fig. 9). Under laboratory conditions the concentration, c, of the LMWOP molecule in question, is known. The time of sampling, t, is recorded, and the mass of the species, m, is determined in accordance with the P analysis method (Sec. 3.5). By rearranging Eq. 1 D for the LMWOP molecules can solved.

When the DGTs are used in the aquatic environment, c is unknown, and Eq. 1 is rearranged to solve for c. It is however more complicated solving c for the LMWOP fraction as the analytical method for P fractionation (Sec. 3.5) cannot differentiate between different LMWOP molecules. In **Paper I**, an assessment of the diffusion coefficient range for LMWOP molecules was conducted, by theoretically calculating the free diffusion coefficient for different LMWOP molecules using various models, calculating the diffusive membrane restriction on the molecules, estimating a potential molecular weight cut-off
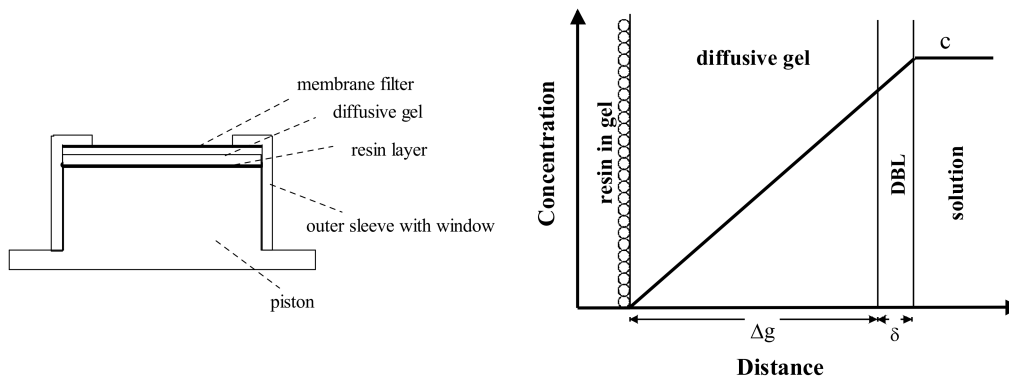
Figure 9: Left: Schematic design of DGT. Right: Diffusive passive sampling concept, where $x = \Delta g + \delta$. Source: Adapted from Zhang [2005].

(i.e. molecule collected on adsorbent over a certain weight are negligible), and calibrating the LMWOP fraction D for a particular stream.

All phosphates undergo proton dissociation with changing pH. As such, the distribution of phosphates change with pH, and D in turn needs to account for the distribution of the phosphate species. Additionally temperature is important to consider as it also influences the diffusion coefficients, due to the change in the viscosity of water and the energy of the species. **Paper I** addresses both these topics and how they should be corrected for in field application.

3.3 Photo- and Biodegradation of Dissolved Organic Matter (Paper II)

Paper II investigates how photodegradation changes the physicochemical properties of DOM, and how these changes influence the biodegradation that follows. Stream water from the forested catchment, *Dalen*, was used as the DOM source in this study for the photo- and biodegradation studies. Additionally thoroughly characterised reference material powder of natural organic matter, from different stream and lake water sites in Scandinavia, were used to help in the assessment of how the degradation influences changes in physicochemical properties.

Prior to the photo- and biodegradation experiments, all the raw stream water used was filtered using sterile 0.2 μm cellulose acetate filter membranes. This removes microorganisms, hindering any further biodegrdation of the DOM sample prior to the experiments. It also removes the particulate organic matter fraction, allowing the study to focus solely on the DOM fraction.

Photodegradation of the DOM samples was done by irradiating the sample in increments for 0 to 20 hours with artificial sunlight (Q-SUN® Xe-1 Xenon Test Chamber). The irradiated samples were then followed up by biodegradation, where the samples were incubated in sealed jars at room temperature in the dark for 25 days with inoculum native

to the stream. A small vial containing 1M NaOH solution was placed in the jars on a floating mat. The NaOH solution acts as a CO_2 trap, capturing the emitted CO_2 from microbial respiration as CO_3^{2-}. The vials were taken out after 13 days and replaced for the remaining 12 days. The vials were measured for CO_2 (Sec. 3.5.6). Unfortunately the amount of CO_2 captured between the 13th and 25th was below the limit of detection (LOD), and therefore excluded. The solutions for all degradation combinations are analysed for pH, conductivity, DOC, UV-Visible absorption spectroscopy (UV-Vis) and fluorescence excitation-emission matrix (EEM) spectroscopy (Table 2).

Table 2: Brief overview of the photo- and biodegradation experimental setup.

		Irradiation Time						
		0 h	1 h	4 h	8h	12 h	16 h	20 h
Incubation with Inoculum	0 days	pH, conductivity, DOC, UV-Vis, EEM						
	13 days	CO_2						
	25 days	pH, conductivity, DOC, UV-Vis, EEM						

3.4 Aquatic Speciation Analysis from Mixing Water (Paper III)

Paper III studies the water chemistry, from mixing of forest and agricultural stream water, both experimentally and theoretically.

Water was collected from the forest and agriculture catchment streams, *Dalen* and *Støa* respectively, and mixed at different ratios (Fig. 10).
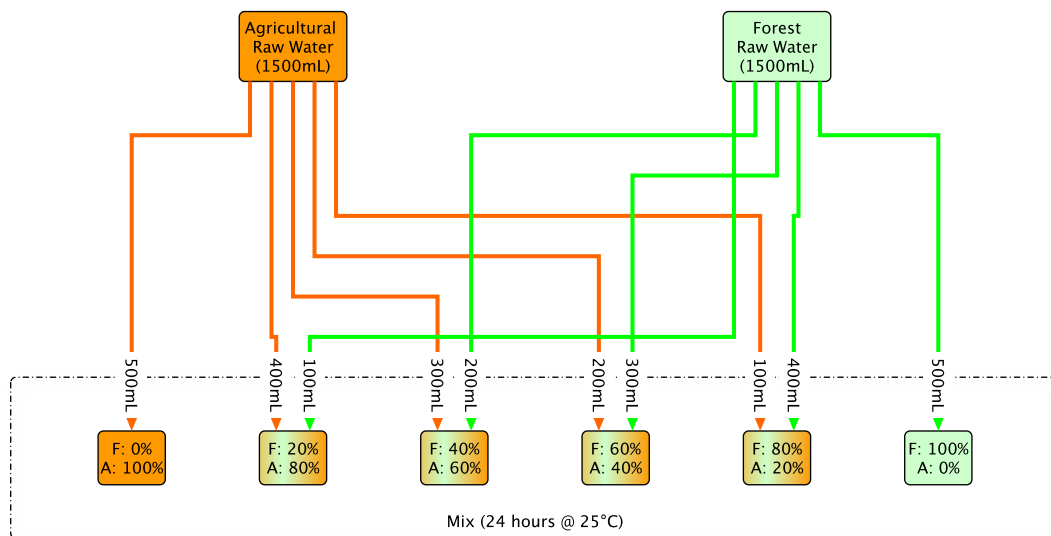
Figure 10: Schematic diagram of the experimental mixing of forest and agriculture stream water.

The mixing experiment was conducted both for the current water chemistry and for a 1980's water chemistry. Only the forest water chemistry is expected to have changed from the 1980's, in which DOC and Al_i was half and three times the concentration, respectively, of what it is today. The 1980's forest water chemistry was achieved by diluting the forest water with deionised water and spiking the solution with $KAl(SO_4)_2 \cdot 10\,H_2O$. The solutions were analysed for particulate matter (PM), major and trace cations, major anions, alkalinity, DOC, and dissolved reactive phosphorus (DRP)/orthophosphate. In addition the PM is analysed by scanning electron microscopy (SEM) and Energy-dispersive X-ray spectroscopy (EDX) (see Fig 11 and Sec. 3.5).

Theoretical mixing was done by simulating the mixes with the geochemical speciation software PHREEQC [Parkhurst and Appelo, 2013] with the humic ion binding model [Tipping et al., 2011] included (Sec. 3.6.3). Unlike the experimental mixing, the theoretical simulations only account for the mixing of dissolved solutes. The water chemistry of dissolved solutes is taken from the analytical measurements of pure forest and agriculture solutions for 2015 and the 1980's.

Figure 11: Schematic diagram of sample physicochemical analyses for the mixing experiment.

3.5   Physicochemical Analysis Methods

3.5.1   Conductivity and pH

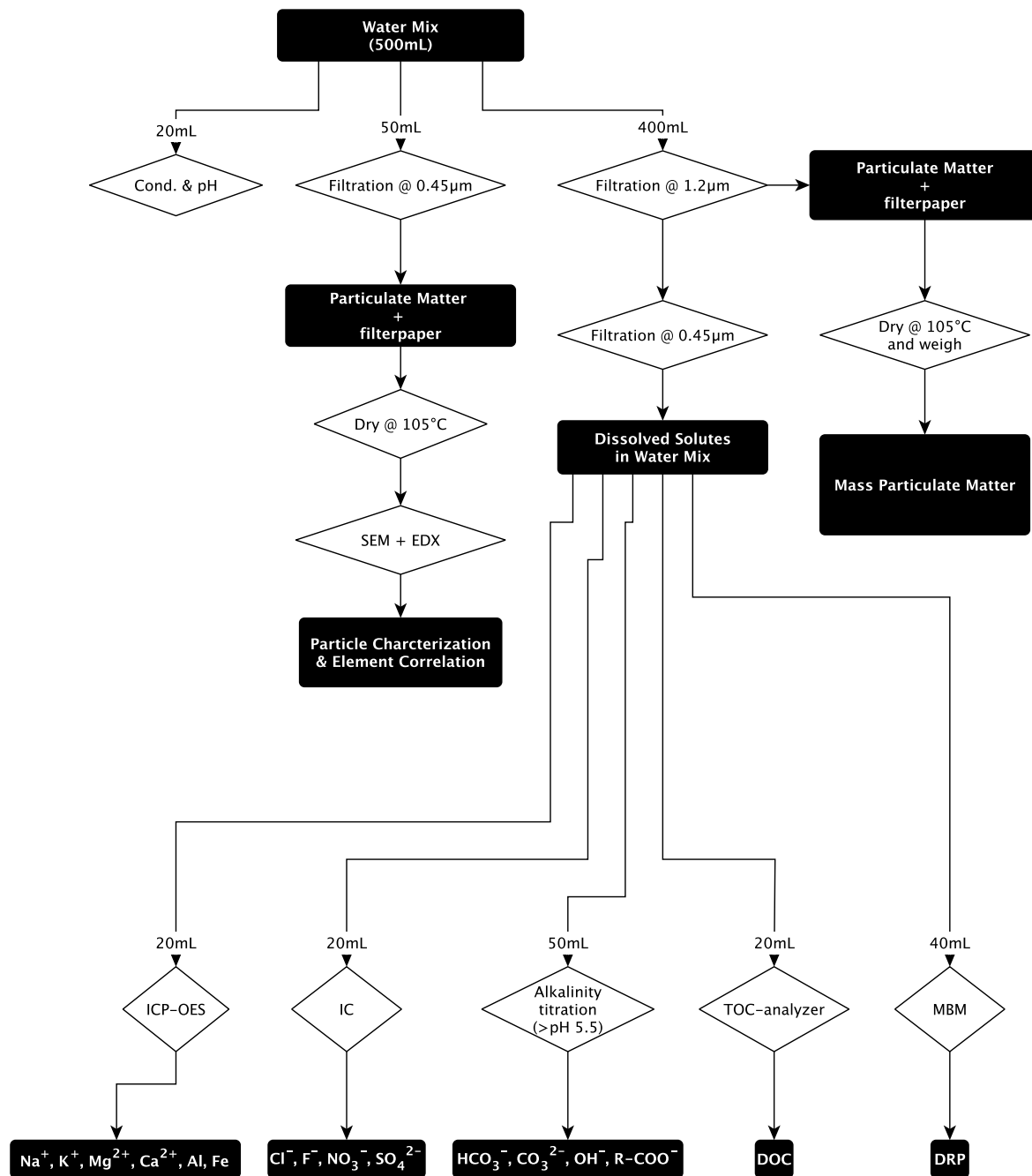In all papers, measurement of conductivity and pH are performed for all the samples. Both measurements are generally conducted on the raw sample. The exception is in **Paper II**, where the samples are pre-filtered with 0.2 μm CA filter membranes, before any analysis is conducted.

Conductivity was measured with a FiveGoTM (FG3) hand held operating device from METTLER-TOLEDO Inc. pH was measured using an 8102 ROSS® Combination pH Electrode combined with an Orion Research Expandable ionAnalyzer EA920 from Thermo Fisher Scientific Inc.

3.5.2   P fractionation

Only the studies in **Paper I** and **III** present measurements for P in the samples. Originally this was attempted also in the DOM photodegradation study (**Paper II**), where the idea was to assess the bioavailability of P with DOM photodegradation. However, P concentrations were found below the limit of quantification (LOQ) or below LOD such that further pursuit of answering P bioavailability was dropped.

P fractionation, presented in Fig. 12, mainly results in four P fractions; total reactive P (TRP), total P (TP), dissolved reactive phosphorus (DRP) and total dissolved P (TDP). All of these P fractions are traditionally measured using the wet chemical spectrophotometric molybdenum blue method (MBM) developed by Murphy and Riley [1962]. The method is selective for orthophosphate, and it is the inclusion and exclusion of the pretreatments, filtration and digestion, that define the four P fractions.

DRP, in which filtration is first conducted followed by MBM, is approx. equal to the concentration of orthophosphate. Even though the method is selective for orthophosphate, the reagents used are highly acidic and reducing, which changes the natural equilibrium in the sample, thereby likely resulting in overestimation of orthophosphate [Rigler, 1973]. For this reason, DRP is a more correct term for the fraction. It is this fraction which is considered bioavailable.

The TDP fraction has filtration followed by digestion before MBM. Traditionally potassium persulphate ($K_2SO_4O_8$) autoclave digestion is used [Jeffres et al., 1979]. This converts all the dissolved P compound into orthophosphate, thereby allowing for it to be measured by MBM. It is generally assumed that the fraction of TDP, which is not measured by DRP, is the dissolved organic phosphorus fraction (DOP $\approx$ TDP $-$ DRP). However, condensed inorganic phosphates and phosphonates are also expected to be found under the same fraction, despite generally being found at far lower concentrations. The LMWOP is the fraction of DOP <1000 Da, and is generally considered to be bioavailable.
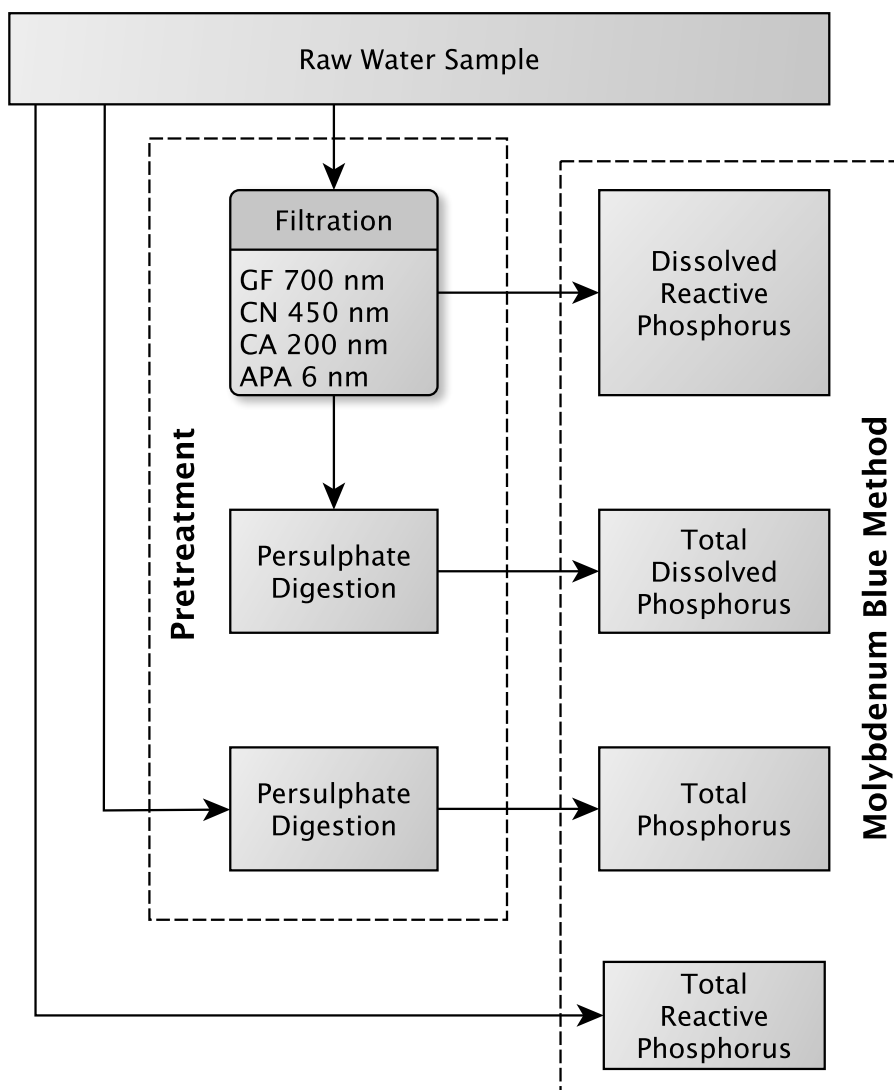
Figure 12: Schematic diagram of P fractionation. GF = glass microfibre, CN = cellulose nitrate, CA = cellulose acetate, and APA = agarose polyacrylamide.

There is also expected to be discrepancies among dissolved fractions depending on filtration cut-off size. In **Paper I**, grab samples are filtered by 0.7 μm glass microfibre filter membranes (Whatman®, Grade GF/F), and passive sampling by DGTs have an agarose polyacrylamide (APA) diffusive gel with a cut-off of $\approx$6 nm. There is therefore expected some discrepancy in the dissolved fraction, as even colloidal particles and bacteria can be found below 0.7 μm in size. **Paper III** uses 0.45 μm filter membranes (Sartorius AG cellulose nitrate Ø47 mm). The 0.45 μm cut-off is generally considered to be the operationally defined separation size between particulate and dissolved matter. Again here there exists colloidal particles and bacteria below this value.

In **Paper I**, the DRP and TDP measurements for both grab samples and DGT extracts, were determined using a customized continuous flow auto-analyser (SKALAR San++ Automated Wet Chemistry Analyser). **Paper III** follows the more traditional

MBM in accordance with ISO 6878 [2004]. However, for **Paper III** measurements of TDP were omitted due to technical issues.

TP and TRP are two fraction not included in these studies, but are worth mentioning as they were initially measured during the EUTROPIA monitoring program. TP differs from TDP in that it includes the particulate P fraction ($PP \approx TP - TDP$). TRP represent the total labile phosphate; i.e. in addition to the free labile orthophosphate ($\approx$DRP), orthophosphate loosely bound to particulate matter may become labile after the addition of the MBM reagents. These two fractions were eventually dropped by the EUTROPIA monitoring program as the continuous flow auto-analyser system ran into complications due to the particulate matter.

3.5.3 UV-Visible Absorption Spectrophotometry

Absorbency spectrum from 200 - 700 nm was recorded for the samples presented in **Paper II**. The spectrophotometer was a Shimadzu UV-1800 fitted with a 10 mm quartz cell.

3.5.4 Fluorescence Excitation-Emission Matrix analysis

In **Paper II** fluorescence EEM spectrums were captured at 200 - 450 nm (10 nm intervals) and 300 - 600 nm (1 nm intervals), for excitation and emission respectively, using a Varian Cary Eclipse Fluorospectrometer with a 10×10 mm quartz cell.

EEMs are particularly interesting, because the two dissolved humic substances (HS), fulvic acid (FA) and humic acid (HA), have peaks in separate regions of the spectrum matrix (Fig. 13). By analysing the change in the FA and HA peak intensities, it is possible to assess the transformation DOM undergoes during photo- and biodegradation.

3.5.5 Dissolved Organic Carbon

DOC was determined by analysis of non-purgeable organic carbon (NPOC) after filtration. NPOC is the measurement of organic carbon as CO_2, in which the DOC in the samples undergoes combustion at 700 - 800 °C after the sample has been first acidified with HCl and purged with CO_2 free air. The acidification removes all carbonate and bicarbonate, and the gassing purges the sample free of CO_2. The process may also result in the loss of volatile organic carbons. This is however assumed to be a fairly small fraction of the DOC.

Paper I samples are filtered using 0.7 μm membrane filters (Whatman®, Grade GF/F Ø47 mm) and analysed on the Shimadzu TOC-5000A Total Organic Carbon Analyzer. **Paper II** samples are filtered using 0.2 μm membrane filters (Sartorius AG sterile cellulose acetate Ø47 mm) and analysed on the Shimadzu TOC-V$_{CPH}$ Total Organic Carbon Analyzer. **Paper III** samples are filtered using 0.45 μm membrane filters (Sartorius

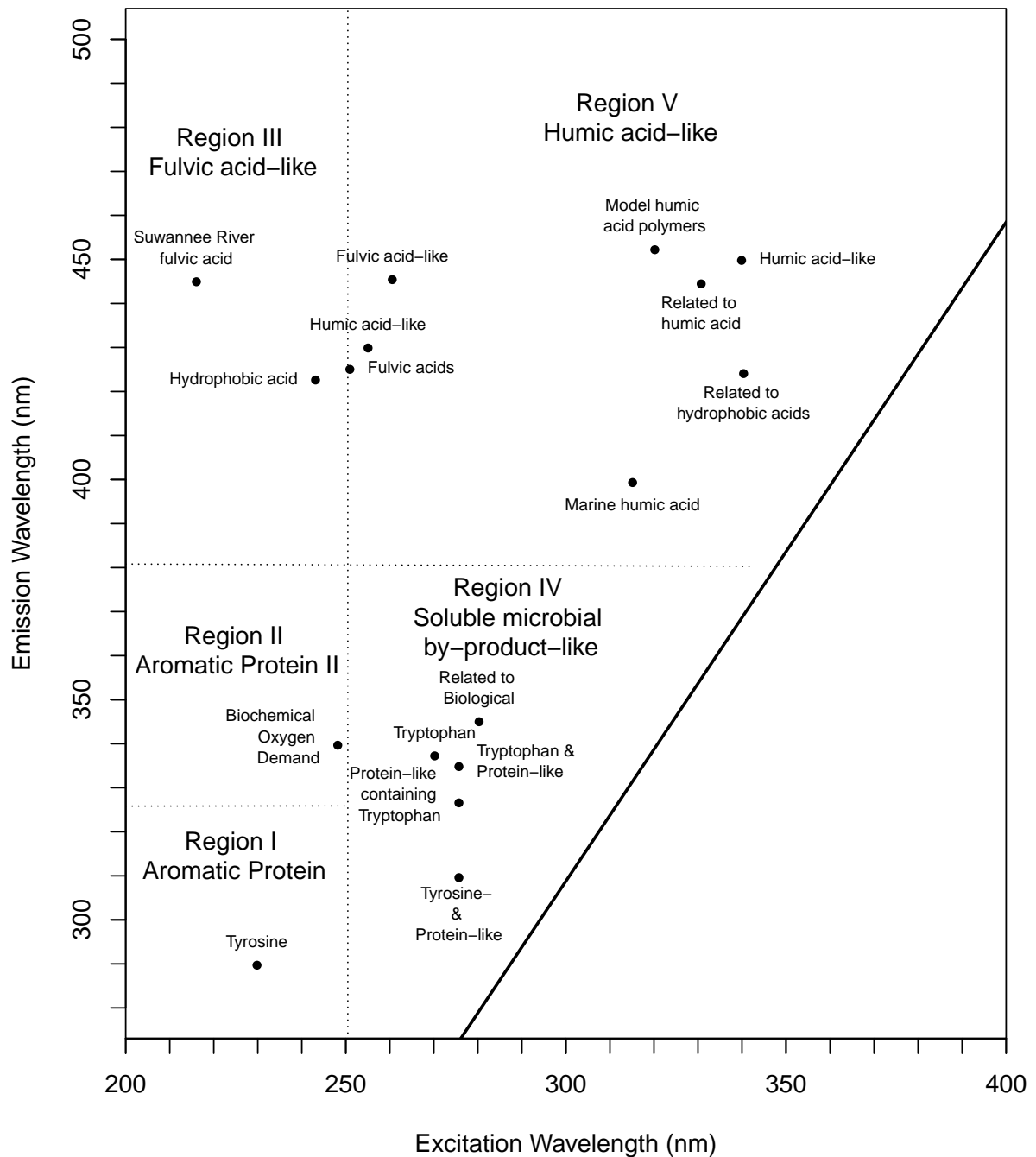AG cellulose nitrate Ø47 mm) and analysed on the Shimadzu TOC-V$_{CPH}$ Total Organic Carbon Analyzer.

Figure 13: Location of Excitation-Emission Matrix peaks for different water samples from literature. The peaks are found in different regions of the spectrum representing different types of organic matter. Source: Adapted from Chen et al. [2003].

3.5.6 CO_2 measurements

In **Paper II** respiration analysis from the biodegradation experiment was conducted by measuring captured CO_2 (Sec. 3.3). An automated customised set-up is used in which a peristaltic pump draws the NaOH solution from the vial to a reaction chamber, adding 1 M H_2SO_4. This reacts with CO_3^{2-} releasing the CO_2. The CO_2 is then carried with Argon gas to a 14 cm flowcell and measured by infrared absorbency using a LI-820 CO_2 Gas Analyzer (LI-COR$^®$). Before reaching the detector, the gas is led through a H_2O trap, containing anhydrous $MgSO_4$, thereby reducing the spectral interference of water.

3.5.7 Total Dissolved Elements / Cations

The total dissolved concentration of the elements Na, K, Mg, Ca, Al and Fe were determined for sample(s) presented in **Paper II** and **III**. In **Paper II** only the non-irradiated and non-incubated sample had the elements determined. The purpose of the element analysis was to theoretically assess the changes to Fe and Al species with photo- and biodegradation. For **Paper III** speciation analysis is a fundamental part of the study, and so every sample is analysed. Element determination was conducted by inductively coupled plasma optical emission spectroscopy (ICP-OES; Varian Vista AX CCD simultaneous axial view), after filtration (0.2 and 0.45 μm for **Paper II** and **III**, respectively) and acidification. The samples were acidified with 1% (v/v) 32.5% (m/v) HNO_3 with 50000 ppm Cs. The Cs acts as an ion suppressor in the plasma; reducing the element ionisation, thereby increasing the intensity of the atomic optical emission lines (particularly Na and K).

3.5.8 Major Anions

The concentration of the major anions were determined by ion chromatography (IC), for both **Paper II** and **III**, using a Dionex ICS-2000. However, in **Paper II** determination of anions was not conducted for the samples undergoing photo- and biodegradation. Instead measured median values acquired by the EUTROPIA monitoring program, for the same stream, were used.

3.5.9 Particulate Matter

The concentration particulate matter (PM) mass was determined only for **Paper III**. Determination of PM mass concentration was done by filtrating raw samples through 1.2 μm glass fibre filter membranes (Whatman$^®$ Grade GF/C Ø47 mm). The filter membranes with particles are dried at 105°C for 6 hours, then placed in desiccator for 24 hours and then weighed. The PM mass concentration is determined by taking the difference in weight of the filter membrane before and after filtration, divided by the

filtered volume. PM was also collected on 0.45 μm filter membranes for characterisation (Sec. 3.5.10).

3.5.10 Scanning Electron Microscopy and Energy-Dispersive X-ray Spectroscopy

In **Paper III** the Field Emission Gun Scanning Electron Microscope (FEG-SEM; FEI Quanta 200) equipped with an Energy Dispersive X-ray Spectrometer (EDX; EDAX Pegasus 2200) operating in low vacuum (60-80 Pa) were utilised to study the PM collected on the 0.45 μm filter membrane. EDX element map images were converted from a matrix of pixels to a vector of pixels, allowing for linear regression correlation between the vectors. The method allows for identification of correlation between the elements on the membrane filter.

3.6 Computation, Statistical Methods, and Visualisation

All statistical methods, calculations and visualisation of the data were conducted using the statistical computing language R [R Core Team, 2015]. The utilisation of script based programming language, such as R, made it possible to solve highly complicated and tedious calculations efficiently. The large number of packages available for R made it a powerful tool for advanced statistical analysis and visualisation.

3.6.1 The Wilcoxon rank-sum test

In **Paper I** comparison of P fractions from grab samples and the DGTs was done by using the Wilcoxon rank-sum statistical test (also known as the Mann-Whitney U test). The test is a nonparametric test for the null hypothesis of two sample groups originating from the same population. The main advantage of the Wilcoxon test is its efficiency and robustness in comparing populations, which are not necessarily normally distributed and vary in the number of observations, i.e. non-paired test. Since the DGTs are TWA measurements and the grab samples are momentary measurements, the two sampling methods cannot be paired and have skewed distributions.

The Wilcoxon rank-sum statistical test was also used in reverse, in which DGT diffusion coefficients (D_{DGT}) for the LMWOP were calibrated by comparing the grab sample DOP concentrations with the DGT-LMWOP concentrations for different D_{DGT}, in search of the"best match"/"best fit".

3.6.2 Multivariate Statistics

In **Paper II** multivariate statistical analysis techniques principal component analysis (PCA), corrgrams, and hierarchical clustering on principal components (HCPC) were used to compare the physicochemical properties of the reference DOM samples with FA and HA EEM peaks (Sec. 3.3 and 3.5.4).

PCA is a multivariate statistical technique used to correlate multiple variables with each other while at the same time reducing the dimensionality, thereby making a simplified visualisation of the relationship between variables.

Many of the physicochemical properties, in this study, are assessed from nuclear magnetic resonance (NMR) and Fourier transform infrared (FTIR) spectroscopy. Regions of the spectra are related to chemical bonds / functional groups. However, due to much overlap between the spectra regions and the chemical properties, visualisation by corrgrams are mainly used to identify which spectra regions can be combined to reduce the number of variables.

Finally HCPC is used to cluster the DOM samples with similar physicochemical properties and determine what physicochemical properties makes the clusters unique from each other.

Overall these multivariate statistical analysis techniques help in the assessment of identifying the physicochemical transformations of DOM with photo- and biodegradation.

3.6.3 PHREEQC

Both **Paper II** and **III** use the software PHREEQC for chemical speciation analysis. PHREEQC is a computer program developed for geochemical studies with particular focus on groundwater chemistry. The software uses different databases, with thermodynamic data for chemical reactions, in order to calculate the distribution of species in solutions [Parkhurst and Appelo, 2013].

In **Paper II** the software was used to theoretically assess the speciation and precipitation of Al and Fe with changing pH due to DOM photodegradation. In **Paper III** the software was used far more extensively, calculating the chemical speciation distribution and precipitation for the mixing of forest and agricultural water at different ratios, both for 2015 and 1980's conditions. Additionally in **Paper III** the highly complex Humic Ion-Binding Model VII, developed by Tipping et al. [2011], was incorporated into the PHREEQC Minteq (version.4) thermodynamic database in order to calculate the binding of metal ions to humic and fulvic acid. In **Paper II** the humic ion-binding model is not as advanced, and uses a simplified thermodynamic database by Ball and Nordstrom [1991], in which humic and fulvic acid perform bidentate metal ion-binding based on thermodynamic data for oxalic acid.

4 Results and Discussions

4.1 Passive Sampling of P fractions with Diffusive Gradients in Thin films (Paper I)

The major findings of **Paper I** showed that DGTs are suitable for passively sampling both DRP and LMWOP, and thus two bioavailable P fractions. The study indicated that $\ll 25\%$ of the DOP collected by the DGT, is likely to be HMWOP. Despite the fact that the two largest fractions of DOP *in situ* are found to be associate with molecular weight (Mw) <1000 and >10000 Da [Ged and Boyer, 2013], DGT uptake, i.e D_{DGT}, declines with increasing molecular size. This is because the free diffusion coefficient in water ($D_{\mathrm{H_2O}}$) and membrane resistance from the APA diffusive gel, decreases and increases, respectively, with molecular size (Fig. 14).

The models tested to determine D_{DGT} for LMWOP molecules from molecular size and mass are still in their infancy and require more experimental data for further development. The development of these models could prove very useful in the future, should there be a need to determine the concentration of specific LMWOP molecule.

The application of the DGTs in the field study for streams provided a fairly good match between P fractions for the DGT and the grab samples (The Wilcoxon rank-sum test found no significant difference; $p > 0.05$). D_{DGT} of AMP and IP6 seem to be good estimates for the maximum and minimum D_{DGT} range, since the DOP concentration from the grab samples fall between the determined upper and lower estimated DGT-LMWOP concentration. However, upper and lower LMWOP concentration estimates are impractical. Especially the upper limit, as the LMWOP fraction concentration cannot be higher than the DOP concentration. For this reason, a practical compromise was found by determining a "best fit" D_{DGT} for each study site that results in the least significant difference between the DGT and grab samples. By sweeping through different D_{DGT} a maximum p-value can be found (Fig. 15).
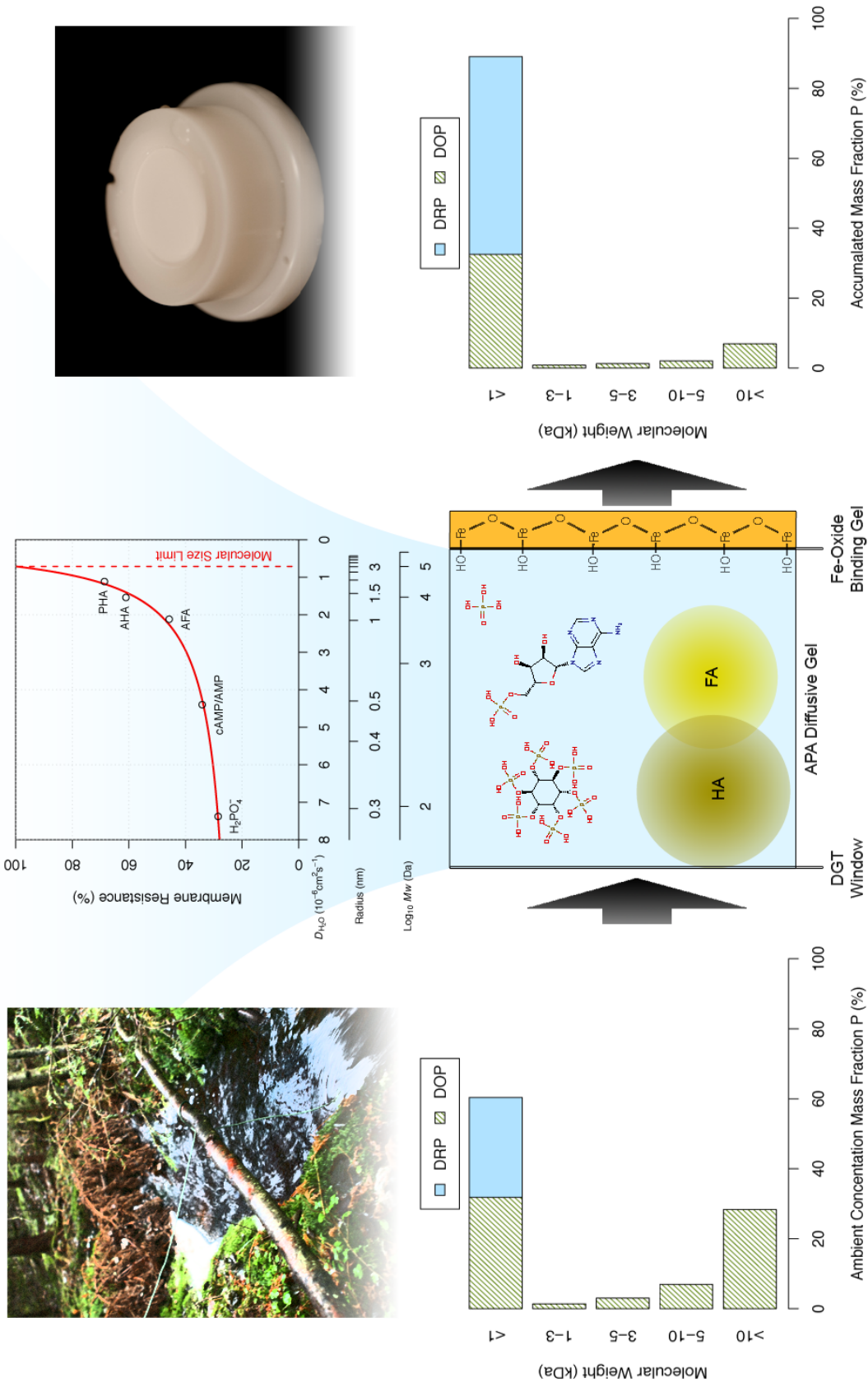
Figure 14: Concept illustration of DGT size-exclution of dissolved P fractions (cAMP/AMP = cyclic adenosinemonophosphate/adenosinemonophosphate; AFA = aquatic fulvic acid; AHA = aquatic humic acid; PHA = peat humc acid).
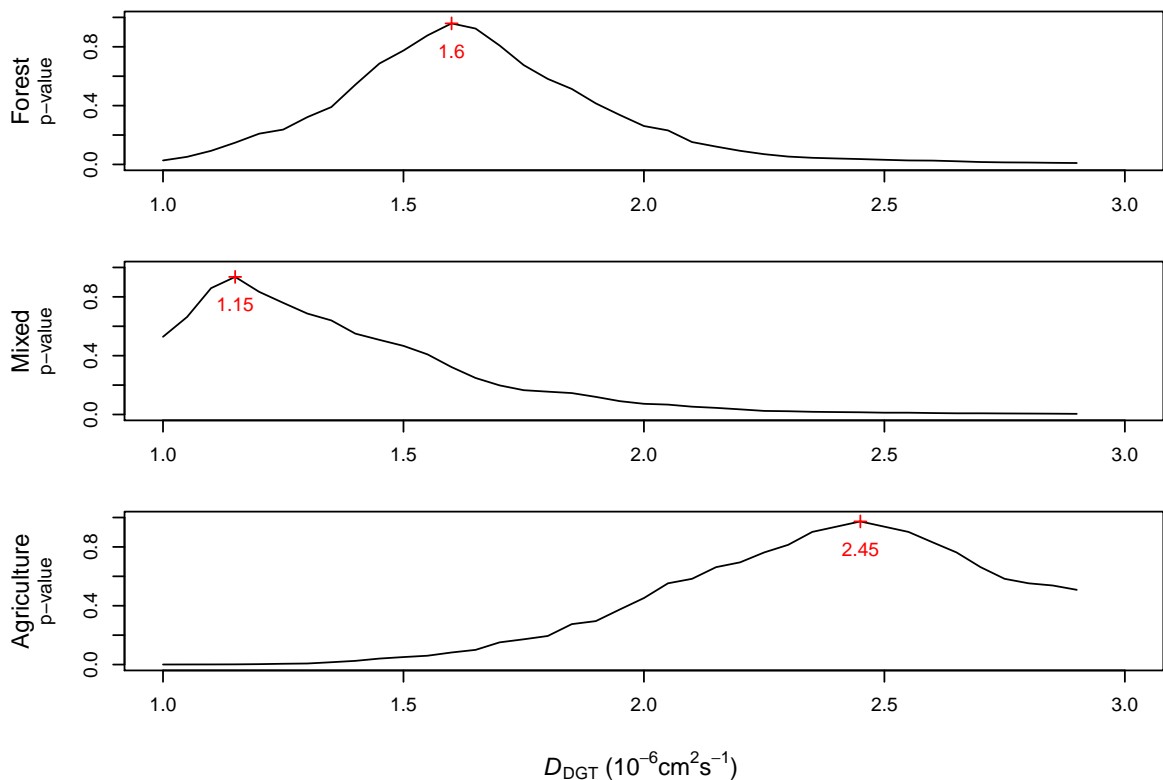
Figure 15: Wilcoxon-rank-sum sweep test: By changing D_{DGT} for the LMWOP/DOP fraction, the"best fit" between the DGT and grab sample DOP concentration can be determined.

The DGT lake study at *Grepperødfjorden* provided insight into lake P cycling, not easily achieved, or overlooked, by grab sampling techniques. The DGTs suggested that the highest concentration of LMWOP/DOP and DRP are found near the surface. The DGT-DRP was so high it closely matches the concentration found for the stream from the mixed catchment (Table 3). It was postulated in **Paper I**, that this may be indication of photodegradation of DOP (i.e fragmentation of HMWOP into LMWOP and DRP) and/or phytoplankton death due to damaging UV radiation. In the forest stream more LMWOP can be found than DRP. Considering that there has been a doubling in the concentration of DOM over the last 30 years, could also mean that there has been an equivalent increase in LMWOP. This may have had a significant impact on P cycling, resulting in more eutrophication.

Table 3: Summary of P fraction concentrations from DGT field study.

Sampling Site	Stat.	DRP-water (μg P L^{-1})	DRP-DGT (μg P L^{-1})	DOP-water (μg P L^{-1})	LMWOP-DGT (μg P L^{-1})
Forest	mean	3.2	2.1	6.1	$\geq$2.7
	median	1.7	2.0	4.6	$\geq$2.6
Mixed	mean	12.3	14.4	8.1	$\geq$4.0
	median	9.0	13.5	7.4	$\geq$2.8
Agriculture	mean	79.1	48.6	14.9	$\geq$11.5
	median	68.8	44.7	13.1	$\geq$10.8
Lake ($\sim$0 m)	mean	-	11.4	-	$\geq$3.2
	median	-	7.7	-	$\geq$3.2
Lake (2.5 m)	mean	13.2	2.8	1.9	$\geq$1.8
	median	-	2.0	-	$\geq$1.5
Lake (3.75 m)	mean	-	1.8	-	$\geq$1.4
	median	-	2.1	-	$\geq$1.3
Lake sediment ($\sim$4 m)	mean	-	6.9	-	$\geq$2.8
	median	-	-	-	-

4.2 Photo- and Biodegradation of Dissolved Organic Matter (Paper II)

After 20 hours of irradiating the samples with DOM, as much as 26% of the DOC was photo-mineralised. Furthermore, the photodegradation greatly enhanced the biodegradability of the remaining DOM, which enhanced the overall mineralisation rate. Irradiating the samples from 0 to 20 hours, resulted in a change from 3 to 39% bio-mineralisation of the remaining DOC, respectively. It is evident from the experiments that there is a synergistic effect between photo- and biodegradation, in which they together play a crucial role on the DOM mineralisation rates.

Analysis of the simultaneous changes in UV-Vis absorbency and DOC suggested there are fluctuations in the photodegradation rates of DOM singular and double bonds. This seems to be linked to fluctuations in direct and indirect (radicals) photodegradation. The photochemical reactions additionally caused the rise in pH. UV-Vis absorbency spectra analysis and theoretical speciation calculation with PHREEQC indicate that this resulted in the production of colloidal $Fe(OH)_3$ and $Al(OH)_3$. It can therefore be postulated whether DOM photodegradation may have a negative impact on P bioavailability, considering that $Fe(OH)_3$ and $Al(OH)_3$ are likely to co-precipitate with phosphates.

Fluorescence EEM analysis suggest that FA is a product from the photo- and biodegradation of HA, and possibly other non-humic substances. FA is a product which continuously increases with photo- and biodegradation, which suggests that it is a recalcitrant fraction resulting from HA degradation. The findings are supported by the statistical PCA

and HCPC analysis of reference material. However, the results from the multivariate analyses also reflect that the nature of DOM is fairly complex, and that spectral properties to a large degree overlap. Furthermore, considering that there is increased biodegradability of the remaining DOM after photodegradation, suggests that in addition to FA production, there is also a production of fairly labile aliphatic LWM organic matter (LMWOM) (Fig. 16).

In the natural environment the daily and seasonal cycles will likely have a substantial role in regulating the DOM degradation rate. The impact is likely to be greater in the western basin of Lake Vansjø, *Vanemfjorden*, due to the shallow water depth (average depth of 3.7 m). However, overall it is difficult to assess the impact DOM degradation has on eutrophication as there is no data on P bioavailability in this paper. However, HS contain N and P, two elements essential for microbial growth. By degrading HS, both N and P may become more bioavailable to phytoplankton. For bacteria and other heterotrophs, the rise in DOM over last 30 years, will likely be contributing to more bioavailable C. Another aspect is the decline in light attenuation due to the increasing colour of the water, brought on by the rise in DOM. This will likely force the phytoplankton to move closer to the surface in order to get enough light, which could put them at risk of becoming damaged from exposure to UV. Overall there are a large number of processes occurring together in the lake during DOM photo- and biodegradation, which illustrates the complexity of the system as a whole.
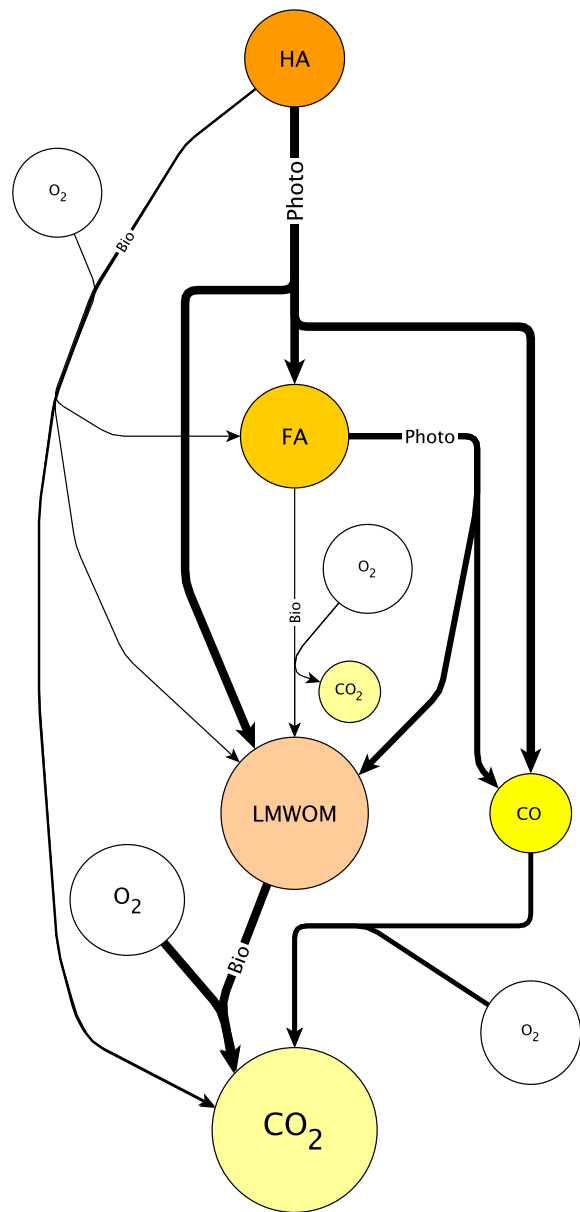

Figure 16: Conceptual diagram of humic substance degradation pathways based on findings, where major and minor pathways are indicated by the size of the arrows. (Photo = Photodegradation, Bio = Biodegradation, LMWOM = Low-Molecular-Weight Organic Matter)

4.3 Aquatic Speciation Analysis from Mixing Water (Paper III)

The theoretical and experimental results from the forest and agriculture stream water mixing study, found that there was substantially far less bioavailable P (DRP/orthophosphate) in the 1980's than in 2015 due to the environmental impacts of acid rain. The theoretical results from PHREEQC mixing indicated that precipitation of Al along with P ($Al_{1.4}PO_4(OH)_{1.2}$) would have occurred during the 1980's for a 90%/10% - 35%/65% forest / agriculture mix ratio, but not during 2015. At an 80%/20% mix ratio, >50% of the P was found to be precipitated out as $Al_{1.4}PO_4(OH)_{1.2}$.

The experimental mix results not only confirmed precipitation at that ratio, but found it to be even greater: Orthophosphate concentrations in the 1980's were found to be only $\frac{1}{5}$ of what it was in 2015.

The SEM images suggest that there is considerable flocculation of humic substanses for the 1980's 80%/20% mix, which is resulting in co-precipitation with Al and other PM (Fig. 17). EDX image correlation confirm that there is a stronger correlation between P and Al, Fe and Si for 1980's 80%/20% than any other mix (not including the pure agriculture solution).

The particular importance of the 80%/20% mix ratio finding is that the land-use distribution, in the Morsa catchment, is approx. 85% forest and 15% agriculture. It is therefore highly likely that a similar water mix ratio will be found in Lake Vansjø.
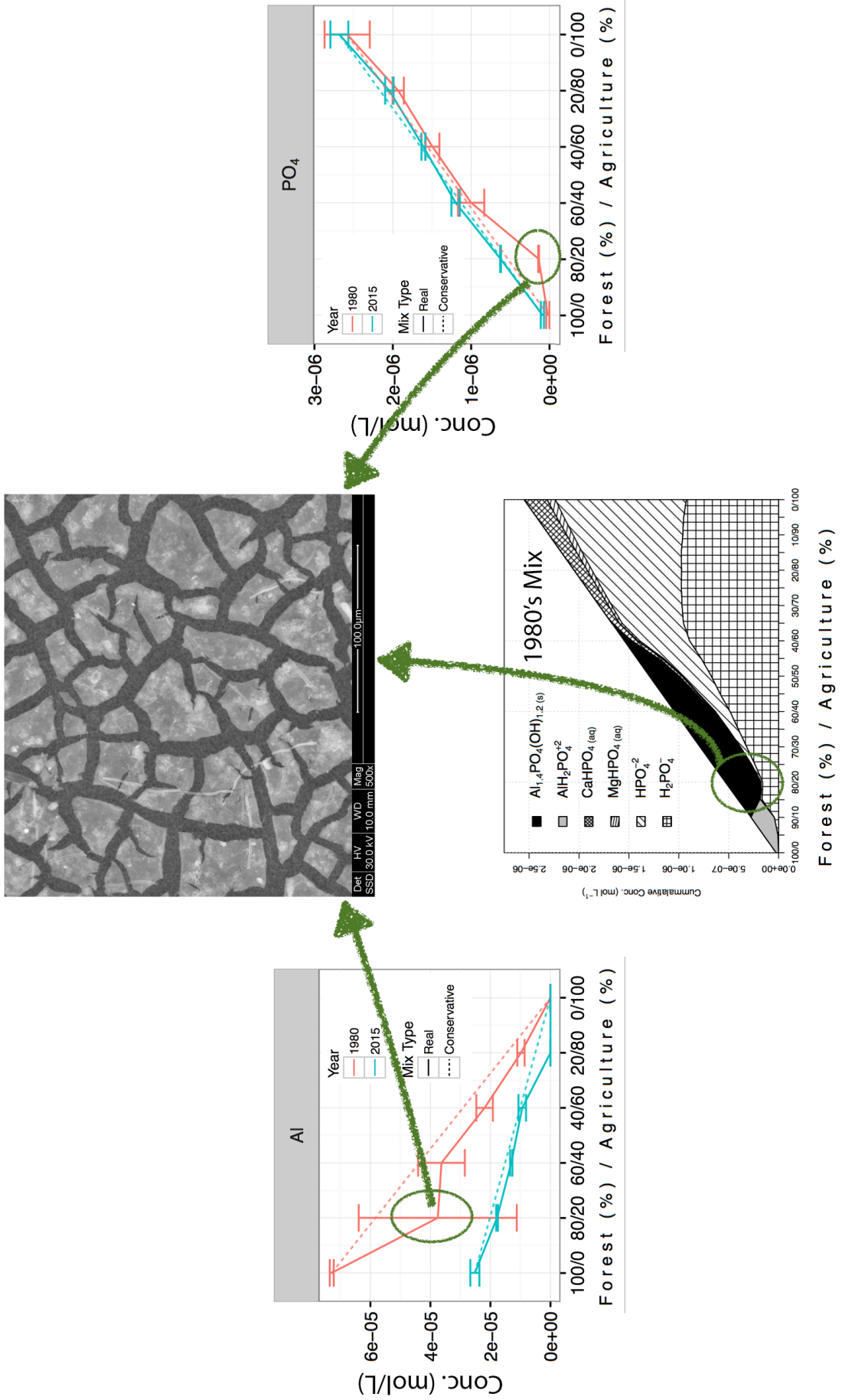
Figure 17: Summery of graphs and SEM image from **Paper III** showing the co-precipitation of Al and P for the 1980's 80%/20% mix ratio.

29

5 Conclusion

Our research looked into different aspects of DOM and P fraction processes and their impact on eutrophication at Lake Vansjø in relation to a changing environment over the last 30-40 years. **Paper III** clearly shows that acid rain in the 1980's, which contributed to considerable Al leaching from forested catchments, is highly likely to have kept the concentration of orthophosphate in the lake (and possibly all phosphates including LMWOP), substantially lower ($\approx \frac{1}{5} \times$) than today. With orthophosphate almost always being the limiting nutrient for phytoplankton growth (particularly cyanobacteria) [Schindler, 1977], there should be little doubt that eutrophication was strongly inhibited by the environmental impacts of acid rain. In other words, the reduction in acid rain over the last 30 years, has masked or countered the affects of the abatement action to reduce P runoff to the lake.

The impact the doubling in DOM concentration has had on eutrophication remains more uncertain. The findings of **Paper II** suggest that photodegradation greatly enhances the biodegradability of DOM. The increase in DOM can therefore cause a shift in the biodiversity of microbial organisms, increasing the dominance of certain bacteria. This in turn may result in more nutrients becoming available to phytoplankton, either through excretion or eventual cell death of the bacteria. The production of radicals from the DOM photodegradation, creates a high-risk environment for microorganism near the lake surface. Furthermore, because of the exponential light attenuation downward in the water column, which is further enhanced by DOM, phytoplankton attempt to get closer to the surface, where they risk death due to the harmful UV radiation and radials. The increase in DOM over the last 30 to 40 years, may in fact be shifting the water column microbial food-web cycle towards the surface. The DGT study at *Grepperødfjorden* (**Paper I**) suggests that this type of cycling may be occurring, as more bioavailable P was found near the surface of the lake than any other depth. The DGT study also suggests that there is more LMWOP than orthophosphate in the forested water. If the concentration of LMWOP has doubled, along with the rest of the DOM, then potentially the forested areas ($\approx 85\%$ of the catchment) are contributing substantially more bioavailable P to Lake Vansjø, than they were in the 1980's.

References

L. Arvola, M. Rask, J. Ruuhijärvi, T. Tulonen, J. Vuorenmaa, T. Ruoho-Airola, and J. Tulonen. Long-term patterns in pH and colour in small acidic boreal lakes of varying hydrological and landscape settings. *Biogeochemistry*, 101(1-3):269–279, jun 2010. ISSN 0168-2563. doi: 10.1007/s10533-010-9473-y. URL http://link.springer.com/10.1007/s10533-010-9473-y.

F. Auvray, E. D. van Hullebusch, V. Deluchat, and M. Baudu. Laboratory investigation of the phosphorus removal (SRP and TP) from eutrophic lake water treated with aluminium. *Water research*, 40(14):2713–9, aug 2006. ISSN 0043-1354. doi: 10.1016/j.watres.2006.04.042. URL http://www.ncbi.nlm.nih.gov/pubmed/16814358.

J. W. Ball and D. K. Nordstrom. User's Manual for Wateq4F, with Revised Thermodynamic Data Base and Test Cases for Calculating Speciation of Major, Trace, and Redox Elements in Natural Waters. Technical Report 80225, U.S. Geological Survey, Menlo Park, California, 1991. URL http://wwwbrr.cr.usgs.gov/projects/GWC_chemtherm/pubs/wq4fdoc.pdf.

K. Bjørndalen, T. Andersen, and P.-J. Færøving. Utredninger Vansjø - Kartlegging av vannkvalitet i 2006. Technical report, Norwegian Institute for Water Research, Oslo, Norway, 2007.

A. Blankenberg, S. Turtumøygard, A. Pengerud, H. Borch, E. Skarbøvik, L. Øyegarden, M. Bechmann, N. Syversen, and N. Vagstad. Tiltaksanalyse for Morsa: "Effekter av fosforreduserende tiltak i Morsa 2000 - 2006". Technical report, Bioforsk, Jord og Miljø, Ås, Norway, 2008.

D. Q. Bowen. Last Glacial Maximum. In V. Gornitz, editor, *Encyclopedia of Paleoclimatology and Ancient Environmnets*, pages 493–495. Springer, Dordrecht, The Netherlands, 2007. ISBN 978-1-4020-5197-5.

D. J. A. Brown and K. Sadler. The Chemistry and Fishery Status of Acid Lakes in Norway and Their Relationship to European Sulphur Emissions. *The Journal of Applied Ecology*, 18(2):433, aug 1981. ISSN 00218901. doi: 10.2307/2402404. URL http://www.jstor.org/stable/2402404?origin=crossref.

W. Chen, P. Westerhoff, J. A. Leenheer, and K. Booksh. Fluorescence ExcitationEmission Matrix Regional Integration to Quantify Spectra for Dissolved Organic Matter. *Environmental Science & Technology*, 37(24):5701–5710, dec 2003. ISSN 0013-936X. doi: 10.1021/es034354c. URL http://pubs.acs.org/doi/abs/10.1021/es034354c.

W. D. Collins, P. Friedlingstein, A. T. Gaye, J. M. Gregory, A. Kitoh, R. Knutti, J. M. Murphy, A. Noda, S. C. Raper, I. G. Watterson, A. J. Weaver, and Z.-C. Zhao. Global Climate Projections. In S. Solomon, D. Qin, M. Manning, M. Marquis, K. Averyt, M. M. Tignor, H. L. Miller, and Z. Chen, editors, *Climate Change 2007: The Physical Science Basis. Contribution of Working Group I to the Fourth Assessment Report of the Intergovernmental Panel on Climate Change*, chapter 10, pages 747 – 846. Cambridge University Press, Cambridge, United Kingdom and New York, USA, 2007. ISBN 9780521880091. URL http://www.ipcc.ch/publications_and_data/ar4/wg1/en/contents.html.

E. L. Cussler. *Diffusion: mass transfer in fluids systems*. Cambridge University Press, 3 edition, 2009. ISBN 978-0-521-87121-1.

European Commission. The EU Water Framework Directive - integrated river basin management for Europe, 2010. URL http://ec.europa.eu/environment/water/water-framework/index_en.html.

Ø. Garmo, L. B. Skancke, and T. Høgasen. Monitoring long-range transboundary air pollution. Water chemical effects 2013. Technical report, Norwegian Institute for Water Research, Oslo, Norway, 2014.

E. C. Ged and T. H. Boyer. Molecular weight distribution of phosphorus fraction of aquatic dissolved organic matter. *Chemosphere*, 91(7):921–7, may 2013. ISSN 1879-1298. doi: 10.1016/j.chemosphere.2013.01.113. URL http://www.ncbi.nlm.nih.gov/pubmed/23466281.

R. W. Gensemer and R. C. Playle. The Bioavailability and Toxicity of Aluminum in Aquatic Environments. *Critical Reviews in Environmental Science and Technology*, 29(4):315–450, oct 1999. ISSN 1064-3389. doi: 10.1080/10643389991259245. URL http://www.tandfonline.com/doi/abs/10.1080/10643389991259245.

S. Haaland, D. Hongve, H. Laudon, G. Riise, and R. D. Vogt. Quantifying the Drivers of the Increasing Colored Organic Matter in Boreal Surface Waters. *Environmental Science & Technology*, 44(8):2975–2980, apr 2010. ISSN 0013-936X. doi: 10.1021/es903179j. URL http://dx.doi.org/10.1021/es903179j.

I. Hanssen-Bauer, E. Førland, I. Haddeland, H. Hisdal, S. Mayer, A. Nesje, J. Nilsen, S. Sandven, A. Sandø, A. Sorteberg, B. Ådlandsvik, L. Andreassen, S. Beldring, A. Bjune, K. Breili, C. A. Dahl, A. Dyrrdal, K. Isaksen, H. Haakenstad, J. Haugen, H. Hygen, H. Langehaug, S.-E. Lauritzen, D. Lawrence, K. Melvold, A. Mezghani, O. Ravndal, B. Risebrobakken, L. Roald, H. Sande, M. Simpson, Ø. Skagseth, T. Skaugen, M. Skogen, E. Støren, O. Tveito, and W. Wong. Klima i Norge 2100. Kunnskaps-

grunnlag for klimatilpasning oppdatert i 2015. Technical Report 2, Norsk Klimaservicesenter, 2015. URL www.miljodirektoratet.no/20804.

D. Hongve, G. Riise, and J. F. Kristiansen. Increased colour and organic acid concentrations in Norwegian forest lakes and drinking water – a result of increased precipitation? *Aquatic Sciences*, 66(2):231–238, jun 2004. ISSN 1015-1621. doi: 10.1007/s00027-004-0708-7. URL http://link.springer.com/10.1007/s00027-004-0708-7.

P. H. Hsu. Interaction Between Aluminum and Phosphate in Aqueous Solution. In R. A. Baker, editor, *Trace Inorganics In Water*, volume 73 of *Advances in Chemistry*, pages 115–127. American Chemical Society, Washington, D.C., jun 1968. ISBN 0-8412-0074-2. doi: 10.1021/ba-1968-0073. URL http://dx.doi.org/10.1021/ba-1968-0073.ch005.

ISO 6878. Water quality - Determination of phosphorus - Ammonium molybdate spectrometreic method. Technical report, International Organization for Standardization, 2004.

E. R. Ivins and T. S. James. Bedrock response to Llanquihue Holocene and present-day glaciation in southernmost South America. *Geophysical Research Letters*, 31(24):1–4, 2004. ISSN 00948276. doi: 10.1029/2004GL021500.

E. R. Ivins and T. S. James. Antarctic glacial isostatic adjustment: a new assessment. *Antarctic Science*, 17(04):541, 2005. ISSN 0954-1020. doi: 10.1017/S0954102005002968. URL http://www.journals.cambridge.org/abstract_S0954102005002968.

E. R. Ivins, C. G. Sammis, and C. F. Yoder. Deep mantle viscous structure with prior estimate and satellite constraint. *Journal of Geophysical Research: Solid Earth*, 98(B3): 4579–4609, 1993. ISSN 2156-2202. doi: 10.1029/92JB02728. URL http://onlinelibrary.wiley.com/doi/10.1029/92JB02728/abstract.

D. S. Jeffres, F. P. Dieken, and D. E. Jones. Performance Of The Autoclave Digestion Method For Total Phosphorus Analysis. *Water Research, Pergamon Press*, 13:275–279, 1979.

E. Jennings, M. Järvinen, N. Allott, L. Arvola, K. Moore, P. Naden, C. N. Aonghusa, T. Nõges, and G. A. Weyhenmeyer. Impacts of Climate on the Flux of Dissolved Organic Carbon from Catchments. In G. George, editor, *The Impact of Climate Change on European Lakes*, pages 199–220. Springer Netherlands, Dordrecht, 2010. ISBN 978-90-481-2944-7. doi: 10.1007/978-90-481-2945-4. URL http://link.springer.com/10.1007/978-90-481-2945-4.

A. Jones. The European Environment — State and Outlook 2010. Technical report, European Commission JRC, Luxembourg, jul 2010.

Kartverket. Land-use map data, 2016. URL http://www.kartverket.no.

T. Klemsdal. Landformene i Østfold. *Natur i Østfold*, 21(1-2):7–31, 2002.

S. J. Köhler, D. Kothawala, M. N. Futter, O. Liungman, and L. Tranvik. In-lake processes offset increased terrestrial inputs of dissolved organic carbon and color to lakes. *PloS one*, 8(8):e70598, jan 2013. ISSN 1932-6203. doi: 10.1371/journal.pone.0070598. URL http://journals.plos.org/plosone/article?id=10.1371/journal.pone.0070598.

S. Kosten, V. L. M. Huszar, E. Bécares, L. S. Costa, E. Donk, L.-A. Hansson, E. Jeppesen, C. Kruk, G. Lacerot, N. Mazzeo, L. Meester, B. Moss, M. Lürling, T. Nõges, S. Romo, and M. Scheffer. Warmer climates boost cyanobacterial dominance in shallow lakes. *Global Change Biology*, 18(1):118–126, jan 2012. ISSN 13541013. doi: 10.1111/j.1365-2486.2011.02488.x. URL http://doi.wiley.com/10.1111/j.1365-2486.2011.02488.x.

S. H. Kværnø and L. Øygarden. The influence of freeze-thaw cycles and soil moisture on aggregate stability of three soils in Norway. *Catena*, 67(3):175–182, 2006. ISSN 03418162. doi: 10.1016/j.catena.2006.03.011.

K. Lambeck. Glacial Isostasy. In V. Gornitz, editor, *Encyclopedia of Paleoclimatology and Ancient Environments*, pages 374–380. Springer, Dordrecht, The Netherlands, 2007. ISBN 978-1-4020-5197-5.

D. T. Monteith, J. L. Stoddard, C. D. Evans, H. a. de Wit, M. Forsius, T. Høgåsen, A. Wilander, B. L. Skjelkvåle, D. S. Jeffries, J. Vuorenmaa, B. Keller, J. Kopácek, and J. Vesely. Dissolved organic carbon trends resulting from changes in atmospheric deposition chemistry. *Nature*, 450(7169):537–540, 2007. ISSN 0028-0836. doi: 10.1038/nature06316.

J. Murphy and J. P. Riley. A modified single solution method for the determination of phosphate in natural waters. *Analytica Chimica Acta*, 27:31–36, 1962.

Norges vassdrags- og energidirektorats (NVE). Hydrological map data, 2016. URL https://www.nve.no.

S. Odén. The acidity problem ? An outline of concepts. *Water, Air, and Soil Pollution*, 6(2-4):137–166, 1976. ISSN 0049-6979. doi: 10.1007/BF00182862. URL http://link.springer.com/10.1007/BF00182862.

D. L. Parkhurst and C. Appelo. Description of input and examples for PHREEQC version 3–A computer program for speciation, batch- reaction, one-dimensional transport, and inverse geochemical calculations: U.S. Geological Survey Techniques and Methods. In *U.S. Geological Survey Techniques and Methods (Book 6)*, chapter A43, page 497. U.S.

Department of the Interior & U.S. Geological Survey, 2013. URL http://pubs.usgs.gov/tm/06/a43.

W. Peltier. Global Glacial Isostasy And The Surface Of The Ice-Age Earth: The ICE-5G (VM2) Model and GRACE. *Annual Review of Earth and Planetary Sciences*, 32(1): 111–149, may 2004. ISSN 0084-6597. doi: 10.1146/annurev.earth.32.082503.144359. URL http://www.annualreviews.org/doi/10.1146/annurev.earth.32.082503.144359.

R Core Team. *R: A Language and Environment for Statistical Computing.* R Foundation for Statistical Computing. R Foundation for Statistical Computing, Vienna, Austria, 2015. ISBN 3-900051-07-0. URL http://www.r-project.org.

F. H. Rigler. A Dynamic View of the Phosphorus Cycle in Lakes. In E. J. Griffith, A. Beeton, J. M. Spencer, and D. T. Mitchell, editors, *Environmental Phosphorus Handbook*, pages 539–572. John Wiley and Sons., New York, 1973.

B. Rosseland, F. Kroglund, M. Staurnes, K. Hindar, and A. Kvellestad. Tolerance to Acid Water Among Strains and Life Stages of Atlantic Salmon (Salmo Salar L.). *Water, Air, and Soil Pollution*, 130(1-4):899–904, 2001. ISSN 1573-2932. doi: 10.1023/A:1013807618283.

N. Roulet and T. R. Moore. Environmental chemistry: browning the waters. *Nature*, 444 (7117):283–4, nov 2006. ISSN 1476-4687. doi: 10.1038/444283a. URL http://dx.doi.org/10.1038/444283a.

D. W. Schindler. Evolution of Phosphorus Limitation in Lakes. *Science*, 195(4275): 260–262, jan 1977. ISSN 0036-8075. doi: 10.1126/science.195.4275.260. URL http://www.sciencemag.org/cgi/doi/10.1126/science.195.4275.260.

E. Skarbøvik, M. Bechmann, T. Rohrlack, and S. Haande. Overvåking Vansjø/Morsa 2009-2010. Technical Report 31, Bioforsk, Ås, Norway, 2011.

E. Skarbøvik, S. Haande, M. Bechmann, and S. Birger. Overvåking Morsa 2014-2015. Technical Report 2, Norwegian Institute of Bioeconomy Research, Ås, Norway, 2016.

B. L. Skjelkvåle, J. Mannio, a. Wilander, and T. Andersen. Recovery from acidification of lakes in Finland, Norway and Sweden 1990–1999. *Hydrology and Earth System Sciences*, 5(3):327–338, 2001a. ISSN 1607-7938. doi: 10.5194/hess-5-327-2001.

B. L. Skjelkvåle, J. L. Stoddard, and T. Andersen. Trends in Surface Water Acidification in Europe and North America (1989-1998). *Water, Air, and Soil Pollution*, 130(1-4): 787–792, 2001b. ISSN 1573-2932. doi: 10.1023/A:1013806223310.

A. L. Solheim. Tiltaksanalyse for Morsa (Vansjø-Hobøl-vassdraget). Technical report, Norwegian Institute for Water Research, Oslo, Norway, 2001.

A. L. Solheim and J. Moe. Eutrofierings-tilstand i norske innsjøer og elver 1980-2008. Technical Report 1042/2009, Norwegian Institute for Water Research, Oslo, Norway, 2008.

I. Spikkeland. Der det er vann er det liv. Ferskvann og våtmark i Østfold. *Natur i Østfold*, 22(1-2):27–33, 2003. URL http://www.nhm.uio.no/botanisk/nbf/ofa/nio2003/4_vann. pdf.

E. Tipping, S. Lofts, and J. E. Sonke. Humic Ion-Binding Model VII: a revised parameterisation of cation-binding by humic substances. *Environmental Chemistry*, 8(3): 225–235, 2011. ISSN 1448-2517. doi: 10.1071/EN11016. URL http://www.publish. csiro.au/?paper=EN11016.

B. L. Turner, M. J. Papházy, P. M. Haygarth, and I. D. McKelvie. Inositol phosphates in the environment. *Philosophical transactions of the Royal Society of London. Series B, Biological sciences*, 357(1420):449–69, apr 2002. ISSN 0962-8436. doi: 10.1098/rstb. 2001.0837. URL http://rstb.royalsocietypublishing.org/content/357/1420/449.short.

UNECE. 1979 Convention On Long-Range Transboundary Air Pollution, 1979. URL http://www.unece.org/env/lrtap/lrtap_h1.html.

R. Vogt. Increase in colour and amount of organic matter in surface waters. Technical Report 009, NORDTEST, Espoo, Finland, 2003.

R. D. Vogt, O. K. Røyset, P. Aagaard, T. Andersen, L. Gottschalk, T. M. Saloranta, D. Barton, C. Auterives, G. Orderud, K. B. Stokke, J. Naustdalslid, E. Romstad, M. Bechmann, and H.-M. Bjørnsen. Watershed EUTROphication management through system oriented process modelling of Pressures, Impacts and Abatement actions., 2008. URL https://www.mn.uio.no/kjemi/english/research/projects/eutropia/ presentations/eutropia-project-descrpiption.pdf.

G. A. Weyhenmeyer, Y. T. Prairie, and L. J. Tranvik. Browning of boreal freshwaters coupled to carbon-iron interactions along the aquatic continuum. *PloS one*, 9(2):e88104, jan 2014. ISSN 1932-6203. doi: 10.1371/journal.pone.0088104. URL http://journals. plos.org/plosone/article?id=10.1371/journal.pone.0088104.

H. Zhang. DGT - for measurements in water, soil and sediments. Technical report, DGT Research Ltd, Lancaster, United Kingdom, 2005.

H. Zhang, W. Davidson, R. Gadi, and T. Kobayashi. In situ measurement of dissolved phosphorus in natural waters using DGT. *Analytica Chimica Acta*, 340:29–38, 1998.

Papers

Paper I

An in-depth assessment into simultaneous monitoring of dissolved reactive phosphorus (DRP) and low-molecular-weight organic phosphorus (LMWOP) in aquatic environments using diffusive gradients in thin films (DGT).

Mohr, C.W., Vogt, R.D., Røyset, O., Andersen, T., Parekh, N.A.,

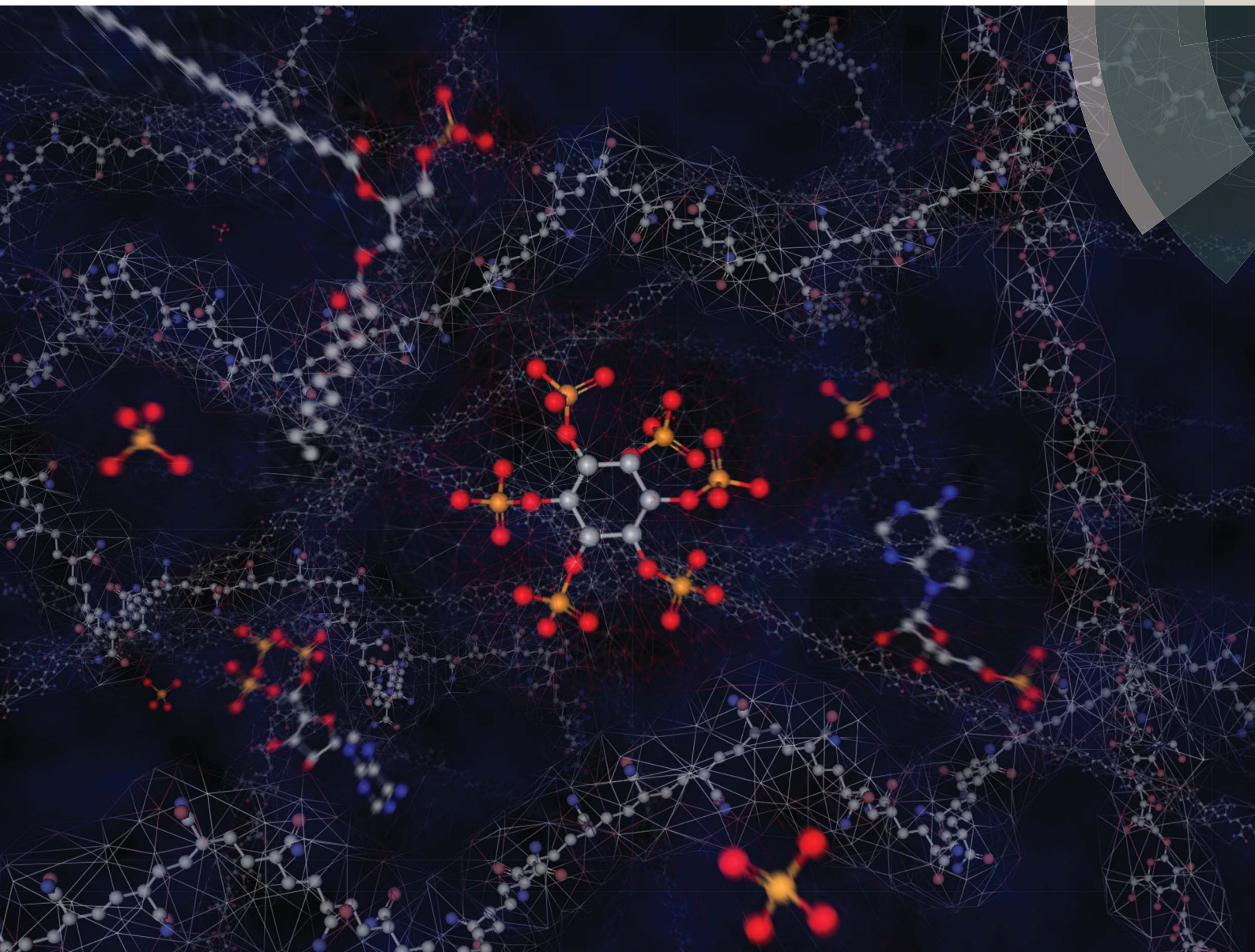# Environmental Science
Processes & Impacts

PAPER

An in-depth assessment into simultaneous monitoring of dissolved reactive phosphorus (DRP) and low-molecular-weight organic phosphorus (LMWOP) in aquatic environments using diffusive gradients in thin films (DGT)

Christian Wilhelm Mohr,[*a] Rolf David Vogt,[a] Oddvar Røyset,[b] Tom Andersen[c] and Neha Amit Parekh[a]

Long-term laborious and thus costly monitoring of phosphorus (P) fractions is required in order to provide reasonable estimates of the levels of bioavailable phosphorus for eutrophication studies. A practical solution to this problem is the application of passive samplers, known as Diffusive Gradient in Thin films (DGTs), providing time-average concentrations. DGT, with the phosphate adsorbent Fe-oxide based binding gel, is capable of collecting both orthophosphate and low molecular weight organic phosphorus (LMWOP) compounds, such as adenosine monophosphate (AMP) and myo-inositol hexakisphosphate (IP6). The diffusion coefficient (D) is a key parameter relating the amount of analyte determined from the DGT to a time averaged *ambient* concentration. D at 20 °C for AMP and IP6 were experimentally determined to be 2.9×10^{-6} cm^2 s^{-1} and 1.0×10^{-6} cm^2 s^{-1}, respectively. Estimations by conceptual models of LMWOP uptake by DGTs indicated that this fraction constituted more than 75% of the dissolved organic phosphorus (DOP) accumulated. Since there is no one D for LMWOP, a D range was estimated through assessment of D models. The models tested for estimating D for a variety of common LMWOP molecules proved to be still too uncertain for practical use. The experimentally determined D for AMP and IP6 were therefore used as upper and lower D, respectively, in order to estimate minimum and maximum ambient concentrations of LMWOP. Validation of the DGT data was performed by comparing concentrations of P fractions determined in natural water samples with concentration of P fractions determined using DGT. Stream water draining three catchments with different land-use (forest, mixed and agriculture) showed clear differences in relative and absolute concentrations of dissolved reactive phosphorus (DRP) and dissolved organic P (DOP). There was no significant difference between water sample and DGT DRP ($p > 0.05$). Moreover, the upper and lower limit D for LMWOP proved reasonable as water sample determined DOP was found to lie in-between the limits of DGT LMWOP concentrations, indicating that on average DOP consists mainly of LMWOP. "Best fit" D was determined for each stream in order to practically use the DGTs for estimating time average DOP. Applying DGT in a eutrophic lake provided insight into P cycling in the water column.

Environmental impact

It is well known that eutrophication is a continuous growing environmental problem, as the increase in human activity associated with urbanization and agricultural practices results in nutrient pollution in the aquatic and marine environment from point and non-point sources. However, a less known issue is the possible impact climate change and acid rain reduction may have on eutrophication in many Nordic countries with marine clay soil becoming phosphorus rich (due to the rising of land from the sea during the post-glacial period). This paper focuses on the monitoring of dissolved reactive phosphorus (DRP) and dissolved organic phosphorus (DOP), and especially the DOP subfraction low-molecular-weight organic phosphorus (LMWOP), which are known to be bioavailable. The method chosen for monitoring is passive sampling by using Diffusive Gradients in Thin-films (DGTs).

[a]Department of Chemistry, University of Oslo, Norway. E-mail: c.w.mohr@kjemi.uio. no

[b]Norwegian Institute for Water Research (NIVA), Oslo, Norway

[c]Department of Bioscience, University of Oslo, Norway

1 Introduction

1.1. The role of background P flux in eutrophication

Deterioration of water resources due to the increased rate of eutrophication has been a large and increasing environmental

This journal is © The Royal Society of Chemistry 2015

Environ. Sci.: Processes Impacts, 2015, **17**, 711–727 | **711**

problem in most parts of the world. The problem is related to excessive input of nutrients (mainly phosphorus (P) and nitrogen (N)) from human activities: agriculture, industry, and sewage disposal. Abatement actions used in order to reduce the anthropogenic nutrient loading to water bodies have been shown to counter eutrophication.[1,2] However, the progression in resolving the eutrophication problems is generally very slow, such as in the lake Vansjø, south-eastern Norway. Despite numerous and costly abatement actions, such as redirecting sewage wastewater and reducing the P input from agricultural sites in the catchment, the water quality remains poor. This has brought attention to the role of the background flux of P.[3] The main natural transport mechanism of P from forested watersheds to surface waters is associated with Dissolved Natural Organic Matter (DNOM). With 85% of the Vansjø catchment being forested, and approx. 90% of the land being below the marine limit, it is found that this background flux accounts for 39% of the total P flux to the lake.[4] The contribution of P to DNOM is thus a considerable portion of the total P flux to the lake. Moreover, the concentrations of DNOM in streams have increased significantly in the southern parts of the Nordic countries since the 1980's.[5–7] It is hypothesized that this has caused an increased flux of P bound to the DNOM, and that this partly compensates for the decreased anthropogenic P loading – thereby disguising the effect of abatement actions.[3] It is furthermore likely that a considerable fraction of the P associated with DNOM is bioavailable low-molecular-weight (molecular weight <1 kDa)[8] organic phosphorus (LMWOP) compounds. Nucleic acid derivatives, phospholipids, sugar phosphates and inositol polyphosphates are all bioavailable LMWOP species commonly found in the soil and water.[9–16] The concentrations of these molecules, as well as the inorganic orthophosphate species, fluctuate, but are generally held low even in eutrophic freshwaters. This is due to rapid fixation by algae and other microorganisms as well as precipitation/co-precipitation with aluminium, iron, calcium and manganese. The fluctuating and very low concentrations of these compounds present major challenges in the monitoring of the bioavailable P fraction by standard methods.

1.2. Diffusive gradients in thin films

The use of Diffusive Gradient in Thin films (DGTs), a passive sampler based on diffusive uptake, represents a major breakthrough in environmental water-chemistry monitoring for a number of chemical species commonly present in concentrations close to the limit of detection. The DGTs' ability to accumulate specific chemical species linearly over time (within limits) makes it possible to determine the time average concentrations of specific species. Furthermore, because DGTs accumulate the analyte, even species with concentrations near the detection limit can be determined with good precision and accuracy.[17]

The DGTs' linear uptake of an analyte is based on Fick's law for steady-state diffusion in dilute solutions.[18] The diffusion flux (J) over the permeable thin-film membrane of the DGT is dependent on the area of cross-section (A), the diffusion coefficient (D) and the concentration gradients across the membrane and diffusive boundary layer combined ($\mathrm{d}c/\mathrm{d}x$) (eqn (1)).

$$J = -AD\frac{\mathrm{d}c}{\mathrm{d}x} \qquad (1)$$

The analyte that has diffused across the membrane is rapidly and completely bound to the binding gel. The concentration of dissolved analyte in the binding gel is thus practically zero, simplifying the flux equation (eqn (2)).

$$J = \frac{m}{t} = AD\frac{c}{x} \qquad (2)$$

in which m is the accumulated mass on the binding gel over a period of time (t), c can be simplified to the ambient solute concentration outside the membrane and x is the thickness of the membrane and the diffusive boundary layer combined.[17] This equation implies that the linear slope of m as a function of time will be linearly proportional to the ambient concentration (c).

DGTs fitted with Fe-oxide binding gel have been shown to adsorb phosphate, arsenate and selenate.[19,20] The strong affinity of Fe-oxide for phosphate makes it a suitable adsorbent also for many LMWOP compounds. Fe-oxide binding gel has been tested in regards to some organic and condensed phosphates that are commonly encountered in the aquatic environment.[21] These findings are strongly supported by a review of organic P sorption studies by Celi and Barberis.[22] In this study LMWOP compounds were shown to adsorb to ferric oxide surfaces in the soil. Moreover, the sorption properties were linked to the phosphate functional group. Similar sorption–desorption properties were found to be common with the well-studied orthophosphate.

Other DGT phosphate binding gel materials, such as titanium dioxide[23] and amorphous zirconium oxide,[24] have been assessed. Both produced promising results regarding dissolved reactive phosphorus (DRP) in terms of sorption capacity and binding gel stability over time. Zirconium oxide has also been shown to adsorb LMWOP.[25] It is therefore likely that titanium dioxide also adsorbs LMWOP, due to its similar properties to zirconium oxide in binding to orthophosphate. However, a minimum elution strength of 1 M NaOH is required in order to efficiently extract phosphate from both titanium dioxide and zirconium oxide.[23,24] In the case of zirconium oxide this has been shown to increase the risk of hydrolysis for some P compounds.[25] In this study only the Fe-oxide binding gel has been studied, based on its well-established record as a phosphate adsorbent and commercial availability (DGT Research Ltd).

Employing DGTs to sample LMWOP is not novel in itself, as both Moorlegham et al.[21] and Sun et al.[25] have studied the adsorption of LMWOP by the DGTs. However, the question how to use the amount of analyte determined from the DGTs to predict the *ambient* concentration of LMWOP is yet unresolved. In the study by Dougherth et al.[26] it was shown that total dissolved phosphorus (TDP) runoff from peat soil could be empirically estimated from time average measured DRP in soil pore water using soil deployment DGT with Fe-oxide binding gel. However the application of this study in a real world

712 | *Environ. Sci.: Processes Impacts*, 2015, **17**, 711–727

This journal is © The Royal Society of Chemistry 2015

scenario is limited to risk assessment of runoff from peat soil, and not actual monitoring of water bodies for a variety of land-use. Furthermore in the study only an inorganic fertilizer was applied to the peat soil, which makes it highly likely that the relationship found between TDP in the runoff and DRP from the DGTs is actually fundamentally a relationship between DRP in the runoff and DRP from the DGTs, since TDP in this case is likely approx. equal to DRP. This is not always the case, since different land-uses will have different DRP to dissolved organic P (DOP = TDP − DRP) ratios as will be presented in the field studies in Chapter. 4.7.

Operationally defined, LMWOP is the fraction of organic molecules containing P that are small enough to diffuse through the APA-gel of the DGT and accumulate in the Fe-oxide binding gel. LMWOP is operationally determined as the difference between the TDP and the DRP, based on the amounts extracted from the DGT binding gels, see Chapter 2.4. The average *ambient* concentration of a phosphorus species (c) is calculated by solving eqn (2) in regards to c (eqn (3)), using the D determined for the specific molecular compound.

$$c = \frac{mx}{tDA} \qquad (3)$$

LMWOP constitutes a continuum of a poorly defined group of compounds that exhibit large spatial variation.[11] This represents a challenge when converting the amount of LMWOP measured in the binding gel to the *ambient* concentration of the LMWOP fraction. A single diffusion coefficient for the LMWOP fraction cannot be applied since diffusion coefficients are species specific. A more accurate perspective would be to view the concentration of LMWOP (c_{LMWOP}) as the sum of the concentration of the individual LMWOP species (c_i; eqn (4)).

$$c_{LMWOP} = \sum_{i=1}^{n} c_i = \sum_{i=1}^{n} \frac{m_i x}{t D_i A} \qquad (4)$$

where m_i and D_i are the accumulated amount in the DGT binding gel and diffusion coefficient of the individual LMWOP species (i), respectively. The problem is that this is not practically possible since the specific distribution of LMWOP species in the gel and most of their D_i are unknown. In this study the suggested and applied approach for assessing c_{LMWOP} is instead to first estimate the possible range of LMWOP concentrations. This is achieved by estimating the upper and lower diffusion coefficient values for the LMWOP molecules in water. The estimated range is compared with the measured concentration of DOP fraction in the water samples. This comparison is based on the assumption that high molecular weight DNOM (>1 kDa; such as much of humic substances (HS)) contributes minimally to the overall amount of DOP accumulated by the DGT. This assumption, which is based on that compounds with a large molecular size will not pass through the DGT membrane, is assessed and found valid in this study through field measurements and experimentally and theoretically determined DGT diffusion coefficients.

Using a LMWOP D range is to some degree impractical for the application of monitoring water bodies by DGT, as it only results in giving a possible LMWOP concentration range. However for the sake of practicality it is possible to estimate a "best fit" D for the entire DOP fraction by testing different D values until the bulk temporal distribution of monitored DGT LMWOP matches the bulk temporal distribution of monitored water sample DOP. This makes it possible to "tailor" the LMWOP D for a specific water body, *i.e.* a form of calibrating the D for time average determination of DOP. In this study the Wilcoxon rank-sum statistical test was used to search for a "best fit" D. The test was also used for the validation of DGT DRP data, discussed in depth in Chapter 4.7.

2   Materials and methods

All DGTs used in this study were solution deployment style DGTs purchased from DGT Research Ltd. Each unit consisted of a piston-cap with a 2.0 cm diameter sampling window fitted with 0.12 mm thick cellulose nitrate membranes and 0.8 mm thick agarose polyacrylamide (APA) diffusive gel situated over the Fe-oxide binding gel.[17] All data were processed using R statistical software.[27]

2.1.   Experimental determination of the range of LMWOP diffusion coefficients

Adenosine monophosphate (AMP) and inositol hexakisphosphate (IP6; or phytic acid) were selected as model compounds since the sizes of these two compounds span most of the molecular weight range of LMWOP. Moreover, they represent nucleoside poly-phosphates and inositol polyphosphates, two LMWOP compounds commonly encountered in the environment.[11]

The diffusion coefficients (D) for these model compounds were experimentally determined by placing the DGTs in a 40–45 L solution containing the model compounds. The DGTs were mounted on 3 central rotating disks in the container and submerged face down into the solution. The rotor was set to a fixed rotating speed of 6 rpm (equivalent speed of 5–10 cm s^{-1} depending on the mounting distance from the center point) to ensure a low laminar diffusive boundary layer (<0.1 mm) during the experiments.[28]

The DGTs were collected from the AMP solution over a period of 19 days at intervals of approx. 2 days (2 replicates). The sampling scheme for the DGTs in the IP6 solution was daily samples for 8 days (1 replicate). Aliquots of 30 mL test solution were sampled along with the DGTs for determining the concentration of P fractions in the test solution. Temperature was measured during DGT and test solution sample collection and was shown to remain relatively constant (22.4 ± 0.6 and 23.6 ± 0.5 °C for the AMP and IP6 solution respectively). Collected DGTs and water samples were refrigerated at 4 °C and kept in the dark until extraction and analysis of P fractions. Non-exposed DGTs were used as DGT blanks for background correction and determination of the limit of detection ($n = 4$).

The 45 L test solution containing 25 μg P/L AMP was prepared by dissolving disodium adenosine-5′-monophosphate salt ($C_{10}H_{12}N_5Na_2O_7P$, brand: Merck, purity: ≥99%) in deionized water. In order to match natural water pH and ionic

strength (IS), the pH was adjusted to 5.0 by adding 0.1 M ammonium acetate (CH_3COONH_4) and IS was increased by adding NaCl to a final concentration of 1 mM.

In a similar manner the 40 L test solution containing 32 μg P/L IP6 was prepared by dissolving phytic acid dipotassium salt ($C_6H_{16}O_{24}P_6K_2$, brand: Sigma-Aldrich, purity: ≥95%) in deionized water. The pH in the tank was buffered to 5.5 by adding 1 M sodium acetate/acetic acid buffer (CH_3COO^-/CH_3COOH). The IS was increased by adding NaCl to a final concentration of 1 mM. Both solutions were left to stabilize for 24 h prior to the experiment.

2.2. Monitoring of P fractions in stream and lake water with DGTs

The concentration of dissolved reactive phosphorus (DRP; *i.e.* mainly orthophosphate) and LMWOP in streams was measured using DGTs. The DGTs were placed in three 1st order streams draining catchments which differ in land-use; *Dalen* is a boreal forested catchment (Forest), *Huggenes* is a mixed catchment (Mixed), comprised of approx. 32% forest, 59% agriculture and 9% other land-use, while *Støa* is an agricultural catchment (Agricultural).[29] The streams drain into the eutrophic western basin of Vansjø, a lake located south of Oslo, Norway. The concentrations of P fractions in the stream water were monitored as a part of the Eutropia research project.[3] The streams were therefore known to differ in the level and composition of P fractions. All DGTs were deployed in the streams for 1 to 2 week intervals over a period of approx. 3 months from June to September, 2011. Water temperature was measured at the time of deployment and collection to correct diffusion coefficients for temperature differences. Water samples for the determination of P fractions were collected along with the deployment and collection of DGTs, and occasionally more frequently during increased runoff periods. Evaluation of compliance between the DGT measured DRP and grab sample DRP was performed using the Wilcoxon rank-sum test.

A practical performance study using DGTs was performed in *Grepperødfjorden*, a shallow sub-basin of lake Vansjø. DGTs were placed at depths ~0 m (*i.e.* just below the surface), 2.5 m, 3.75 m and in the sediment at ~4 m (DGT window faced down into the sediment under buoy anchor). The DGTs were deployed in replicates of 3 at each depth, except in the sediment in which only a single DGT was used. All DGTs placed in the lake water were fitted with a nylon net mesh coated with an antifouling agent (Seajet 034 spray, Sola Shipping AS) situated a few mm from the DGT window. The purpose of the net was to reduce algae growth on the DGT window. The DGTs were placed in the lake for 13 days during mid-August, 2012. Water samples at 2.5 m depth were collected and water temperature profiles were measured during deployment and collection of the DGTs. Differences in P fractionation between depths were analyzed by one-way ANOVAs on log-transformed variables. Log-transformation was necessary to stabilize variances.

2.3. Elution of P from the DGT binding gel

DGTs were dissembled and the Fe-oxide binding gels were placed in polypropylene tubes. 0.7 mL deionized water was added to the

tube, followed by 0.3 mL of 4 M H_2SO_4, giving an initial concentration of 1.2 M H_2SO_4. The binding gels were left for 24 h ensuring a complete dissolution of the Fe-oxides in the binding gel. The final acid concentration was adjusted to 0.04 M H_2SO_4 by dilution with deionized water, matching the acid concentration of the standards used for the phosphate determination.

2.4. Phosphorus fractionation and analysis

The two P fractions, Total Dissolved P (TDP) and Dissolved Reactive P (DRP), were determined in the water samples by combining potassium peroxodisulfate ($K_2S_2O_8$) digestion[30] and non-digestion of filtered (0.7 μm Whatman® glass microfiber filters, Grade GF/F) samples as pre-treatment steps prior to the determination of DRP by the molybdate blue method (MBM)[31] (see Fig. 1). 0.7 μm Whatman® glass microfiber filters (Grade GF/F) were employed as this was required for the concurrent monitoring within the Eutropia research project for studying the characteristics of particulate matter. TDP and DRP fractions in the DGT extracts were analyzed in a similar manner, though without the filtration step. Still, only dissolved P compounds are sampled by DGTs as only molecules smaller than 5–10 nm pass through the APA diffusive gel of the DGTs. Discrepancies are expected between TDP determined in the water samples and DGTs due to the smaller pore-sizes of the DGT membranes (700 nm *versus* 5–10 nm), causing size exclusion of the fraction of large dissolved molecules by the DGT.

MBM is considered a wet chemical selective method for the determination of orthophosphate. However studies have shown that the reagents added in the MBM method alter the natural equilibrium in the water sample, resulting in an overestimation of the orthophosphate.[32] It is nevertheless assumed here that the DRP fraction is approximately equal to the free aqueous orthophosphate concentration in solution.

The concentrations of TDP and DRP in the water and DGT samples were determined using a customized
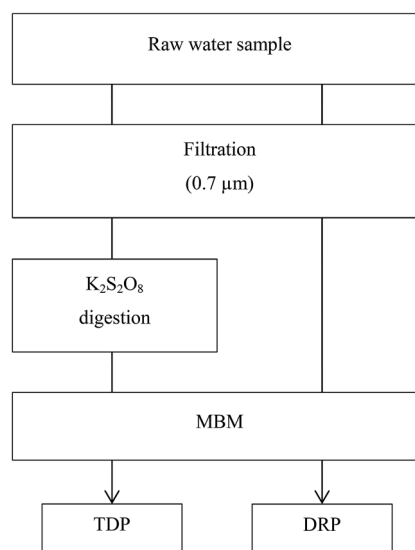

Fig. 1 P fractionation scheme for water samples.

continuous flow auto-analyzer (SKALAR San[++] Automated Wet Chemistry Analyser), with online digestion prior to analysis of TDP. pH was measured and dissolved organic carbon (DOC) was determined in all water samples. DOC was determined using a Shimadzu TOC-5000A total organic carbon analyzer after 0.7 μm filtration. pH measurements were used to determine the protonated distribution of orthophosphates, and correct the orthophosphate diffusion coefficients for this distribution.

3 Modelling

3.1. Relating range in size, mass and charge of P fractions to DGT diffusion coefficients

The Stokes–Einstein equation (eqn (5a)) can be used to theoretically predict diffusion coefficients of organic molecules in liquid media:

$$D = \frac{k_B T}{f} \tag{5a}$$

where f is the friction coefficient, T the temperature and k_B is Boltzmann's constant. The Stokes–Einstein equation simplifies the diffusion process by treating the organic molecules as spherical particles moving at a constant velocity. The f for a spherical particle can be calculated by Stokes' relationship (eqn (5b)):

$$f = 6\pi\eta r_0 \tag{5b}$$

where η is the viscosity of the media/solvent and r_0 is the solute radius of the spherical particle.[18,33] The problem when using the Stokes–Einstein equation is that there is no simple way to determine the solute size of a molecule based on its chemical structure. Major shortcomings are that molecules are generally not spherical and they interact with each other, the solvent and other solutes. These factors which affect the diffusion coefficient are not accounted for in the calculation of the friction coefficient. Molecular interactions are especially important for charged molecules in polar solvents. DNOM has a net negative charge at the pH range of natural waters due to the large number of weak acid functional groups. This is especially the case with LMWOP, due to the negatively charged phosphate group. This net negative charge of LMWOP molecules produces a hydration sphere, thereby increasing the solvent radius.[33] IP6, with 6 phosphate groups, may carry a charge ranging from 0 to −12 depending on the pH. Within the pH range of 5–7, commonly found in natural water, IP6 speciation is dominated by species charged in the range of −6 to −8, with overlapping distribution.[34] The pH is therefore likely to be highly influential on the solute radius of IP6, but also, to a varying degree, for all LMWOP molecules. However, with sophisticated molecular geometry computational models it is possible to estimate the solvent accessible surface area (SASA).[35,36] Assuming a spherical surface area it is then possible to calculate a solute radius (r_0) (eqn (6)) that can be used in eqn (5) to calculate the diffusion coefficient.

$$r_0 = \sqrt[2]{\frac{SASA}{4\pi}} \tag{6}$$

This theoretical approach is explored in order to estimate the D for a number of LMWOP molecules lacking experimentally derived D, and thereby help assess the upper and lower diffusion coefficient values for the LMWOP molecules.

3.2. Assessing humic substance uptake by DGT

The main DNOM fraction in water is humic substances (HS), constituting approx. 60% of the total organic carbon (TOC) in freshwater.[37] The molecular size of HS are generally on average larger than the low molecular weight (LMW) compounds,[38] comprising LMWOP, and thereby considered as a high molecular weight fraction (HMW). HS are also assumed to contain P, though the mass percentage of P in HS is relatively low compared to LMWOP compounds (e.g. nucleoside phosphates, inositol phosphates, some phospholipids, etc., see Table 1). Still, the abundance of HS implies that this fraction constitutes not only a significant amount of the high molecular weight organic P (HMWOP), but also the total DOP in surface waters. It is therefore necessary to assess to what degree HS may be adsorbed by the DGTs. Depending on the size, some of the HS may be able to pass through the APA membrane owing to the molecular cut-off of 5–10 nm.[39] If successful in passing the membrane they are assumed to be efficiently adsorbed by the Fe-oxide binding gel, as HS and phosphate strongly compete for adsorption sites on Fe-oxide.[40] A theoretical solute radius for HS cannot be determined using eqn (6) as there is no specific chemical structure. Therefore, it is not possible to determine a theoretical diffusion coefficient for the HS using the Stokes–Einstein equation (eqn (5)). The diffusion coefficient can instead be semi-empirically estimated using eqn (7), developed by Buffle,[41] providing a relationship between molecular weight (M) and D in water at 20 °C (eqn (7)).[42] The coefficient in this equation is based on a study of a number of organic molecules in the molecular weight range of 200–10[5] Da. The friction coefficient, ϕ/ϕ_0, is ideally equal to one, however it has been shown to increase with molecular size. For HS a friction coefficient of 1.16 was found to

Table 1 Molecular weight and P content of commonly found organic P compounds and fractions[a]

Substance	M (Da)	P content (w/w%)	P/C mass ratio
G6P	260	12	0.431
AMP	347	9	0.258
ATP	507	18	0.775
DLPA	536	5.8	0.095
IP6	660	28	2.584
FA (average)	500–2800[b]	~0.004[c]	~7.6 × 10[−5c]
HA (average)	1300–6500[b]	~0.013[c]	~2.5 × 10[−4c]

[a] ATP, adenosine tri-phosphate; G6P, glucose 6-phosphate; DLPA, 1,2-dilauroylphosphatidic acid. [b] Perdue and Ritchie.[37] [c] IHSS: Suwannee River FA and HA fractions.[44]

give the best fit,[43] and has thus been used in this study for the calculation of diffusion coefficients for HS.

$$D = \frac{\frac{\phi_0}{\phi} 3.3 \times 10^{-5}}{\sqrt[3]{M}} \qquad (7)$$

HS in freshwater consists of mainly fulvic acids (FA) and humic acids (HA). Their number- and weight-average molecular weights (M_n and M_w respectively) given in the literature vary greatly, mainly due to variations in sampling sites and the operationally defined analytical techniques used for their determination. In a comprehensive review by Perdue and Ritchie[37] the combined range of M_n and M_w for FA and HA was found to range from approx. 500 to 2800 and 1300 to 6500 Da, respectively.

The smaller molecular weight FA fraction will have a higher diffusion coefficient, and can therefore accumulate at a higher rate than the larger molecular weight HA fractions. It is therefore necessary to assess both the *ambient* concentration of both FA and HA bound P and the molecular weight distribution of these two humic fractions in order to calculate the total amount of accumulated HS bound P.

The concentrations of FA and HA bound P (c_{FA-P} and c_{HA-P}) are calculated using eqn (8a) and (8b), based on dissolved organic carbon (DOC) concentration in the collected water samples, weighted by the relative fractions of HA and FA (f_{FA-C} = 46 and f_{HA-C} = 13% from Perdue and Ritchie[37]) and their P to C ratio (P/C) for FA and HA (Table 1).

$$c_{FA-P} = DOC \times f_{FA-C} \times P/C \qquad (8a)$$

$$c_{HA-P} = DOC \times f_{HA-C} \times P/C \qquad (8b)$$

It has been shown that the molecular weight distributions of FA follows a log-normal distribution. A log-normal Gaussian distribution of the molecular weight can be calculated only if M_n and M_w[45] are known (eqn (9a)):

$$f_i = \frac{1}{\sigma \sqrt{2\pi}} e^{-\left(\log \frac{M_g}{M_i}\right)^2 / 2\sigma^2} \qquad (9a)$$

where f_i is the molar frequency of the ith molecular weight fraction, M_i. σ and M_g are calculated according to eqn (9b) and (9c):

$$\sigma = \sqrt{\log \frac{M_w}{M_n} / 2.303} \qquad (9b)$$

$$M_g = \frac{M_n \sqrt{M_n}}{\sqrt{M_w}} \qquad (9c)$$

Due to the polydisperse nature of HS it is presumed that HA, like FA, also follows a log-normal distribution. On the basis of this assumption the molecular weight distribution of freshwater FA and HA can be calculated by taking the mean M_n and M_w for a number of observations derived from different analytical

methods (vapour pressure osmometry (VPO), cryoscopy (CRY), size exclusion chromatography (SEC), UV scanning ultracentrifugation (UV-UCGN) and flow field-flow fractionation (FFF)) from the review paper of Perdue and Ritchie.[37] The mean M_n and M_w are weighted for the number of observations for each analytical method. A probability density plot for the molecular weight is then created based on the determined molar frequency (Fig. 2).

Using the probability density data the probability of every molecular weight fraction, $p(x_i)$, from 100 to 10 000 Da can be calculated for both FA and HA by multiplying $p(x_i)$ with the calculated concentration of FA and HA bound P (c_{FA-P} and c_{HA-P}, respectively), with the assumption that the P content in FA and HA is constant for the molecular weight distribution within each fraction (eqn (10a) and (10b)).

$$FA-P_i = p(x_i) \times c_{HA-P} \qquad (10a)$$

$$HA-P_i = p(x_i) \times c_{HA-P} \qquad (10b)$$

The total flux of FA-P and HA-P across the DGT membrane is then calculated using eqn (11):

$$\sum_{i=1}^{n} \frac{m_i}{t} = \sum_{i=1}^{n} A D_i \frac{c_i}{x} \qquad (11)$$

where c_i and D_i are the P concentration and diffusion coefficient, respectively, of the ith molecular weight fraction. D_i is calculated using Buffle's equation (eqn (7)) for the mean molecular weight of the ith fraction, followed by the DGT APA membrane retention correction (eqn (17)) and then temperature correction (eqn (14)). c_i is FA-P_i and HA-P_i calculated from eqn (10a) and (10b). The total flux of FA and HA is the summed accumulated mass $\left(\sum_i^n m_i\right)$ of each molecular weight fraction divided by time (t).

3.3. Accounting for diffusion retention by the DGT APA membrane

Zhang et al.[20] measured a 29% lower diffusion coefficient (D) for $H_2PO_4^-$ using DGT compared to D measured in water. This was

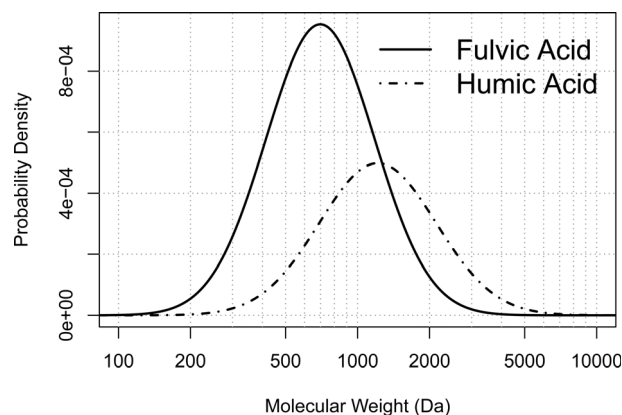Fig. 2 Probability density plot of the molecular weight distribution of FA and HA calculated from a log-normal model (eqn (9)) based on the mean M_n and M_w data from Perdue and Ritchie.[37]

716 | Environ. Sci.: Processes Impacts, 2015, 17, 711–727

This journal is © The Royal Society of Chemistry 2015

explained by phosphate retention due to positively charged sites on the APA diffusive gel.[20] Similar reduced diffusion in DGTs is thus likely to be a factor for all negatively charged compounds. Furthermore, as the molecular size increases there is likely to be an increase in friction as the molecular size approaches the pore size (5–10 nm) of the APA membrane. It is therefore important that the free-diffusion in water, as calculated by the Stokes–Einstein (eqn (5)) or Buffle's equation (eqn (7)), is corrected for the reduced diffusion caused by the APA membrane. Three empirical regression fit models, $y = \alpha x + \beta$, $y = \alpha x^{\beta}$ and $y = \dfrac{\alpha x^2}{1 + bx}$, were tested on experimentally determined free and DGT restricted D in order to assess the best model for D correction.

3.4. Theoretical determination of diffusion coefficients for LMWOP molecules

The molecular composition of the LMWOP fraction ($M_w < 1$ kDa) in any specific surface water is generally unknown as it varies in time and space. A single averaged diffusion coefficient can therefore not be theoretically calculated or directly derived from experimental data for the LMWOP fraction. Instead the adopted approach is to determine the upper and lower diffusion coefficients, covering the range of LMWOP compounds expected to be encountered in surface waters. As introduced in Chapter 1.1 the most dominant group of LMWOP compounds are nucleic acids, phospholipids, sugar phosphates and inositol polyphosphates. Some of the most common as well as most studied LMWOP compounds in soil and water are presented in Table 1.[11] The exception is DLPA (1,2-dilauroylphosphatidic acid), which only serves as a representative of a small phospholipid, of which there are numerous varieties.

Three conceptually based models were used for theoretically estimating the upper and lower diffusion coefficients:

• Buffle's model: estimation by Buffle's semi-empirical equation (eqn (7)), where molecular weight is the only variable and the friction coefficient (ϕ/ϕ_0) is set by default to 1.

• ChemAxon-Stokes–Einstein model: estimation using the Stokes–Einstein equation (eqn (5)), based on the friction coefficient (f) achieved using the solute radius (r_0), which was based on the computational model for determining SASA from the chemical structure, pH and the radius of the solute water molecule (radius = 1.4 Å). pH was used to calculate the dominant molecular species. SASA was calculated at pH 5 since the pH in the experimental determination of diffusion coefficients for AMP and IP6 was 5.0 and 5.5, respectively (Chapter 2.1).

• ChemAxon-Wilke–Chang model: estimation by the Wilke–Chang correlation[46] (eqn (12a)):

$$D = \frac{7.4 \times 10^{-8} (\phi M)^{1/2} T}{\eta V^{0.6}} \tag{12a}$$

where D is the diffusion coefficient, ϕ is the association parameter (2.6 for water), M is the molecular mass of the solvent molecule in Daltons (18 Da for water), T is the temperature in Kelvin, η is the viscosity in centipoise (1 centipoise = 10 kg m^{-1} s^{-1}) and V is the molecular volume given in cm^3 mol^{-1}. SASA is used to calculate the molecular radius (eqn (6)) used for estimating the assumed spherical volume (eqn (12b)):

$$V = 4\pi r_0^3 N/3 \tag{12b}$$

where N is Avogadro's constant.

Evaluation of the three models was done by comparing the modelled D of AMP and IP6 with the experimentally derived D.

4   Results and discussion

4.1.   Experimental determination of diffusion coefficients

In Fig. 3 the accumulated amounts of TDP and DRP by DGTs are plotted against their deployment time in the test solutions.

The results presented in Fig. 3 show a clear linear uptake of AMP and IP6 with time, where all TDP measurements are above LOD (1.7 µg P L^{-1}). Based on correlation slopes the uptake rates for AMP and IP6 were found to be 182 ± 2.7 ng P day^{-1} ($p < 10^{-11}$) and 150 ± 7.0 ng P day^{-1} ($p < 10^{-6}$), respectively.

In the AMP experiment the amount of DRP found in the extract remained below LOD (1.2 µg P L^{-1}), with no clear increasing trend with time (0.15 ± 0.27 ng P day^{-1}, $p = 0.58$). This indicates that there was negligible or no AMP degradation in the tank or when bound to the DGT binding gel, or during the extraction step. The IP6 experiment, on the other hand, showed a slight indication of an increase in DRP concentration with time (3.0 ± 1.5, $p = 0.086$). This may be due to degradation. However, this is conceptually unlikely since IP6 had a shorter experiment time than AMP. A possible explanation may instead lie in the relatively lower purity of the IP6 chemical reagent compared to the AMP chemical reagent (≥95% vs. ≥99% purity, respectively). Nevertheless DRP measurements for IP6 experiment were below LOD.

Uptake flux rates for the two experiments cannot be directly compared due to different concentrations of analyte and temperatures. In order to compare the uptake of AMP with IP6 the diffusion coefficient (D) for each TDP measurement presented in Fig. 3 must therefore first be calculated by eqn (13), derived by rearranging eqn (3).

$$D = \frac{mx}{tcA} \tag{13}$$

Moreover, the concentration of analytes (measured as TDP) in the tanks decreased over time during both experiments.
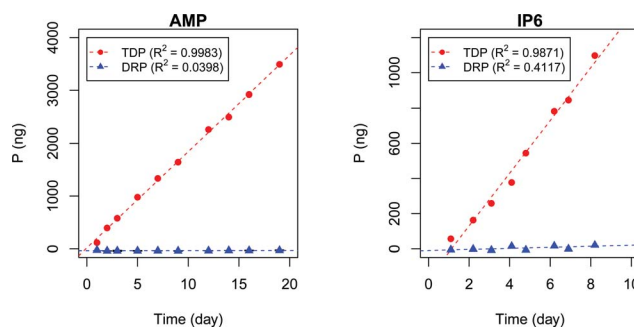

Fig. 3   DGT uptake of AMP and IP6 with time.

Interpolation through linear regression was therefore used to estimate the time average concentration (c). D needs to be corrected for different ambient temperatures. The correction is calculated by eqn (14) (derived from the Stokes–Einstein equation, eqn (5)), in which D_{T_1} is the diffusion coefficient for temperature T_1, η_1 is the viscosity of water at temperature T_1, D_{T_2} is the diffusion coefficient for temperature T_2, and η_2 is the viscosity of water at temperature T_2, where temperature is given in Kelvin and viscosity in kg m^{-1} s^{-1}.

$$\frac{D_{T_2}}{D_{T_1}} = \frac{T_2 \eta_1}{T_1 \eta_2} \tag{14}$$

The water viscosity is calculated using a quadratic empirically based equation (eqn (15)), where T is the temperature given in Kelvin. The constants $a = 5.53 \times 10^{-7}$, $b = -3.51 \times 10^{-4}$ and $c = 5.65 \times 10^{-2}$ were determined using a second degree regression model ($R^2 = 0.998$) to fit the equation to measured viscosities for water at different temperatures (0 to 40 °C in 5 °C increments) taken from Zwolinski and Eicher.[47] Eqn (15) is only applicable for temperatures between 0 and 40 °C.

$$\eta = aT^2 + bT + c \tag{15}$$

From these equations the diffusion coefficient at 20 °C was calculated. The average D for AMP and IP6 were found to be $2.9 \pm 0.4 \times 10^{-6}$ cm^2 s^{-1} and $1.0 \pm 0.3 \times 10^{-6}$ cm^2 s^{-1}, respectively.

4.2. Elution efficiency from DGT

The elution of AMP and IP6 from the Fe-oxide binding gel was conducted using 1.2 M H$_2$SO$_4$. This acid concentration is far stronger than the 0.25 M H$_2$SO$_4$ recommended by Zhang et al.[20] The higher acidity was used to ensure a total recovery of orthophosphate, which has been shown to increase with increased acid concentration.[20] Since organic phosphates and orthophosphate have similar adsorption/desorption chemistry (Chapter 1.2) it is fair to assume complete elusion. On the other hand, a high sulphuric acid strength increases the risk of

hydrolysis (*i.e.* of the ester-bonds linking phosphate to the adenosine or inositol molecule) decomposing the organic compounds. As addressed in Chapter 4.1 the DRP concentration remained low in the test solution (Fig. 3), which documents that AMP and IP6 were not significantly hydrolysed. However, the study by Moorlegham et al.[21] suggests that a few LMWOP compounds are susceptible to hydrolysis under strong acidic conditions (pH $\leq$ 0). It is therefore perceivable that some LMWOP compounds accumulated by the DGT from the natural aquatic environment may have hydrolysed during elusion.

4.3. DGT APA membrane resistance

The plots presented in Fig. 4 show the relationship between the determined D for water (D_{H_2O}) with the determined D for DGTs with APA diffusive gel (D_{DGT}). Out of the three models presented, the linear regression fit model, $y = \alpha x + \beta$ (left plot), shows the strongest correlation with the D data ($R^2 = 0.9997$), with the estimated values for parameters, α and β, highly significant for explaining the variations ($p < 0.001$). It should be noted that the linear empirical model is not applicable for correcting all D_{H_2O}, as it intersects the x-axis at $D_{H_2O} = 0.71$. The non-linear model, $y = \alpha x^\beta$ (centre plot), also shows a strong correlation with the data ($R^2 = 0.9967$). However it remains the weakest correlation of the three plots. The advantage of the equation $y = \alpha x^\beta$ is that as D_{H_2O} decreases towards 0, D_{DGT} also decreases towards 0, making the model applicable for all D_{H_2O}. The third model, $y = \dfrac{\alpha x^2}{1 + bx}$ (right plot), is a combination of a quadratic and linear equation ($R^2 = 0.9989$). The choice of this equation is because it supports the linear trend as D_{H_2O} increases $\left(\lim\limits_{x \to \infty} \dfrac{\alpha x^2}{1 + bx} = \dfrac{\alpha}{b}x\right)$, while allowing a non-linear trend towards 0 as D_{H_2O} decreases $\left(\lim\limits_{x \to 0} \dfrac{\alpha x^2}{1 + bx} = 0\right)$, thereby making the model applicable for all D_{H_2O}.

The main difference between the linear model and the two non-linear models is the conceptual understanding of the
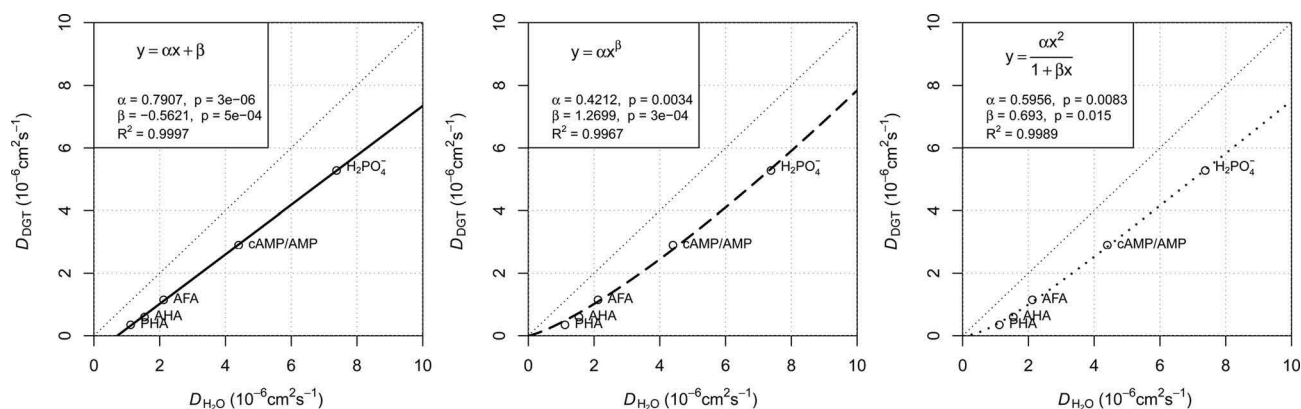
Fig. 4 Three regression models fitted to diffusion coefficients in water and DGT data for H$_2$PO$_4^-$ (Zhang et al.[20]), aquatic derived FA and HA (AFA and AHA respectively), peat derived HA (PHA) (Zhang and Davison[39]) and cAMP in water (Dworkin and Keller[48]) with AMP for DGTs, all corrected for 20 °C. Water diffusion coefficients for AFA, AHA and PHA are calculated using Buffle's equation (eqn (7), with friction coefficient = 1.16) based on the M_w for the fractions (2400, 6300 and 16 500 Da respectively).[49]

718 | *Environ. Sci.: Processes Impacts*, 2015, **17**, 711–727

This journal is © The Royal Society of Chemistry 2015

relationship between D_{H_2O} and D_{DGT} as a result of membrane resistance. Presented in Fig. 5, where membrane resistance (MR) can be calculated from D_{H_2O} and D_{DGT} (eqn (16)), the linear model presents the cut-off point (100% retention) for $D_{H_2O} = 0.71$, while the non-linear models show a continuous increase in retention only reaching 100% once $D_{H_2O} = 0$.

$$MR = \left(1 - \frac{D_{DGT}}{D_{H_2O}}\right) \times 100\% \tag{16}$$

Using the Stokes–Einstein equation (eqn (5)) the molecular radius can be calculated to be approx. 3 nm for $D_{H_2O} = 0.71$. This is a diameter of approx. 6 nm, which is within the range of the pore size, 5–10 nm, for the APA membrane. It seems therefore likely that molecules larger than ~6 nm in diameter are unable to diffuse through the APA membrane. This is a molecular weight of approx. 64 000–100 000 Da calculated by Buffle's equation (eqn (7)) for a friction coefficient = 1.16–1, respectively. On the basis of this concept and the good fit with the data, the linear model (eqn (17)) is chosen for correcting the free D for MR.

$$D_{DGT} = 0.7907 D_{H_2O} - 0.5621 \tag{17}$$

4.4. Assessment of the amount of adsorbed humic substance P and HMWOP by DGT

Based on the model approach presented in Chapter 3.2 followed by MR correction, an assessment was made to estimate the amount of phosphorus associated with HS accumulated by the DGT. Mean concentrations of DOC in the water samples (Table 2) were used in eqn (8a) and (8b) to determine the amount of FA and HA bound P (FA-P and HA-P) for each of the three studied sites (Table 2).

The mean total flux of DOP was calculated by taking the accumulated amounts of DOP (TDP–DRP) adsorbed and dividing by the field deployment time of the DGTs. The mean HA-P and FA-P flux could then be calculated, in accordance with eqn (7)–(11), (14) and (17), as a fraction of the mean total DOP flux for each study site. The non-HS DOP, which is presumed to be accounted for by the LMWOP, was calculated by subtracting the HA-P and FA-P flux from the total DOP flux. The results given in Table 3 show that the amounts of HA-P and FA-P (i.e. comprising HMWOP) accumulated by the DGTs are negligible compared to the LMWOP fraction.

The negligible contribution is mainly attributed to the extremely low P/C ratio reported for the FA-P and HA-P fractions (Table 1). These data are based on HS that were isolated using the XAD solid phase column extraction method and fractionated by precipitation of FA at pH < 1 (IHSS Suwannee River FA and HA fractions[44]). It is possible that the XAD alters the natural equilibrium of phosphate bound to Al and Fe complexed by HS. The low pH (1–2) and high pH (13) used in the XAD extraction method may desorb phosphate bound to the Al and Fe (ref. 50 and 51) on the HS. In the review by Copper et al.,[52] it was shown that even after isolating HMW organic matter (>1 kDa) from
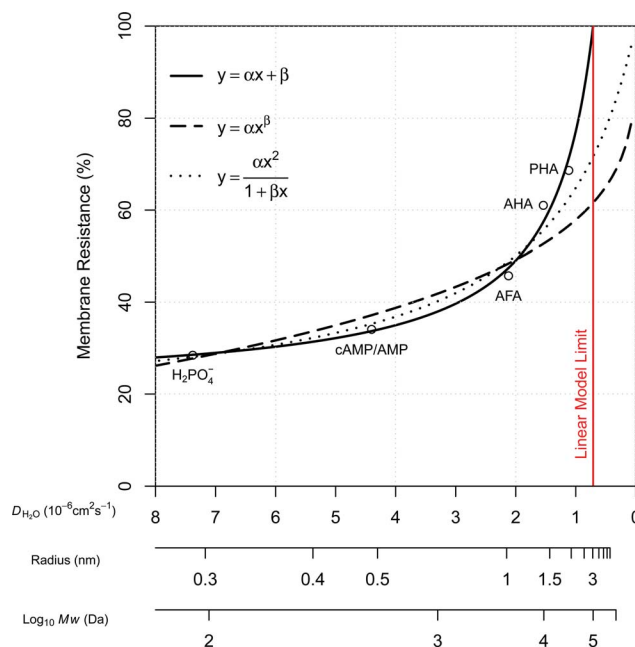

Fig. 5 Comparison of the three regression fit models, where the diffusion coefficient in water is plotted against DGT APA membrane resistance. The additional x-axis denotes the solute radius and molecular weight scale calculated by Stokes–Einstein and Buffle's equations (friction coefficient = 1) in order to show the change in membrane resistance as a function of molecular size.

natural waters, the large majority of organic phosphorus species determined for this fraction by mass spectrometry techniques were below 1 kDa. The confounding result was assumed to be a result of disruption of ionic interaction between large humic-like substances and LMWOP species, due to the electrospray ionization step, i.e. they were separated before analysis, despite being naturally found to be weakly linked together in natural waters. A study of freshwater from the Everglades, by Ged and Boyer[8] showed that approx. 40% of their DOP was associated with compounds larger than 10 kDa. That being said the study also showed that approx. 44% of the DOP was associated with low molecular weight species (<1 kDa), leaving only ~16% DOP in the molecular weight fraction between 1 and 10 Da. Based on these DOP data a rough estimated calculation of DOP uptake by the DGTs can be conducted in which the flux is calculated using the concentration of DOP for each fraction (c) and D of the middle molecular weight of each molecular weight fraction. Unfortunately, no middle molecular weight can be estimated for >10 kDa, so a "worst case scenario" is used in which the average molecular weight for the >10 kDa fraction is assumed to be equal to 10 kDa. The results presented in Table 4 show that despite the relatively high concentration of DOP associated with HMW compounds, the relative flux of >10 kDa DOP into the DGT is only 16% vs. approx. 75% being associated with <1 kDa. However unlike the first assessment made from Table 3, where HS are shown to be negligible, these data show that >1 kDa or HMWOP may account for approx. 25% of the accumulated DOP fraction. Since much of DNOM larger than 1 kDa is HS, it cannot be exactly concluded to what degree HS contributes to the

This journal is © The Royal Society of Chemistry 2015

Environ. Sci.: Processes Impacts, 2015, 17, 711–727 | 719

Table 2 Statistical data of the determined concentration of dissolved organic carbon at the studied sites

| Location | Dissolved Organic Carbon (DOC) | | | |
	Mean (mg C L^{-1})	Stdev (mg C L^{-1})	RSD (%)	n
Forest	38	2.5	6.7	26
Mixed	17	3.3	20.2	8
Agricultural	12	1.4	11.5	12

Table 3 The FA and HA fraction of the DGT DOP flux

Site	HA-P (%)	FA-P (%)	LMWOP (%)
Forest	0.21	0.31	99.46
Mixed	0.03	0.05	99.91
Agricultural	0.02	0.04	99.94

fraction of DOP adsorbed by the DGT. Instead it can be concluded that more than 75% of the DOP accumulated by the DGT is associated with LMWOP.

4.5. Assessment of *ambient* LMWOP from adsorbed DOP by the DGT

Diffusion coefficients at 20 °C for five LMWOP compounds (Table 5) were calculated using the three theoretically based methods discussed in Chapter 3.4, and corrected for MR using the linear empirical model derived in Chapter 4.3 (eqn (17)).

The estimated lower and upper D ranges were found to be 2.4–3.5, 1.2–2.6 and 1.2–4.7 for Buffle, ChemAxon-Stokes–Einstein and ChemAxon-Wilke–Chang models, respectively. ChemAxon-Wilke–Chang gave a much larger range, with a difference of 3.5 from the lowest to the highest D, compared to the spans of Buffle and ChemAxon-Einstein–Stokes (1.1 and 1.4, respectively). Overall, Buffle produced slightly higher D values than ChemAxon-Einstein–Stokes. All three models show G6P to have the highest D. The lowest D, however, varies among the Buffle and ChemAxon models. The Buffle equation indicates that IP6 is the slowest molecule, because it has the largest mass of the five compounds. However based on the molecular structure the largest r_0 is DLPA, which is why the ChemAxon model indicates that this compound has the lowest D. This

reflects the weakness of using Buffle's equation for LMWOP. Buffle's semi-empirical equation is based on that the organic molecules have a mole fraction dominated by the atoms ^{12}C, ^{1}H, ^{16}O and small amounts of ^{14}N. This generates rather similar molecular densities for the organic molecules. However, molecules dense in ^{31}P, such as IP6, have considerably higher molecular density. However, the phosphate groups cause the compound to have a relatively high net negative charge, producing a large hydrodynamic radius (possibly not accounted for by the ChemAxon model) and retention by the DGT APA membrane. IP6 has a strong negative charge of −6 to −8 at the pH range of 5–7 (Chapter 3.1), encountered in the studied water bodies. This results in a high absolute charge to mass/size ratio, explaining the relatively lower diffusion coefficient than what might be expected considering mass and size based on structure.

Deviations between experimentally measured diffusion coefficients for AMP and IP6 (Chapter 4.1) and their three theoretically derived constants are given in Table 6. The diffusion coefficients of AMP and IP6 are assumed to cover the range of D values encountered by LMWOP. Estimated D based on Buffle's equation deviates only 9% from the observed value for AMP, while both the ChemAxon models have an absolute error of 23%. Moreover, all models perform extremely poorly in estimating D for IP6. The estimated values using the ChemAxon-Stokes–Einstein model is slightly closer, with only 81% deviation, though still too high to be useful for any meaningful prediction of D. Apparently, retardation of the charged IP6 by the slightly positively charged APA gel (Chapter 3.3) considerably reduces the diffusion of the molecule causing the experimentally observed D value to be significantly lower than the modelled D estimates.

ChemAxon-Wilke–Chang appeared to be the poorest model in this test. The other two models performed slightly better, but were also poor predictors for lower and upper D of LMWOP. However, the combined D range of Buffle and ChemAxon-Stokes–Einstein models for the five studied compounds (1.2–3.5; Table 5) does not deviate much from the experimental D range of 1.0–2.9, captured by measuring IP6 and AMP.

The experimentally derived values of D for AMP and IP6 will be used for determining the ambient LMWOP concentration in the catchment study (Chapter 4.7) since they span the theoretically derived D values based on a set of LMWOP with large differences in physiochemical characteristics.

Table 4 DGT DOP flux assessment based on data from Ged and Boyer[8]

Molecular weight fraction (kDa)	Middle molecular weight (kDa)	Relative DOP concentration (%)	DOP flux[b] (%)
<1	0.5	44	74.9
1–3	2	2	1.9
3–5	4	4	2.7
5–10	7.5	10	4.7
>10	10[a]	40	15.9

[a] Worst case scenario of 10 kDa is chosen. [b] Diffusion coefficients for the flux were calculated using Buffle's eqn with a friction coefficient = 1.

Table 5 Buffle and ChemAxon estimated and MR corrected DGT diffusion coefficients for five selected LMWOP at pH 5

Substance	M (Da)	Solute radius (Å)	Estimated D_{DGT} (10^{-6} cm^2 s^{-1})		
			Buffle	ChemAxon-Stokes–Einstein	ChemAxon-Wilke–Chang
G6P	260	5.3	3.5	2.6	4.7
AMP	346	6.1	3.2	2.2	3.5
ATP	507	7.1	2.7	1.8	2.5
DLPA	535	9.7	2.7	1.2	1.2
IP6	656	7.1	2.4	1.8	2.5

4.6. pH correction of dissolved reactive phosphate (DRP)

The common D constant used for determining ambient DRP from DGT measurements is 5.28×10^{-6} cm^2 s^{-1} for $H_2PO_4^-$ (Zhang *et al.*[20]). The problem however is that $H_2PO_4^-$ is not the dominant species at all pH commonly encountered in the environment. *E.g.*, the median pH during the monitoring period for the Forest, Mixed and Agricultural catchment streams was 4.4, 6.9 and 7.8, respectively. Within this range the dominant species of orthophosphate differ between $H_2PO_4^-$ and HPO_4^{2-}. As each of these species has its own D the distribution of $H_2PO_4^-$ and HPO_4^{2-} with pH needs to be accounted for. The distribution (α) for each species can be calculated from eqn (18) and (19), where the pK_a values for H_3PO_4, $H_2PO_4^-$ and HPO_4^{2-} are 2.16, 7.21 and 12.3, respectively.

$$\alpha_1 = \frac{Ka_1[\text{H}^+]^2}{[\text{H}^+]^3 + Ka_1[\text{H}^+]^2 + Ka_1 Ka_2[\text{H}^+] + Ka_1 Ka_2 Ka_3} \quad (18)$$

$$\alpha_2 = \frac{Ka_1 Ka_2[\text{H}^+]}{[\text{H}^+]^3 + Ka_1[\text{H}^+]^2 + Ka_1 Ka_2[\text{H}^+] + Ka_1 Ka_2 Ka_3} \quad (19)$$

In the forest catchment stream, with pH 4.4, 99.3% (α_1) is in the form of $H_2PO_4^-$ and 0.2% (α_2) is HPO_4^{2-}. In the mixed catchment stream, having pH 6.9, 63.2% is in the form of $H_2PO_4^-$ and 36.8% is HPO_4^{2-}, while for the agricultural catchment stream, with pH 7.8, only 34.9% is in the form of $H_2PO_4^-$ and 65.1% is HPO_4^{2-}. The challenge is that there exists no experimentally DGT determined D value for HPO_4^{2-}. There is however a water determined D for HPO_4^{2-} (6.40×10^{-6} cm^2 s^{-1} at 20 °C),[53] which after correction for DGT retardation due to MR (eqn (17)) is calculated to be 4.50×10^{-6} cm^2 s^{-1}. One can then calculate a pH adjusted D for DRP at any given pH by multiplying the fractional contribution of the two species, with their corresponding D and adding the two products (eqn (20)).

$$D_{1,2} = D_1 \frac{\alpha_1}{\alpha_1 + \alpha_2} + D_2 \frac{\alpha_2}{\alpha_1 + \alpha_2} \quad (20)$$

It should be noted that the reason eqn (20) does not use the fractions directly is due to the fact that the forest catchment stream, with a median pH of 4.4, also contains the H_3PO_4 species (0.5%). There is however a lack of available data on D for H_3PO_4, making it difficult to employ for this special case.

4.7. Field study of DGTs in stream water

Median, mean, variation and range in DRP and DOP concentration, derived from DGTs and water samples collected from the streams draining Forest, Mixed and Agricultural catchments, are shown in Fig. 6. As expected the drainage from agricultural catchment shows a considerably higher concentration of DRP compared to the mixed and forested catchment. The agricultural stream shows also a greater concentration of DRP compared to DOP, while the opposite is the case for the forest stream. The reason is without doubt the large amount of inorganic phosphate fertilizer used in the cultivation of the agriculture sites, governing the higher DRP to DOP ratio. In forest catchments the DRP is kept low as it is efficiently consumed by the perennial forest vegetation. It is the leaching of DNOM from the forest soil which contributes most to the DOP found in the Forest stream. The stream water from the Mixed catchment has inherently a DRP to DOP ratio that lies between the ratios found for the Forest and Agricultural streams.

Validation of the DGT's ability to measure time average concentrations of DRP was performed by comparing the DRP concentrations derived from DGTs with the DRP measured directly in water samples collected from the streams during the DGT deployment period. The Wilcoxon rank-sum statistical test (also known as the Mann–Whitney U test) is a nonparametric

Table 6 Validation of the DGT diffusion coefficient models[a]

Compound	Observed D_{DGT} (10^{-6} cm^2 s^{-1})	Estimated D_{DGT} (10^{-6} cm^2 s^{-1})			Deviation (%)		
		Buffle	C.A.-Stokes–Einstein	C.A.-Wilke–Chang	Buffle	C.A.-Stokes–Einstein	C.A.-Wilke–Chang
AMP	2.9	3.2	2.2	3.5	8.8	−23	23
IP6	1.0	2.4	1.8	2.5	144	81	152

[a] C.A.: abbreviation for ChemAxon.

test for the null hypothesis of two sample groups originating from the same population. The main advantage of the Wilcoxon test is its efficiency and robustness in comparing populations, which are not necessarily normally distributed and vary in the number of observations, *i.e.* non-paired test. This is practical, considering that DGTs are time average measurements, while grab samples are only momentary measurements. For good comparison more grab samples than DGT measurements are required. The test does not require an interval dataset, only that the data is ordinal, which is necessary since sampling intervals varied during the period (Chapter 2.2). The statistical test found no significant difference ($p < 0.05$) between DRP from DGTs and water samples for the Forest, Mixed and Agricultural catchment streams ($p = 0.053$, $p = 0.39$ and $p = 0.078$, respectively).

However it should be noted that both the Forest and Agricultural catchments were borderline to failing the null hypothesis. It is important also to note that without pH correction (Chapter 4.6) the Wilcoxon rank-sum test would have predicted a significant difference ($p = 0.032$) for the Agricultural catchment stream. From the boxplots in Fig. 6 it can be seen that the median values of the forest DRP values for DGT and water sample are close (2.0 µg P L^{-1} and 1.7 µg P L^{-1} respectively), but that the bulk distribution of measurements overlap poorly. The DGT time average measurements show an overall slightly higher DRP concentration than the water samples. For the stream draining the Agricultural catchment there is good agreement between the two distributions of DGT and water sample DRP measurements. However, the DGT show a far
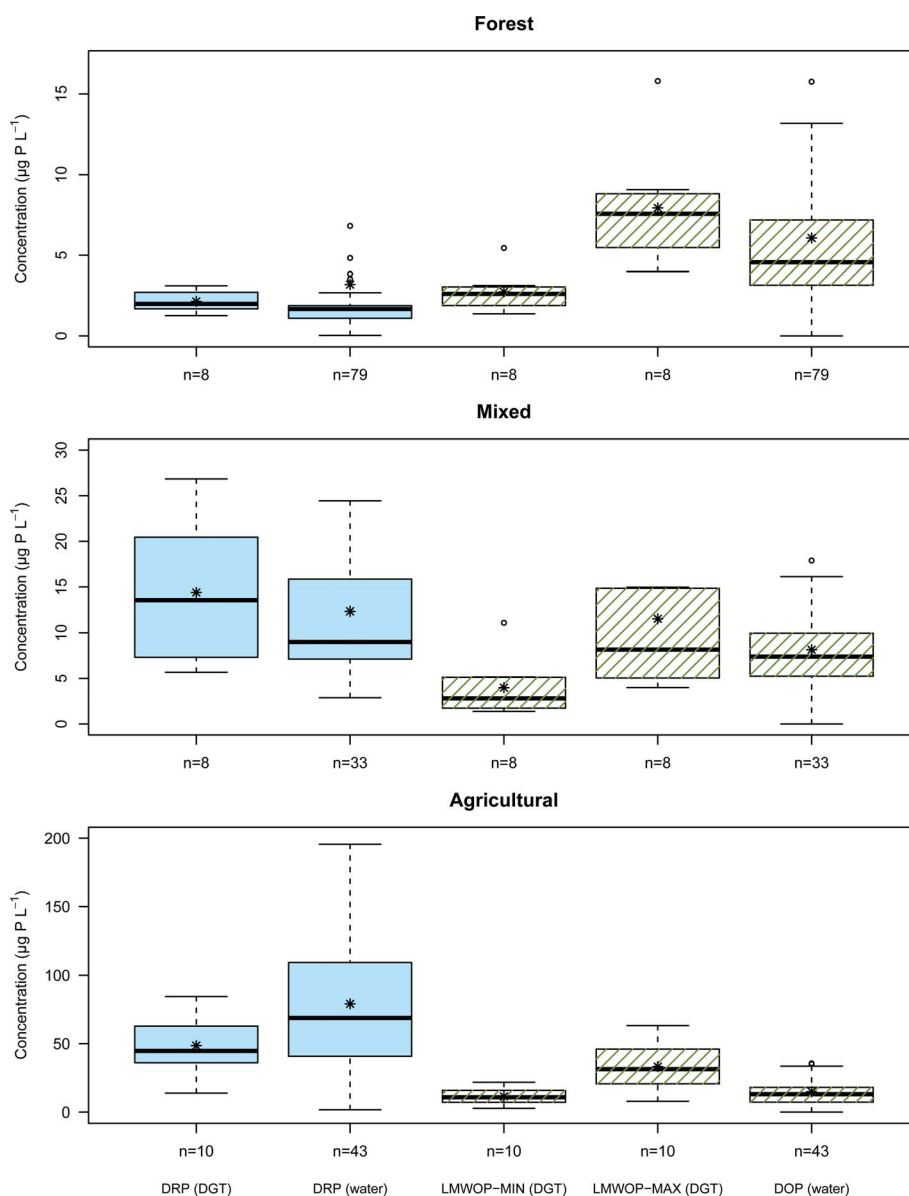

Fig. 6 Boxplots comparing concentrations of P fractions from the DGTs and water samples collected from the study sites, forest, mixed, and agricultural, during the period from June to September. The black star dot (*) denotes the mean value.

722 | *Environ. Sci.: Processes Impacts*, 2015, **17**, 711–727

This journal is © The Royal Society of Chemistry 2015

narrower spread in measurements as these are time averaged values. All the water sample DRP measurements from the median to the 3rd quartile are higher than the main bulk distribution of DGT DRP measurements. It is possible that this larger DRP concentration in the water sample is a result of over-estimation, possibly contributed by P lightly adsorbed to colloid-particles bypassing the 0.7 μm filter (see Chapter 2.4).

Overall there is clearly far less difference between the two methods of DRP determination (*i.e.* DGT and water sample), relative to the difference in DRP concentration between the three catchment streams.

Validation of DOP by comparing significant deviations between DGT determined LMWOP and water samples determined DOP is not sound for the following two reasons:

(1) DOP in the water sample may also contain a significant fraction of HMWOP (Chapter 4.4).

(2) Only minimum and maximum concentrations of LMWOP can be determined. The actual amount remains unknown until further information is acquired regarding the relative distribution of DOP molecular species for the streams draining the different catchments. It can however be assumed, based on the findings in Chapter 4.4, that the large majority of the DGT accumulated DOP is LMWOP (>75%).

For all streams the maximum LMWOP concentration determined is higher than the DOP concentration determined from the water sample. This simply reflects that on average not all of the DOP molecular compounds in the water samples are as large or have a D as low as IP6. The minimum LMWOP concentration has to be smaller than or equal to the DOP in the water samples, since LMWOP is a fraction of the DOP fraction. Based on the good match between DOP in the water sample and the minimum LMWOP concentration in the Agricultural stream it appears that the average size of the DOP molecules in the agricultural runoff is of the size of AMP. The mixed catchment shows closer match with the larger molecular compounds, such as IP6. For the forest stream the DOP on average consists of a medium sized LMWOP. The results clearly show that streams draining from catchments with different land-use have different distributions of LMWOP.

For the practical application of using DGTs to monitor time average DOP we need to determine a "best fit" D, which results in the best match between DGT determined LMWOP and water determined DOP. Using the same Wilcoxon rank-sum test, which was used to validate the DRP data, we can compare the DGT LMWOP with the water sample DOP data for different D from 1.0 to 2.9 in 0.05 increments. The D resulting in the highest p-value for the test will indicate minimum significant difference between the two datasets (Table 7). It should however be noted that this serves only as a practical means of using the DGTs to determine time average DOP, because there is an assumption that the relative distribution of LMWOP/DOP compounds remains constant within each stream, despite changes in the overall LMWOP/DOP concentration. However even if the assumption of constant relative distribution is likely correct, the D determined by this stream calibration method is likely smaller than the true unattainable number average D for

LMWOP, because the DOP concentration in water samples (also containing HMWOP) is always larger than LMWOP.

4.8. Field study of lake water DRP and LMWOP using DGT

The DGT study at the lake basin *Grepperødfjorden* provides some insight into the dynamics of P bioavailability through the water column (Fig. 7). Temperature showed a fairly minor and constant decline with depth, from 21.3 to 18.7 °C. The lake basin is shallow and was non-stratified due to mixing by water turbulence. This is however not always the case, as the lake basin occasionally experiences stratification and hypoxia in the hypolimnion. During the summer and early autumn periods (the warmest months) the lake experiences algae blooms, dominated mainly by *Gonyostomum semen* (phytoplankton fraction approx. 60–80%).[54] This phytoplankton species is typically found in humic lakes and is capable of diel vertical movement (DVM). This means it is able to migrate towards the surface for enough light for photosynthesis during the day and migrate towards the sediments for a source of P, typically during the night.[55,56] It would be expected that the DVM of phytoplankton and lack of stratification would result in a fairly even distribution of DRP and LMWOP concentration through the water column. The DGT results presented in Fig. 7 show however that DRP decreased significantly with depth ($p < 0.05$), while there was no significant difference between depths for LMWOP ($p > 0.05$). The highest concentrations of both DRP and LMWOP were found near the surface. Based on conventional grab samples the levels of bioavailable P species in the photic zone are commonly found to be close to the detection limit even in eutrophic lakes, due to efficient phosphorus assimilation by phytoplankton during the day. On the other hand, DGTs capture the time average concentration, and thus integrate out diurnal variation, while grab samples are usually only taken during the day. This may mean that biochemical processes that may give the net production of DRP and LMWOP during the night are not detected by the conventional sampling method. For instance, it is known that macrozooplankton migrate towards the sediments during the day to avoid predation due to reduced visibility in deeper, darker waters. During the night however they are safe to migrate back towards the surface where they can feed on phytoplankton in the warmer epilimnion.[57] As a result of sufficient food and warmer temperatures, their metabolic rate increases, which results in the release of DRP and LMWOP through excretion.[14] The second explanation for the high DRP and LMWOP near the surface is cell death, which is common near the surface due to the intense solar radiation.

Table 7 "Best fit" diffusion coefficients for minimum difference between DGT LMWOP and water sample DOP, using the Wilcoxon rank-sum test

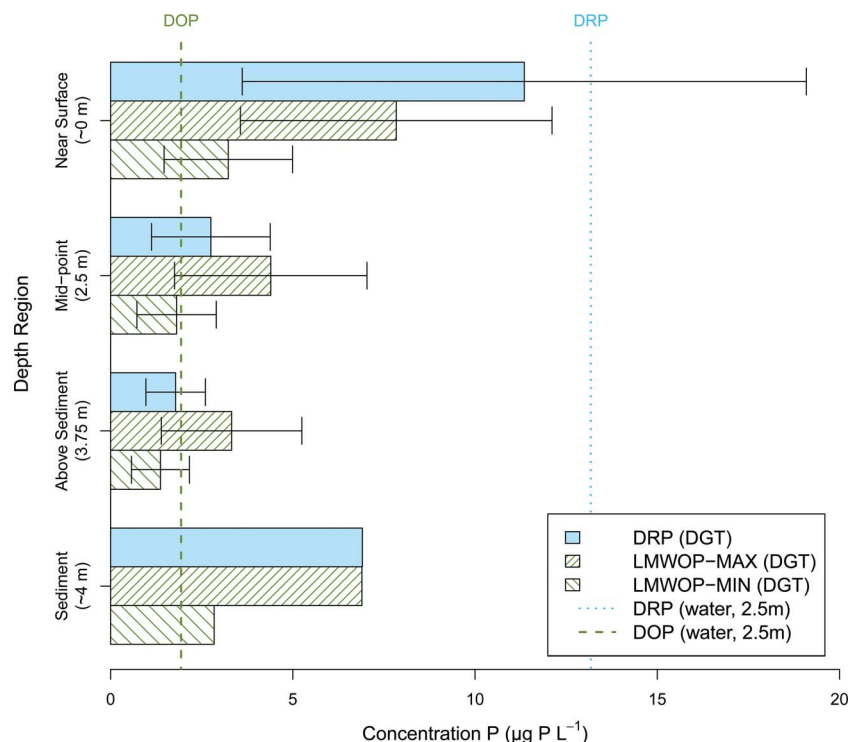| Location	D (10^{-6} cm^2 s^{-1})	p-value
Forest	1.6	0.959
Mixed	1.15	0.936
Agricultural	2.45	0.973

Fig. 7 Bar graph illustrating the variation in average DGT determined P fractions at different depth regions through the water column of the *Grepperødfjorden* lake basin ($n = 3$ for 0 m, 2.5 m, 3.75 m and $n = 1$ for sediment) and average determined P fractions from the water sample from 2.5 m depth ($n = 2$). Error bars represent the standard deviation for the replicates.

Phytoplankton are dependent on getting sufficient photosynthetically active radiation (PAR, ~380–710 nm), which declines exponentially with depth, known as vertical light attenuation. Furthermore UV-radiation, but also wavelengths (WL) in the blue spectrum of PAR, decline exponentially with increase in DNOM.[58] In humic water bodies, such as *Grepperødfjorden*, this results in a thin euphotic zone at the surface of the water. Minimal change in distance from the surface results in large changes in the amount of available PAR. A little too far below the surface results in insufficient photosynthesis to balance their energy demand for metabolic activity.[59] A little too near the surface and the high intensity of light, in particular UV-radiation, result in DNA damage and cell death, not to mention that photo-degradation of DNOM results in reactive oxygen species toxic to biota.[58,60] Cell death is followed by lysis, which results in the release of DOP to the water. In addition many of the enzymes capable of hydrolysing phosphate from DOP are also released as a result of cell lysis, which may explain the high DRP concentration in the surface waters.[14]

At the deeper depths of the water column it appears that P uptake keeps the P concentration low, and the reduced UV-radiation keeps the phytoplankton safe from harmful exposure. Finally the DGT placed in the sediment measures high concentrations of both P fractions, as would be expected due to internal loading from the sediments.

It remains unclear why DRP measured from the water sample collected at 2.5 m is far greater than the DGT determined DRP at 2.5 m. DOP from the water sample remains near the LMWOP determined concentrations.

5 Conclusion

The solution type DGTs fitted with Fe-oxide binding gel proved to be successful in the linear uptake of AMP and IP6, and will therefore most likely capture other LMWOP, and thus bioavailable, compounds in a similar manner. Modelling of HA-P and FA-P uptake indicated that the DGTs only collect negligible amounts of P associated with HS. Even using higher P/C ratios reported by Ged and Boyer,[8] less than approx. 25% of the DOP that was accumulated could be over >1 kDa. It should be noted that a negligible amount of this is associated with HS as this is the largest DNOM fraction. More studies are needed to better quantify the distribution of DOP with molecular weight for a variety of catchments with different land-use. Nonetheless, the results remain fairly conclusive that more than 75% of the DOP accumulated by the DGT is LMWOP.

Both the Buffle and the ChemAxon-Stokes–Einstein models are still in their infancy in regards to predicting DGT diffusion coefficients (D) of LMWOP molecules. This is partly because there is currently insufficient observed/experimental data available to develop good models. More LMWOP molecules need to have their D determined experimentally so that better calibration and validation can be performed. There is little doubt that charge plays an important role in the diffusion of molecules through the DGT APA membrane. It is therefore inherent that the D needs to be determined at different pH, in order to compensate for the changes in negative charge as a result of protonation and de-protonation of phosphate and other weak acid functional groups.

724 | *Environ. Sci.: Processes Impacts*, 2015, **17**, 711–727

This journal is © The Royal Society of Chemistry 2015

The catchment study indicates that there is a reasonable match between the dissolved P fractions determined from water samples and by DGTs, and that molecular weight distribution of LMWOP/DOP is different for the three study sites. However, accurate determination of the concentration of the LMWOP fraction remains infeasible without knowing the distribution of LMWOP molecules in the streams. The application of DGTs will not be practical for the determination of the time average LMWOP fraction if one needs to determine the relative distribution of the LMWOP molecules each time the DGT is used. A practical compromise was however found by determining a "best fit" D for each study site that results in the least significant difference between the two datasets, DGT LMWOP and the water sample DOP. In this way "tailored" D for the individual water bodies can be determined as a means to roughly assess the time average DOP.

The lake study clearly shows the strengths of the DGT as a better means of capturing the spatial variation of DRP and LMWOP in the lake. Further studies are still required to better explain P cycling in the lake. Nevertheless, the use of DGTs provides a far better *ambient* approach to monitoring bioavailable P concentrations than the conventional grab sample, which often fails to capture long-term diel, seasonal and spatial variations due to the practical restraints of sampling.

References

1 S. R. Carpenter, N. F. Caraco, D. L. Correll, R. W. Howarth, A. N. Sharpley and V. H. Smith, Nonpoint Pollution of Surface Waters with Phosphorus and Nitrogen, *Ecol. Appl.*, 1998, **8**, 559–568.

2 M. F. Chslock, E. Doster, R. A. Zitomer and A. E. Wilson, Eutrophication: Causes, Consequences, and Controls in Aquatic Ecosystems, *Nat. Educ. Knowl.*, 2013, **4**, 10.

3 R. D. Vogt, Water Quality in a Changing Environment, *Public Serv. Rev. Eur. Union*, 2012, **23**, 386–387.

4 A. Blankenberg, S. Turtumøygard, A. Pengerud, H. Borch, E. Skarbøvik, L. Øyegarden, M. Bechmann, N. Syversen and N. Vagstad, Tiltaksanalyse for Morsa: "Effekter av Fosforreduserende Tiltak i Morsa 2000–2006; Bioforsk, Jord og Miljø, Ås, Norway, 2008, p. 54.

5 D. Hongve, G. Riise and J. F. Kristiansen, Increased Colour and Organic Acid Concentrations in Norwegian Forest Lakes and Drinking Water – a Result of Increased Precipitation?, *Aquat. Sci.*, 2004, **66**, 231–238.

6 NORDTEST, *Increase in Colour and Amount of Organic Matter in Surface Waters*, The Nordic Council of Ministers, 2003, pp. 1–12.

7 B. L. Skjelkvåle, Overvåkning av Langtransporterte Forurensninger 2009; Klima- og Forurensningsdirektoratet (Eng. Climate and Pollution Agency), 2010, p. 87.

8 E. C. Ged and T. H. Boyer, Molecular Weight Distribution of Phosphorus Fraction of Aquatic Dissolved Organic Matter, *Chemosphere*, 2013, **91**, 921–927.

9 S. Hino, Fluctuation of Algal Alkaline Phosphatase Activity and the Possible Mechanisms of Hydrolysis of Dissolved Organic Phosphorus in Lake Barato, *Hydrobiologia*, 1988, **157**, 77–84.

10 R. C. Dalal, Soil Organic Phosphorus, *Adv. Agron.*, 1977, **29**, 83–117.

11 B. L. Turner, E. Frossard and D. S. Baldwin, *Organic Phosphorus in the Environment*, ed. B. Turner, E. Frossard and D. Baldwin; CABI Publishing, 1st edn, 2005.

12 B. A. Whitton, S. L. Grainger, G. R. Hawley and J. W. Simon, Cell-Bound and Extracellular Phosphatase Activities of Cyanobacterial Isolates, *Microb. Ecol.*, 1991, **21**, 85–98.

13 I. D. McKelvie, B. T. Hart, T. J. Cardwell and R. W. Cattrall, Use of Immobilized 3-Phytase and Flow Injection for the Determination of Phosphorus Species in Natural Waters, *Anal. Chim. Acta*, 1995, **316**, 277–289.

14 A. D. Cembella, N. J. Antia and P. J. Harrison, The Utilization of Inorganic and Organic Phosphorous Compounds as Nutrients by Eukaryotic Microalgae: A Multidisciplinary Perspective: Part 1, *CRC Crit. Rev. Microbiol.*, 1984, **10**, 317–391.

15 A. D. Cembella, N. J. Antia, P. J. Harrison and A. D. Cernbella, The Utilization of Inorganic and Organic Phosphorous Compounds as Nutrients by Eukaryotic Microalgae: A Mulitdiciplinary Perspective: Part 2, *CRC Crit. Rev. Microbiol.*, 1984, **11**, 13–81.

16 P. J. Worsfold, P. Monbet, A. D. Tappin, M. F. Fitzsimons, D. A. Stiles and I. D. McKelvie, Characterisation and Quantification of Organic Phosphorus and Organic Nitrogen Components in Aquatic Systems: A Review, *Anal. Chim. Acta*, 2008, **624**, 37–58.

17 H. Zhang, *DGT - for Measurements in Water, Soil and Sediments*, DGT Research Ltd, Lancaster, 2005, pp. 1–58.

18 E. L. Cussler, *Diffusion: Mass Transfer in Fluids Systems*, Cambridge University Press, 3rd edn, 2009.

19 O. Røyset, S. Eich-Greatorex, T. A. Sogn, Å. R. Almås and E. Bjerke, Simultaneous Sampling of Phosphate, Arsenate, and Selenate in Water by Diffusive Gradients in Thin Films (DGT), Oslo, 2004, p. 17.

20 H. Zhang, W. Davidson, R. Gadi and T. Kobayashi, *In Situ* Measurement of Dissolved Phosphorus in Natural Waters Using DGT, *Anal. Chim. Acta*, 1998, **340**, 29–38.

21 C. Van Moorleghem, L. Six, F. Degryse, E. Smolders and R. Merckx, Effect of Organic P Forms and P Present in Inorganic Colloids on the Determination of Dissolved P in Environmental Samples by the Diffusive Gradient in Thin Films Technique, Ion Chromatography, and Colorimetry, *Anal. Chem.*, 2011, **83**, 5317–5323.

This journal is © The Royal Society of Chemistry 2015

Environ. Sci.: Processes Impacts, 2015, **17**, 711–727 | 725

22 L. Celi and E. Barberis, Abiotic Stabilization of Organic Phosphorus in Environmet, in *Organic Phosphorus in the Environment*, ed. B. Turner, E. Frossard and D. S. Baldwin, CABI Publishing, Wallinford, 2005, pp. 113–132.

23 J. G. Panther, P. R. Teasdale, W. W. Bennett, D. T. Welsh and H. Zhao, Titanium Dioxide-Based DGT Technique for in Situ Measurement of Dissolved Reactive Phosphorus in Fresh and Marine Waters, *Environ. Sci. Technol.*, 2010, **44**, 9419–9424.

24 S. Ding, D. Xu, Q. Sun, H. Yin and C. Zhang, Measurement of Dissolved Reactive Phosphorus Using the Diffusive Gradients in Thin Films Technique with a High-Capacity Binding Phase, *Environ. Sci. Technol.*, 2010, **44**, 8169–8174.

25 Q. Sun, Y. Chen, D. Xu, Y. Wang and S. Ding, Investigation of Potential Interferences on the Measurement of Dissolved Reactive Phosphate Using Zirconium Oxide-Based DGT Technique, *J. Environ. Sci.*, 2013, **25**, 1592–1600.

26 W. J. Dougherty, S. D. Mason, L. L. Burkitt and P. J. Milham, Relationship between Phosphorus Concentration in Surface Runoff and a Novel Soil Phosphorus Test Procedure (DGT) under Simulated Rainfall, *Soil Res.*, 2011, **49**, 523.

27 R Core Team, *R: A Language and Environment for Statistical Computing*, Vienna, Austria, http://www.R-project.org/, 2013.

28 O. A. Garmo, K. R. Naqvi, O. Røyset and E. Steinnes, Estimation of Diffusive Boundary Layer Thickness in Studies Involving Diffusive Gradients in Thin Films (DGT), *Anal. Bioanal. Chem.*, 2006, **386**, 2233–2237.

29 E. Skarbøvik, M. Bechmann, T. Rohrlack and S. Haande, Overvåking Vansjø/Morsa 2008, 2009, vol. 4, p. 108.

30 D. S. Jeffres, F. P. Dieken and D. E. Jones, Performance Of The Autoclave Digestion Method For Total Phosphorus Analysis, *Water Reasearch Pergamon Press*, 1979, **13**, 275–279.

31 J. Murphy and J. P. Riley, A Modified Single Solution Method for the Determination of Phosphate in Natural Waters, *Anal. Chim. Acta*, 1962, **27**, 31–36.

32 F. H. A. Rigler, Dynamic View of the Phosphorus Cycle in Lakes, in *Environmental Phosphorus Handbook*, ed. E. J. Griffith, A. Beeton, J. M. Spencer and D. T. Mitchell, John Wiley and Sons., New York, 1973, pp. 539–572.

33 P. W. Atkins and J. De Paula, Molecules in Motion, in *Atkin's Physical Chemistry*, Oxford University Press, 2006, pp. 747–783.

34 L. Heighton, W. F. Schmidt and R. L. Siefert, Kinetic and Equilibrium Constants of Phytic Acid and Ferric and Ferrous Phytate Derived from Nuclear Magnetic Resonance Spectroscopy, *J. Agric. Food Chem.*, 2008, **56**, 9543–9547.

35 ChemAxon, *Marvin 6.1.2*, http://www.chemaxon.com/, 2013.

36 P. Ferrara, J. Apostolakis and A. Caflisch, Evaluation of a Fast Implicit Solvent Model for Molecular Dynamics Simulations, *Proteins: Struct., Funct., Bioinf.*, 2002, **46**, 24–33.

37 E. Perdue and J. Ritchie, Dissolved Organic Matter in Freshwaters, in *Treatise on Geochemistry, Vol. 5: Surface and Ground Water, Weathering, and Soils*, ed. J. I. Drever, H. D. Holland and K. K. Turekian, Elsevier Ltd, Oxford, 2003, pp. 273–318.

38 S. A. Huber, A. Balz, M. Abert and W. Pronk, Characterisation of Aquatic Humic and Non-Humic Matter with Size-Exclusion Chromatography - Organic Carbon Detection - Organic Nitrogen Detection (LC-OCD-OND), *Water Res.*, 2011, **45**, 879–885.

39 H. Zhang and W. Davison, Diffusional Characteristics of Hydrogels Used in DGT and DET Techniques, *Anal. Chim. Acta*, 1999, **398**, 329–340.

40 E. Tipping, The Adsorption of Aquatic Humic Substances by Iron Oxides, *Geochim. Cosmochim. Acta*, 1981, **45**, 191–199.

41 J. Buffle, Complexation Properties of Homologous Complexants and Choice of Measuring Methods, in *Complexation Reactions in Aquatic Systems an AnlyticalApproach*, ed. R. A. Chalmers and M. R. Masson, Ellis Horwood Limited, Chichester, 1988, pp. 359–363.

42 J. Buffle, *Complexation Reactions in Aquatic Systems an Analytical Approach*, ed. J. Buffle, Ellis Horwood Limited, Chichester, 1988, p. 673.

43 J. Buffle, Z. Zhang and K. Startchev, Metal Flux and Dynamic Speciation at (bio)interfaces. Part I: Critical Evaluation and Compilation of Physicochemical Parameters for Complexes with Simple Ligands and Fulvic/humic Substances, *Environ. Sci. Technol.*, 2007, **41**, 7609–7620.

44 International Humic Substances Society, Elemental Compositions and Stable Isotopic Ratios of IHSS Samples, http://www.humicsubstances.org/elements.html/, accessed Jan 30, 2014.

45 S. E. Cabaniss, Q. Zhou, P. A. Maurice, Y.-P. Chin and G. R. Aiken, A Log-Normal Distribution Model for the Molecular Weight of Aquatic Fulvic Acids, *Environ. Sci. Technol.*, 2000, **34**, 1103–1109.

46 C. R. Wilke and P. Chang, Correlation of Diffusion Coefficients in Dilute Solutions, *AIChE J.*, 1955, **1**, 264–270.

47 B. J. Zwolinski and L. D. Eicher, High-Precision Viscosity of Supercooled Water and Analysis of the Extended Range Temperature Coefficient, *J. Phys. Chem.*, 1971, **75**, 2016–2024.

48 M. Dworkin and K. H. Keller, Solubility and Diffusion Coefficient of Adenosine 3′:5′-Monophosphate, *J. Biol. Chem.*, 1977, **252**, 864–865.

49 J. R. Lead, J. Hamilton-Taylor, N. Hesketh, M. N. Jones, A. E. Wilkinson and E. Tipping, A Comparative Study of Proton and Alkaline Earth Metal Binding by Humic Substances, *Anal. Chim. Acta*, 1994, **294**, 319–327.

50 M. Petrovic and M. Kastelan-Macan, The Uptake of Inorganic Phosphorus by Insoluble Metal-Humic Complexes, *Water Sci. Technol.*, 1996, **34**, 253–258.

51 E. M. Thurman and R. L. Malcolm, Preparative Isolation of Aquatic Humic Substances, *Environ. Sci. Technol.*, 1981, **15**, 463–466.

52 W. T. Cooper, J. M. Llewelyn, G. L. Bennett, A. C. Stenson and V. J. M. Salters, Organic Phosphorus Speciation in Natural Waters by Mass Spectrometry, in *Organic Phosphorus in the Environment*, ed. B. L. Turner, E. Frossard and D. S. Baldwin, CABI Publishing, 2005, pp. 45–74.

53 L. Yuan-Hui and S. Gregory, Diffusion of Ions in Sea Water and in Deep-Sea Sediments, *Geochim. Cosmochim. Acta*, 1974, **38**, 703–714.

54 E. Skarbøvik, M. Bechmann, T. Rohrlack and S. Haande, Overvåking Vansjø/Morsa 2009–2010, Bioforsk, 2011, vol. 6, p. 121.

55 G. Cronberg, The Life Cycle of Gonyostomum Semen (Raphidophyceae), *Phycologia*, 2005, **44**, 285–293.

56 K. Salonen, Advantages from Diel Vertical Migration Can Explain the Dominance of Gonyostomum Semen (Raphidophyceae) in a Small, Steeply-Stratified Humic Lake, *J. Plankton Res.*, 2000, **22**, 1841–1853.

57 J. Kalff, Zooplankton, in *Limnology: Inland Water Ecosystems*, ed. T. Ryu and J. Hakim, Prentice-Hall, Inc., Upper Saddle River, NJ, 2002, pp. 376–407.

58 J. Kalff, Light, in *Limnology: Inland Water Ecosystems*, ed. T. Ryu and J. Hakim, Prentice-Hall, Inc., Upper Saddle River, NJ, 2002, pp. 136–153.

59 S. I. Dodson, Setting the Stage: Water as an Environment, in *Introduction to Limnology*, McGraw-Hill Higher Education, 2005, pp. 39–56.

60 D.-P. Häder, H. D. Kumar, R. C. Smith and R. C. Worrest, Effects of Solar UV Radiation on Aquatic Ecosystems and Interactions with Climate Change, *Photochem. Photobiol. Sci.*, 2007, **6**, 267–285.